PATENT
Docket No. 511582001620

CERTIFICATE OF MAILING BY "FIRST CLASS MAIL"

I hereby certify that this correspondence is being deposited with the United States Postal Service as first class mail in an envelope addressed to: Assistant Commissioner for Patents, Washington, D.C. 20231, on July 29, 2003.

Tami M Procopio
Tami M. Procopio

IN THE UNITED STATES PATENT AND TRADEMARK OFFICE

In the application of:

Daniel E. H. AFAR, *et al.*

Serial No.: 09/455,486

Filing Date: 6 December 1999

For: NOVEL SERPENTINE TRANSMEMBRANE ANTIGENS EXPRESSED IN HUMAN CANCERS AND USES THEREOF

Examiner: Gary B. Nickol, Ph. D.

Group Art Unit: 1642

#31
KD
8/1/03

DECLARATION OF MARY FARIS, PH.D.

UNDER 37 C.F.R. § 1.132

Assistant Commissioner for Patents
Washington, D.C. 20231

Dear Sir:

I, Mary Faris, declare as follows:

1. I hold the position of research Group Leader at Agensys, Inc. This position requires me to generate *in vitro* models for the study of cancer, and to investigate the effect of specific genes and proteins on tumor development, growth, and progression. This position also requires me to attend national and international conferences addressing issues in cancer research, conferences where there are exhibits of established as well as cutting-edge ideas in the cancer field. I have a Ph.D. in Immunology and Microbiology from Ohio State University, and have

OK to enter GW 9/26/03

held two postdoctoral fellowships, one at the University of Virginia and one at the University of California at Los Angeles, School of Medicine. I have worked in the field of molecular biology for over 10 years. A copy of my *curriculum vitae* is attached as Exhibit A.

2. I have reviewed the specification and claims of the above-captioned application. I note that the claims are directed to an isolated STEAP-2 protein and compositions for eliciting an immunological response. I understand that the Office may have taken the position that the specification fails to show how to use the STEAP-2 protein in any predictable manner. I note, however, that consistent with the application as-filed there are several meaningful uses of STEAP-2 protein, as I will discuss below.

3. Of record in the present prosecution is a prior Declaration by me dated 03-June-2002 ("2002 Declaration") describing experimental results indicating that STEAP-2 functions in calcium ion flux, and that its expression results in ion flux. Paragraph 7 of my 2002 Declaration demonstrates that STEAP-2 mediates calcium flux in response to LPA and that the magnitude of calcium flux is comparable to that produced by a known calcium channel.

4. Since STEAP-2 is associated with function as an ion channel, it is useful as a both a target and a screening tool for small molecules that inhibit tumor cells. For example, the specification provides guidance with respect to how to use the STEAP-2 protein as a screening tool as follows: Page 13, lines 11-22 of the application as-filed notes the correlation of STEAP proteins with function as ion channels, transport proteins, or gap junction proteins, and that these functions have been implicated in the proliferation and invasiveness of prostate cancer cells. The paragraph concludes that the art suggests a role for ion channels in prostate cancer and demonstrates that small molecules that inhibit ion channel function interfere with prostate cancer cell proliferation. Weissenbach et al. illustrated the relationship of calcium channels to prostate cancer by demonstrating that expression of the calcium channel CaT-like protein correlates with prostate cancer stage, metastasis and androgen-independence (Weissenbach et al., J. Biol. Chem 2001, 276:19461; Exhibit B). In addition, they and others have shown that regulation of calcium flux and intracellular calcium concentration plays a critical role in prostate cancer survival

(Skryma R et al., J. Physiol 2000, 527:71; Exhibit C). Thus increasing intracellular calcium concentration results in apoptosis of prostates cancer lines (Batra et al., Prostate 1991, 19:2999(Exhibit D); Skryma R et al., J. Physiol 2000, *supra*). Similar observations have been reported with sodium and potassium channels, where expression of ion channels correlates with tumor progression, and inhibition of their function prevents cell growth (Skyrma et al., Prostate 1997, 33:112; Exhibit E). For example, studies on voltage-gated sodium channels (VGSC) revealed that VGSC are associated with increased invasiveness of prostate cancer, and that VGSC blockers inhibit the proliferation of prostate cancer cells (Abdul M. and Hoosein N., Anticancer Res 2002, 22:1727; Exhibit F).

5. Therefore, the STEAP-2 protein is defined as a suitable target for known calcium ion channel inhibitors as well as being a research tool for screening compounds which interact with STEAP-2 so as to inhibit calcium ion flow. Thus, one use disclosed by the specification, and further confirmed by experiment, is the use of the STEAP-2 protein as a research tool for compounds that are useful to treat tumors that express STEAP-2 by inhibiting calcium channel activity.

6. Similarly, data shows that STEAP-2 functions in achieving drug resistance. This is shown by experiments investigating the effect of chemotherapeutic agents on the proliferation and apoptosis of PC3 cells (see 2002 Declaration). Control PC3 cells and PC3 cells expressing STEAP-2 were treated with chemotherapeutic agents currently used in the clinic. Effect of treatment was evaluated by measuring cell proliferation using the Alamare blue assay and by following apoptosis by Annexin V staining. While only 5.2% of PC3-neo cells were able to metabolize Alamare Blue and proliferate in the presence of 5 μM paclitaxel, 44.8% of PC3-STEAP-2 cells survived under the same conditions. A similar outcome was obtained in assays evaluating cell death by apoptosis. These results indicate that expression of STEAP-2 imparts resistance to chemotherapeutic agents such as paclitaxel, and allows survival of prostate cancer cells. These findings have significant *in vivo* implications, as they indicate that STEAP-2

provides a growth advantage for prostate tumor cells in patients treated with common therapeutic agents.

7. Therefore, the STEAP-2 protein is defined as a suitable target for known inhibitors of drug resistance proteins, as well as being a research tool for screening compounds which interact with STEAP-2 so as to inhibit the STEAP-2 drug resistance function. Thus, one use disclosed by the specification, and further confirmed by experiment, is the use of the STEAP-2 protein as a research tool for compounds that are useful to treat tumors that express STEAP-2 by inhibiting its drug resistance function.

8. Interacting STEAP-2 protein with antibodies generated against the STEAP-2 protein is meaningful and useful in several ways. The specification at page 27, for example, states that STEAP proteins are targets for antibody-mediated inhibition of prostate and other cancers that express these proteins. This is verified in the 2002 Declaration as well; that data demonstrate that the presence of STEAP-2 confers resistance on tumor cells to known anticancer agents, such as paclitaxel. Antibodies to STEAP-2 can be used to overcome drug resistance and ion transport conferred by STEAP-2. Another use of STEAP-2 specific antibodies is the inhibition of STEAP-2 function. Altering the functional effect of STEAP-2 by using anti-STEAP-2 antibodies would restore sensitivity to the drug and prevent ion transport, thereby preventing growth and survival of tumor cells. Another application is the use anti-STEAP-2 antibodies to deliver a payload of an antitumor agent to tumor cells. For this purpose, toxin- or drug-conjugated anti-STEAP-2 antibodies are targeted to STEAP-2 expressing cells, delivering the toxin or drug into or in close vicinity to the tumor cell. STEAP-2 protein is thus useful for raising antibodies that are used in this manner.

9. In order to use antibodies raised by the claimed protein to overcome the drug resistance of tumor cells, STEAP-2 needs to be expressed in the tumor. As described in the specification, STEAP-2 expression can be detected using, e.g., antibodies specific to STEAP-2 (Application as-filed pages 23-24). Confirmation that STEAP-2 is present indicates that antibodies or small molecules that interact with STEAP-2 are viable tumor inhibition modalities.

10. In conclusion, the specification, in combination with the data made of record confirming the statements therein, provides guidance for predictable uses of the claimed STEAP-2 protein for immunotherapy of cancer.

I declare that all statements made herein of my own knowledge are true and that all statements made on information and belief are believed to be true; and further, that these statements are made with the knowledge that willful, false statements and the like so made are punishable by fine or imprisonment or both, under Section 1001 of Title 18 of the United States Code and that such willful false statements may jeopardize the validity of the application or any patent issued thereon.

Executed at Santa Monica, California on 25 July 2003.

Mary Faris, Ph.D.

THE JOURNAL OF BIOLOGICAL CHEMISTRY
Vol. 276, No. 22, Issue of June 1, pp. 19461–19468, 2001
Printed in U.S.A.

Expression of CaT-like, a Novel Calcium-selective Channel, Correlates with the Malignancy of Prostate Cancer*

Received for publication, October 30, 2000, and in revised form, February 1, 2001
Published, JBC Papers in Press, February 2, 2001, DOI 10.1074/jbc.M009895200

Ulrich Wissenbach, Barbara A. Niemeyer, Thomas Fixemer‡, Arne Schneidewind, Claudia Trost, Adolfo Cavalié, Katrin Reus§, Eckart Meese§, Helmut Bonkhoff‡, and Veit Flockerzi¶

From the Institut für Pharmakologie und Toxikologie, §Institut für Humangnetik, und ‡Institut für Pathologie der Universität des Saarlandes, D 66421 Homburg, Germany

The regulation of intracellular Ca^{2+} plays a key role in the development and growth of cells. Here we report the cloning and functional expression of a highly calcium-selective channel localized on the human chromosome 7. The sequence of the new channel is structurally related to the gene product of the CaT1 protein cloned from rat duodenum and is therefore called CaT-like (CaT-L). CaT-L is expressed in locally advanced prostate cancer, metastatic and androgen-insensitive prostatic lesions but is undetectable in healthy prostate tissue and benign prostatic hyperplasia. Additionally, CaT-L is expressed in normal placenta, exocrine pancreas, and salivary glands. New markers with well defined biological function that correlate with aberrant cell growth are needed for the molecular staging of cancer and to predict the clinical outcome. The human CaT-L channel represents a marker for prostate cancer progression and may serve as a target for therapeutic strategies.

The link between ion channels and disease has received widespread attention in the last few years as mutations in several ion channels have been shown to be responsible for various forms of neurological disorders (1, 2). Whereas many of these mutations affect well characterized channels of the nervous system, little is known about the situation in non-excitable cells. One new superfamily of channels of widespread expression and function include channels of the Trp family. The prototypical members of this family of six transmembrane domain channel subunits come from the visual system of *Drosophila* where they have been shown to be responsible for the light-activated cationic conductance changes (3). Other members of these growing family of ion channels include osmo- and mechanosensitive ion channels (4, 5), channels responsible for pain and heat perception like the vanilloid receptors (6, 7), and channels involved in agonist/receptor activated cation influx (8) into cells such as Trp-1 to Trp-7. Also new on the scene are the epithelial Ca^{2+} channel, ECaC[1] (also ECaC1 (9)), and the Ca^{2+} transport protein CaT1 (also ECaC2, (10)), implicated to play a role in the reabsorption of Ca^{2+} by the kidney (ECaC) and intestinal epithelial cells (ECaC and CaT1).

Two other identified members of this family of Trp-related proteins, p120 and melastatin, have not yet been demonstrated to function as ion channels. One of these genes, p120 (11), when overexpressed, appears to interfere with normal cell growth, whereas the second, melastatin (12), is abundantly expressed in benign cutaneous nevi but appears to be down-regulated in primary melanomas and, especially, in metastatic lesions.

Here we report the cloning of a new human gene product that is structurally related to the rat CaT1 cDNA and that we tentatively called Ca^{2+} transport protein-like (CaT-L). Unlike CaT1 and ECaC, CaT-L is not expressed in the small intestine (CaT1, ECaC (10, 13)), in colon (CaT1 (10)) and in the kidney (ECaC (9, 13)). CaT-L is abundantly expressed in the placenta, pancreatic acinar cells, and salivary glands. So far, little is known of the Ca^{2+} entry pathways in these tissues. The Ca^{2+}-permeation properties of the CaT-L channel, shown here, renders CaT-L as a good candidate for secretion coupling in these tissues. Most interesting, the CaT-L transcripts are undetectable in benign prostate tissue but are present at high levels in locally advanced prostate cancer, metastatic lesions, and recurrent androgen-insensitive prostatic adenocarcinoma. Hence, molecular classification of prostate cancer subclasses and class prediction by monitoring the level of human CaT-L gene expression is feasible. In addition, functional characterization of the new Ca^{2+} channel suggests a possible link between Ca^{2+} signaling and prostate cancer progression.

EXPERIMENTAL PROCEDURES

Cloning of the CaT-L cDNA from Human Placenta—Total RNA was isolated from human placenta as described (14), and poly(A)$^+$ RNA was obtained using poly(A)$^+$ RNA spin columns (New England Biolabs, Beverly, MA) according to the manufacturer's instructions. To obtain an oligo-(dT)-primed cDNA library, placenta poly(A)$^+$ RNA was reverse-transcribed using the cDNA choice system (Life Technologies, Inc.), and the resulting cDNA was subcloned in λ-Zap phages (Stratagene, La Jolla, CA). After screening the library with the human expressed sequence tag 1404042 (GenBank™), several cDNA clones were identified, isolated, and sequenced. Additional cDNA clones were isolated from two specifically primed cDNA libraries from a second placenta using primers corresponding to amino acids ^{676}HLSLPM and ^{271}GPLTSTL of the CaT-L sequence (Fig. 1*a*) and the 345-bp *NcoI*/*Bam*HI and 596-bp *Eco*RI/*Sst*I cDNA fragments of CaT-L as probes. Thirteen independent cDNA clones were sequenced on both strands. In addition the complete coding region of the CaT-L protein was amplified by PCR, using human cDNA isolated from placenta as template, and eight independent cDNA clones were sequenced on both strands. The nucleotide sequences of CaT-La and CaT-Lb have been deposited in DDBJ/EMBL/GenBank™ under the accession numbers AJ243500 and AJ243501, respectively.

Northern Blot Analysis—For Northern blot analysis 5 μg of human poly(A)$^+$ RNA from human placenta and from prostate (obtained from patients undergoing transurethral prostatectomy because of benign prostatic hyperplasia) were separated by electrophoresis on 0.8% agarose gels and thereafter transferred to Hybond N nylon membranes (Amersham Pharmacia Biotech) as described (14). The membranes were hybridized in the presence of 50% formamide at 42 °C overnight.

* This work was supported in part by the Deutsche Forschungsgemeinschaft. The costs of publication of this article were defrayed in part by the payment of page charges. This article must therefore be hereby marked "*advertisement*" in accordance with 18 U.S.C. Section 1734 solely to indicate this fact.

¶ To whom correspondence should be addressed. Tel.: 49 6841 166400; Fax: 49 6841 166402; E-mail: veit.flockerzi@med-rz.uni-sb.de.

[1] The abbreviations used are: ECaC, epithelial Ca^{2+} channel; bp, base pair; PCR, polymerase chain reaction; GFP, green fluorescent protein; HEK, human embryonic kidney; PBS, phosphate-buffered saline; kb, kilobase pair.

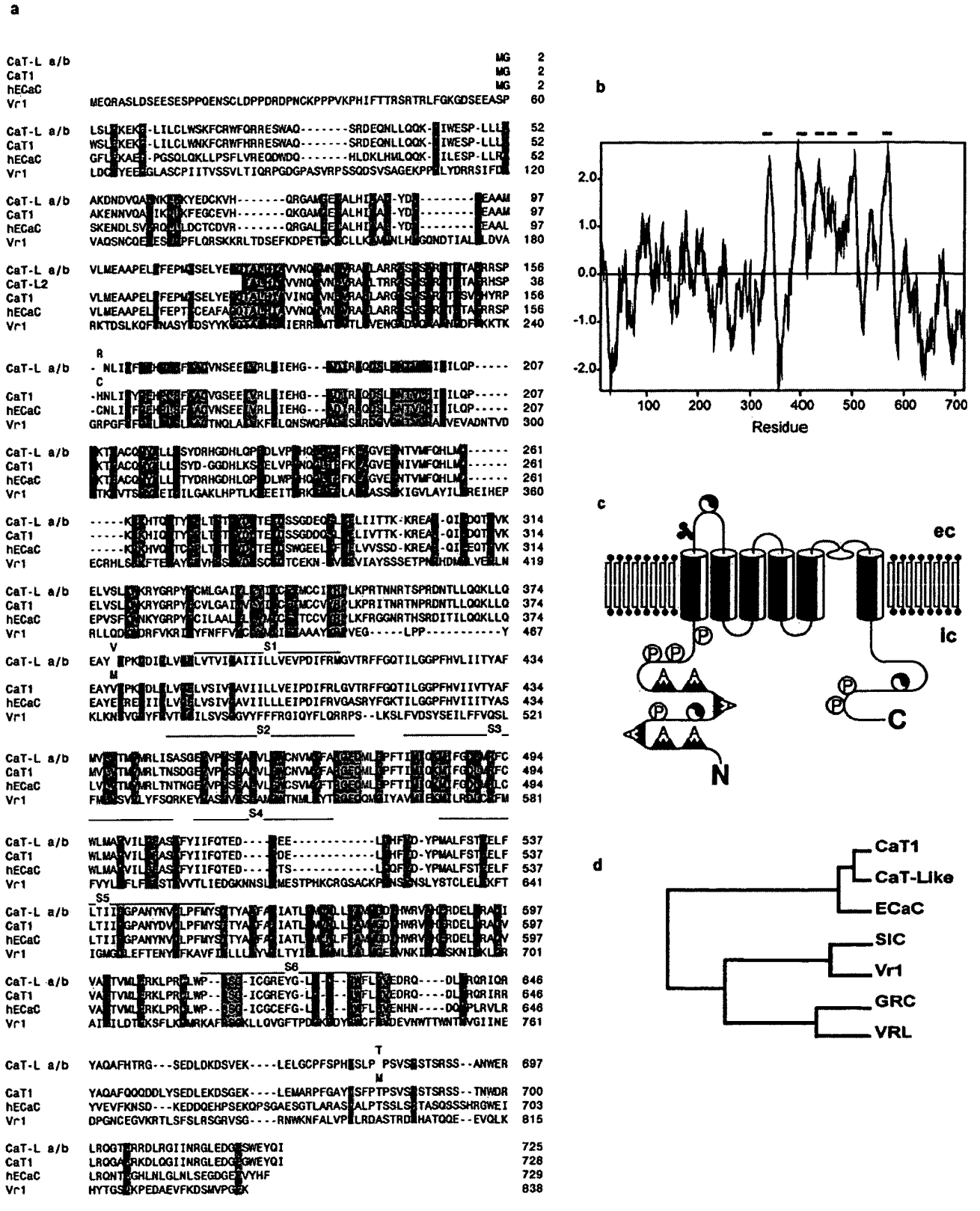

FIG. 1. **Primary structure of human CaT-L.** *a*, alignment of the deduced amino acid sequence of CaT-L with the sequences of human ECaC, rat CaT1, and the rat vanilloid receptor Vr1 (GenBank™ accession numbers AF160798, AJ401155, and T09054). CaT-La and CaT-Lb arise due to polymorphism of the CaT-L gene (see "Results"). Amino acid residues are *numbered* on the *right*. Residues within CaT-L identical to ECaC, CaT1, and Vr1, the putative transmembrane segments (S1–S6), the putative pore region, and the partial CaT-L2 sequence obtained by reverse transcriptase-PCR (see "Results") are indicated. *b*, hydropathy profile (46) of CaT-L. Transmembrane segments S1–S6 were defined as regions with a hydropathy index ≥1.5 using a window of 19 amino acids. *c*, predicted membrane topology of the CaT-L protein. Putative ankyrin repeats (A), an *N*-glycosylation site (*branched circles*) and protein kinase C phosphorylation sites (*circled p*) are indicated. The positions of amino acid exchanges of CaT-La and CaT-Lb are symbolized by ⬭. *d*, phylogenetic tree based on the full-length cDNA sequences of CaT-L-related mammalian gene products ECaC (32), CaT1 (10), SIC (47), Vr1 (6), VRl (7), and GRC (48), respectively.

Alternatively, a human multiple tissue RNA blot (CLONTECH) was hybridized under the same conditions. The probe was a 345-bp *Eco*RI/*Bam*HI fragment spanning the protein coding region of amino acid residues 528–643 of the CaT-L protein (Fig. 1*a*), labeled by random priming with [α,^{32}P]dCTP. Filters were exposed to x-ray films for 4 days.

Construction of Expression Plasmids and Transfection of HEK Cells—To obtain the recombinant dicistronic expression plasmid pdiCaT-L carrying the entire protein-coding regions of CaT-Lb and the GFP (15), the 5′- and 3′-untranslated sequences of the CaT-Lb cDNA were removed, and the consensus sequence for initiation of translation in vertebrates (16) was introduced immediately 5′ of the translation initiation codon; and the resulting cDNA was subcloned into the pCAGGS vector (17), downstream of the chicken β-actin promoter. The internal ribosomal entry site derived from encephalomyocarditis virus (18), followed by the GFP cDNA containing a Ser-65 → Thr mutation (19), was then cloned 3′ to the CaT-Lb cDNA. The internal ribosomal entry site sequence allows the simultaneous translation of CaT-Lb and GFP from one transcript. Thus, transfected cells can be detected unequivocally by the development of green fluorescence. Human embryonic kidney (HEK) 293 cells (ATCC CRL 1573) were transfected with pdiCaT-L using lipofectamine (Qiagen, Hilden, Germany) as described (20).

For measuring $[Ca^{2+}]_i$, HEK cells were cotransfected with the pcDNA3-CaT-Lb and pcDNA3-GFP (21) in a ratio of 4:1. To obtain pcDNA3-CaT-Lb the entire protein coding region of CaT-Lb including the consensus sequence for initiation of translation in vertebrates (16) was subcloned into the pcDNA3 vector (Invitrogen, Groningen, Netherlands). Measurements of $[Ca^{2+}]_i$ and patch clamp experiments were carried out 2 days and 1 day after transfection, respectively.

Chromosomal Localization of the CaT-L Gene—The chromosomal localization of the human CaT-L gene was performed using NIGMS somatic hybrid mapping panel 2 (Coriell Institute, Camden, NJ) described previously (22, 23) and primers corresponding to amino acids ^{115}YEGQTA and ^{158}NLIYFG of the CaT-L sequence (Fig. 3*a*).

Electrophysiological Recordings—Patch clamp recordings on single transfected cells were performed at 22–25 °C in the tight seal whole-cell configuration using fire-polished patch pipettes (3–10 MΩ uncompensated series resistance) 2 days after transfection. Pipette and cell capacitance were electronically canceled before each voltage ramp. Membrane currents were filtered at 1.5 kHz and digitized at a sampling rate of 5–10 kHz. To analyze transfected cells, currents were recorded with an EPC-9 patch clamp amplifier controlled by Pulse 8.3 software (HEKA Electronics). The pipette solution contained (in mM) the following: 140 aspartic acid, 10 EGTA, 10 NaCl, 1 $MgCl_2$, 10 Hepes (pH 7.2 with CsOH). The bath solution contained (in mM) the following: 110 NaCl, 10 CsCl, 2 $MgCl_2$, 50 mannitol, 10 glucose, 20 Hepes (pH 7, 4 with CsOH) and 2 $CaCl_2$, or no added $CaCl_2$ ($-Ca^{2+}$ solution). Divalent free bath solution contained (in mM) the following: 116 NaCl, 10 CsCl, 50 mannitol, 10 glucose, 20 Hepes, 1 EGTA (pH 7, 4 with CsOH) and bath solution without Na^+ contained 110 *N*-methyl-D-glucamine instead of NaCl. Whole-cell currents were recorded every second by applying 200-ms voltage clamp ramps from −100 to +100 mV from a holding potential of either −40 or +70 mV. The holding potential of +70 mV, which reduces Ca^{2+} influx, in combination with high internal EGTA was used to minimize Ca^{2+} dependent feedback mechanisms. Data are given as mean ± S.E. Values were not corrected for liquid junction potentials. Measured currents were normalized to cell capacitance, *i.e.* −25.3 ± 0.4 pA/pF for CaT-L-transfected cells (n = 12) and −1.56 ± 0.54 pA/pF for GFP controls (n = 6) at −80-mV ramp potential in normal bath solution.

Measurements of $[Ca^{2+}]_i$ in Transiently Transfected HEK Cells—Measurements of $[Ca^{2+}]_i$ in single HEK cells were performed with a digital imaging system (T.I.L.L. Photonics). Cells grown on coverslips were loaded with 4 μM fura-2/AM (Molecular Probes, Eugene, OR) for 60 min at 37 °C in minimal essential medium containing 10% fetal calf serum. Cells were washed three times with 300 μl of buffer containing 115 mM NaCl, 2 mM $MgCl_2$, 5 mM KCl, 10 mM Hepes (pH 7.4). Nominal Ca^{2+}-free solutions contained ~2 μM Ca^{2+}. $[Ca^{2+}]_i$ was calculated from the fluorescence ratios obtained at 340 and 380 nm excitation wavelengths as described (24). Experiments were repeated three times.

In Situ Hybridization Analysis—Sense and antisense oligodeoxynucleotides corresponding to the amino acid residues ^{11}LILCLWSK, ^{637}QDLNRQRI, and ^{651}FHTRGSED of the CaT-L sequence (Fig. 1*a*) were synthesized. Using the BLAST sequence similarity search tool provided by the National Center for Biotechnology Information (Bethesda, MD), the antisense sequences show maximal similarity of <71% to sequences in the GenBank™ data base. The oligodeoxynucleotides used for hybridization were biotinylated at the 3′ end.

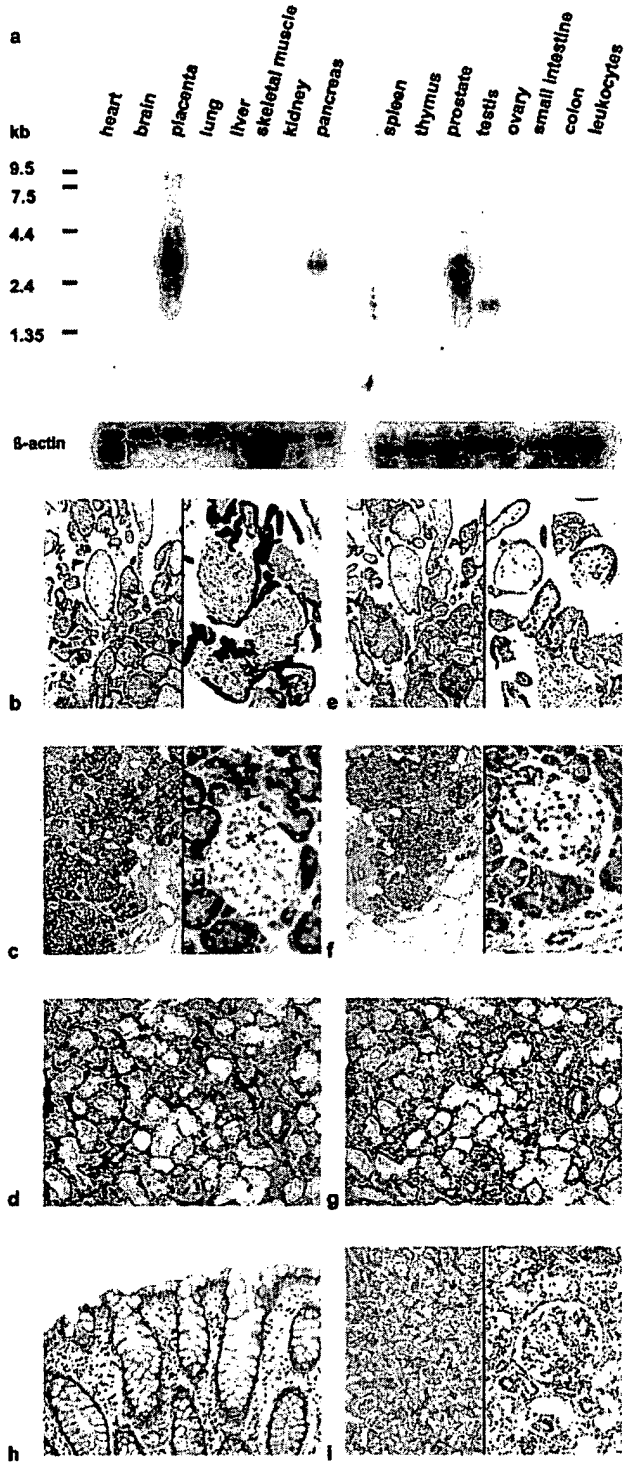

FIG. 2. **Expression of CaT-L mRNA in human tissues.** *a*, autoradiogram of blot hybridization analysis (*lower panel*, signals after hybridization of human β-actin cDNA as control to the same filters). *B–i*, *in situ* hybridization reveals high steady state levels of CaT-L mRNA in trophoblasts and syncytiotrophoblasts of the normal placenta (*b*). Original magnifications are as follows: × 25 (*left*) and × 100 (*right*). Strong expression of CaT-L transcripts are detected in acinar structures of the normal pancreas, whereas pancreatic ductal epithelial cells (*arrows*) and Langerhans islets (*asterisk*) lack CaT-L mRNA. Original magnifications are as follows: × 25 (*left*) and × 200 (*right*). In salivary glands CaT-L mRNA expression is restricted to subsets of myoepithelial cells (*d*). Original magnification, × 100. *In situ* hybridization analyses performed in adjacent tissue sections with the sense probe were distinctively negative (*e–g*). CaT-L mRNA expression was undetectable in other human tissues investigated, including the colon mucosa (*h*) and the normal kidney (*i*). Original magnifications are as follows: *h*, × 100; *i*, × 25 (*left*) and × 100 (*right*).

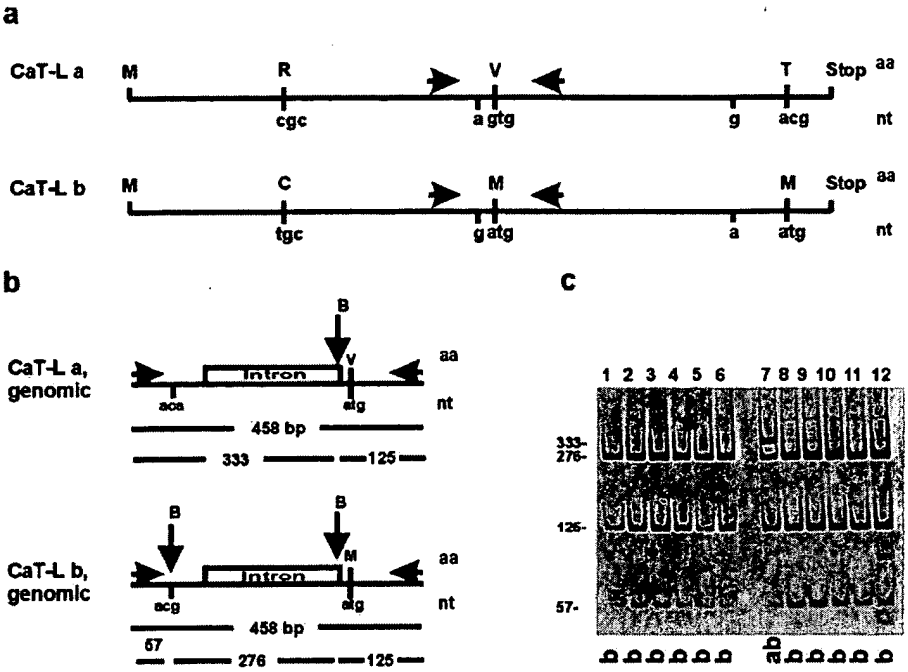

FIG. 3. **Polymorphism of the human CaT-L gene.** *a*, three of the five nucleotide substitutions result in changes of the encoded amino acid (*aa*) residues yielding the CaT-L variants a and b (see "Results"). *b*, PCR amplification of a 458-bp CaT-L fragment from human genomic DNA and expected fragments after cutting with *Bsp*1286I (*b*). *c*, genotyping of 12 human individuals. Both classes of DNA were amplified. Primers are indicated by *arrows*. The nucleotide *a1080g* substitution in the CaT-Lb DNA generates a recognition site for the restriction enzyme *Bsp*1286I. The resulting *Bsp*1286I fragments were separated by polyacrylamide gel electrophoresis. *nt*, nucleotide; *aa*, amino acid; M, methionine; C, cysteine; V, valine; T, threonine, A, arginine.

The non-radioactive *in situ* hybridization method was carried out as described (25) using formalin-fixed slices of 6–8 μm thickness. Briefly, the slices were deparaffinized, rehydrated in graded alcohols, and incubated in the presence of PBS buffer including 10 μg/ml proteinase K (Roche Molecular Biochemicals) for 0.5 h. After prehybridization, the slices were hybridized at 37 °C using the biotinylated deoxyoligonucleotides (0.5 pmol/μl) in the presence of 33% formamide for 12 h. Thereafter, the slices were rinsed several times with 2× SSC and incubated at 25 °C for 0.5 h with avidin/biotinylated tyramide peroxidase complex (ABC, Dako). After several washes with PBS buffer, the slices were incubated in the presence of biotinylated tyramide and peroxide (0.15% w/v) for 10 min, rinsed with PBS buffer, and additionally incubated with ABC for 0.5 h. The slices were then washed with PBS buffer and incubated in the presence of DAB solution (diaminobenzidine (50 μg/ml), 50 mM Tris/EDTA buffer, pH 8.4, 0.15% H_2O_2 in *N,N*-dimethylformamide, Merck). The reaction was stopped after 4 min by incubating the slides in water. Biotinylated tyramide was obtained by incubating NHS-LC biotin (sulfosuccinimidyl-6-[biotinimid]-hexanoate, 2.5 mg/ml, Pierce) and tyramine-HCl (0.75 mg/ml, Sigma) in 25 mM borate buffer (pH 8.5) for 12 h. The tyramide solution was diluted 1000-fold (v/v) in PBS buffer before use.

Tissue Selection—Normal human tissue included placenta (n = 2), prostate tissue (n = 2), colon (n = 2), stomach (n = 2), lung (n = 2), kidney (n = 2), endometrium (n = 2), salivary glands (n = 2), pancreas (n = 2), and parathyroid glands (n = 2). Transurethral resections with benign prostatic hyperplasia were obtained from three patients without clinical and pathological evidence of malignancy. Prostate cancer tissue from five radical prostatectomy specimens was submitted for study. The pathological stages and grades included pT3b (n = 2), pT3a (n = 2), pT2b (n = 1), and primary Gleason grades 5 (n = 2), 4 (n = 2), and 3 (n = 2). Four foci of high grade prostatic intraepithelial neoplasia were identified in the radical prostatectomy specimens. Lymph node metastases were obtained from five staging lymphadenectomies without subsequent prostatectomy. The material further contained palliative transurethral resection specimens from five patients with recurrent androgen-insensitive adenocarcinomas after orchiectomy. All specimens were available as formalin-fixed paraffin-embedded tissue sections.

Miscellaneous Methods—Sequences were analyzed using the Heidelberg Unix Sequence Analysis Resources of the biocomputing unit at the German Cancer Research Center, Heidelberg. The phylogenetic distances of proteins were calculated with the Clustal/Clustree program (26, 27), and the similarity of protein sequences in pairs was calculated with the ClustalW algorithm (28). Photographs were scanned and processed using Corel Photo-Paint/Corel Draw and Adobe PhotoShop.

RESULTS

Primary Structure of Human CaT-L—In search of proteins distantly related to the Trp family of ion channels, a human expressed sequence tag (EST 1404042) was identified in the GenBank™ data base using BLAST programs (29). This EST was used as a probe to screen oligo(dT) and additional specifically primed human placenta cDNA libraries. Several positive cDNA clones were isolated, sequenced, and found to contain the complete sequence of the EST 1404042 clone as well as additional 5′-sequences. These clones cover an mRNA of about 2.9 kb with an open reading frame of 2175 bases (Fig. 1*a*) encoding a protein of 725 amino acid residues that we tentatively called human Ca^{2+} transport protein-like (CaT-L). Downstream of the CaT-L coding sequence an additional open reading frame has been postulated (GenBank™ accession number X83877)[2] to represent a zinc finger type DNA-binding protein. The functional significance of this putative gene product is not known.

Hydropathy analysis reveals a hydrophobic core in the CaT-L protein with six peaks likely to represent membrane-spanning helices (S1 to S6) and a putative pore region between S5 and S6 (Fig. 1*b*). The hydrophobic core is flanked by long presumptive cytoplasmic domains at the N and C termini (Fig. 1*c*). A similar topology has been proposed for the light-activated ion channels in the *Drosophila* compound eye, Trp and TrpL, and related nematode and mammalian gene products (21, 30). The N-terminal region of the CaT-L protein (Fig. 1*c*) contains six amino acid sequence motives (amino acid residues 45–69, 79–102, 116–140, 162–186, 195–219, and 239–263) related to the consensus sequence of ankyrin-like repeats (31).

As shown in Fig. 1, *a* and *d*, amino acid sequence comparison places human CaT-L in close relationship to the rat intestine Ca^{2+} transport protein (CaT1 (10)) and the human renal epithelial Ca^{2+} channel (ECaC (9, 32)), sharing 90 (rat CaT1) and 77% (human ECaC) overall amino acid sequence identity. More distantly related members of this gene family include non-selective cation channels such as the rat vanilloid receptors Vr1 and VRL that share common amino acid sequence motives (21), although overall sequence identity is low (Vr1, 28%; VRL, 27%).

[2] N. Tomilin and V., Boyko, unpublished results.

Expression of CaT-L Transcripts in Human Tissues—To investigate CaT-L expression, Northern analysis was performed using poly(A)$^+$ RNA from different human tissues and a 345-bp *Eco*RI/*Bam*HI fragment of CaT-L cDNA as a probe (Fig. 2*a*). We found that CaT-L transcripts of 3.0 kb are expressed in placenta, pancreas, and prostate. The size of these transcripts corresponds to the size of the cloned CaT-L cDNA (2902 bp). In addition, a shorter transcript of 1.8 kb is detectable in poly(A)$^+$ RNA isolated from human testis, which may result from alternative mRNA processing in this tissue. No CaT-L transcripts were detected in heart, lung, liver, skeletal muscle, spleen, ovary, and leukocytes. Interestingly, no CaT-L transcripts could be detected in small intestine, where both CaT1 and ECaC transcripts have been detected, nor in colon and brain (CaT1) or in kidney (ECaC) where these transcripts are predominantly expressed. The lack of CaT-L expression in human kidney and intestine suggests that CaT-L does not serve the physiological functions in these tissues that have been associated with the ECaC and CaT1 proteins and that include intestinal and renal Ca^{2+} absorption. Therefore, CaT-L is unlikely to represent the human ortholog of rat CaT1. A human cDNA sequence of 446 bp has been deposited to the GenBank™ data base (accession number AJ277909) that is identical to the corresponding sequence reported here. This sequence has been postulated to represent part of human CaT1, but no data are available that support this suggestion. Interestingly a 115-bp fragment, tentatively called CaT-Like2 (CaT-L2), was amplified from human genomic DNA and sequenced. It encodes an amino acid sequence (Fig. 1*a*) that shares 92% sequence identity with human CaT-L, 95% with human ECaC, and 81% with rat CaT1 sequences and may represent a part of an additional ECaC/CaT1-related channel.

To characterize further the cell-specific expression of CaT-L transcripts, *in situ* hybridization experiments were performed, using various human tissue sections (Fig. 2, *b–i*) obtained from placenta (taken from a 10-week-old abort), pancreas (removed from patients with pancreatic cancer), salivary gland, colon, and kidney. In the placenta (Fig. 2*b*) CaT-L transcripts are expressed in trophoblasts and syncytiotrophoblasts. In the pancreas (Fig. 2*c*) CaT-L transcripts are restricted to acinar cells and are not detectable in ductal epithelial cells and Langerhans islets. No CaT-L expression was found in regions of pancreatic carcinomas (data not shown). In salivary glands, CaT-L expression occurs in subsets of myoepithelial cells (Fig. 2*d*). Corresponding to the results obtained by Northern blot analysis, no CaT-L transcripts could be detected in tissue sections of human colon (Fig. 2*h*) and human kidney (Fig. 2*i*). In addition no transcripts could be detected in stomach, endometrium, lung, and parathyroid gland (data not shown).

Polymorphism and Chromosomal Localization of the Human CaT-L Gene—Comparison of the DNA sequences of the various CaT-L cDNA clones obtained from a human placenta revealed that the sequences could be grouped into two classes, which differ in five nucleotide substitutions (Fig. 3*a*). Three of the five substitutions resulted in changes of the encoded amino acid residues, whereas two nucleotide substitutions were silent (*a1080g* and *g1878a*). The resulting two protein sequences that differ in three amino acid residues (R157C, V378M, and T681M) were called CaT-La and CaT-Lb (Figs. 1*a* and 3*a*). This finding was reproduced by isolating CaT-L a and b cDNA clones from a second placenta. In addition, PCR amplification of the full-length CaT-L cDNA from a third placenta yielded only the b variant when eight amplified full-length CaT-L cDNAs were subcloned and sequenced.

The nucleotide substitutions may reflect a coupled polymorphism; alternatively, the underlying mRNAs of the two cDNA classes may be products of different gene loci or may arise by RNA editing. To distinguish between these possibilities, we first designed a primer pair common to both CaT-L a and b isoforms that flanked the silent substitution *a1080g* and the substitution that leads to the amino acid exchange V378M. We then PCR-amplified a DNA fragment of 458 bp from genomic DNA isolated from human T-lymphocytes. Both classes of DNAs were amplified, and both amplification products contained a common intron sequence of 303 bp (Fig. 3*b*). The *a1080g* substitution in the CaT-Lb DNA generates a new rec-

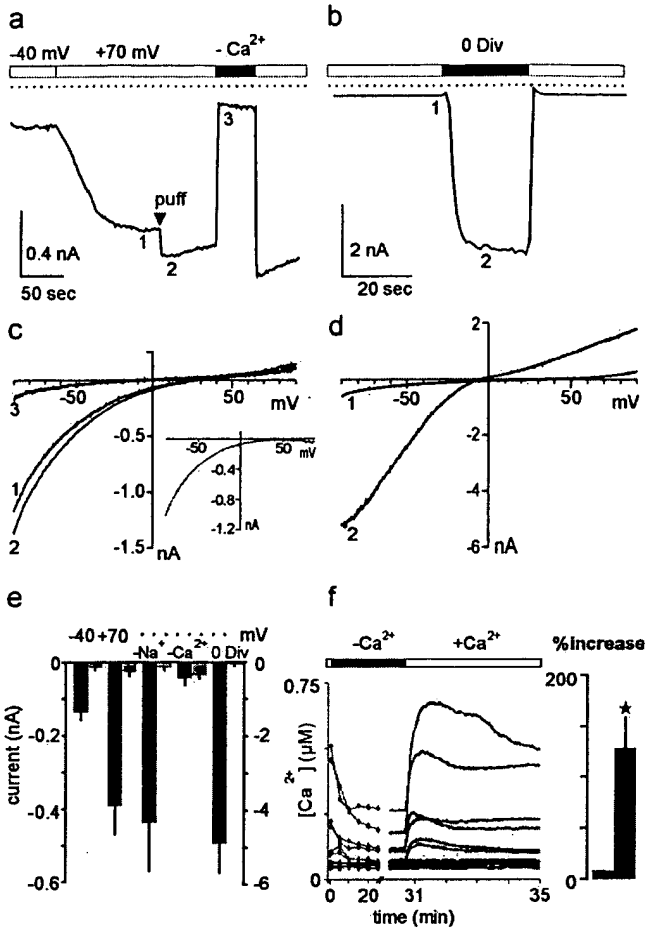

FIG. 4. **The CaT-L protein is a Ca^{2+}-selective ion channel.** *a*, representative current trace obtained from a CaT-L-transfected HEK cell (see "Materials and Methods"). CaT-L-mediated currents are visualized by applying voltage ramps (−100 to +100 mV) from holding potentials of either −40 or +70 mV. Current values measured at −80 mV of the ramp are plotted over time. CaT-L-induced currents increase when the holding potential is switched to positive values. As indicated by the *overlying bar*, the solution was changed from the normal bath solution (2 mM $[Ca^{2+}]_o$) to a solution containing no added Ca^{2+} (*a*) or to an EGTA-buffered solution containing zero divalent cations (*b*). The *numbers* indicate time points from which individual traces shown in *c* and *d* were taken. *c* and *d*, current-voltage relationships, showing the effect of solution switch alone (*c, traces 1* and *2*) and after removal of extracellular Ca^{2+} (*c, trace 3*) with the leak subtracted current (2–3) shown in the *inset*. *d*, current-voltage relationship showing CaT-L currents before (*trace 1*) and after the removal of external divalent cations (*trace 2*). *e*, summary of the currents at −80 mV ramp potential. *Dark*, CaT-L-transfected cells; *red*, control cells. *Columns* from *left* to *right*, CaT-L currents at −40 mV (n = 12) and +70 mV holding potential (n = 12). CaT-L currents in standard bath solution including 110 mM *N*-methyl-D-glucamine without Na^+ (− Na^+, n = 7) and with nominal zero Ca^{2+} ions (− Ca^{2+}, n = 8) or in the presence of 1 mM EGTA with zero divalent cations present (*0 div*, n = 6). *f*, representative changes in $[Ca^{2+}]_i$ in CaT-Lb-transfected HEK cells (*red*) and controls (*black*) in the presence or absence of 1 mM $[Ca^{2+}]_o$. *Inset* to the *right*, relative increase of cytosolic $[Ca^{2+}]_o$ of CaT-L-transfected and control HEK cells after readdition of 1 mM $[Ca^{2+}]_o$.

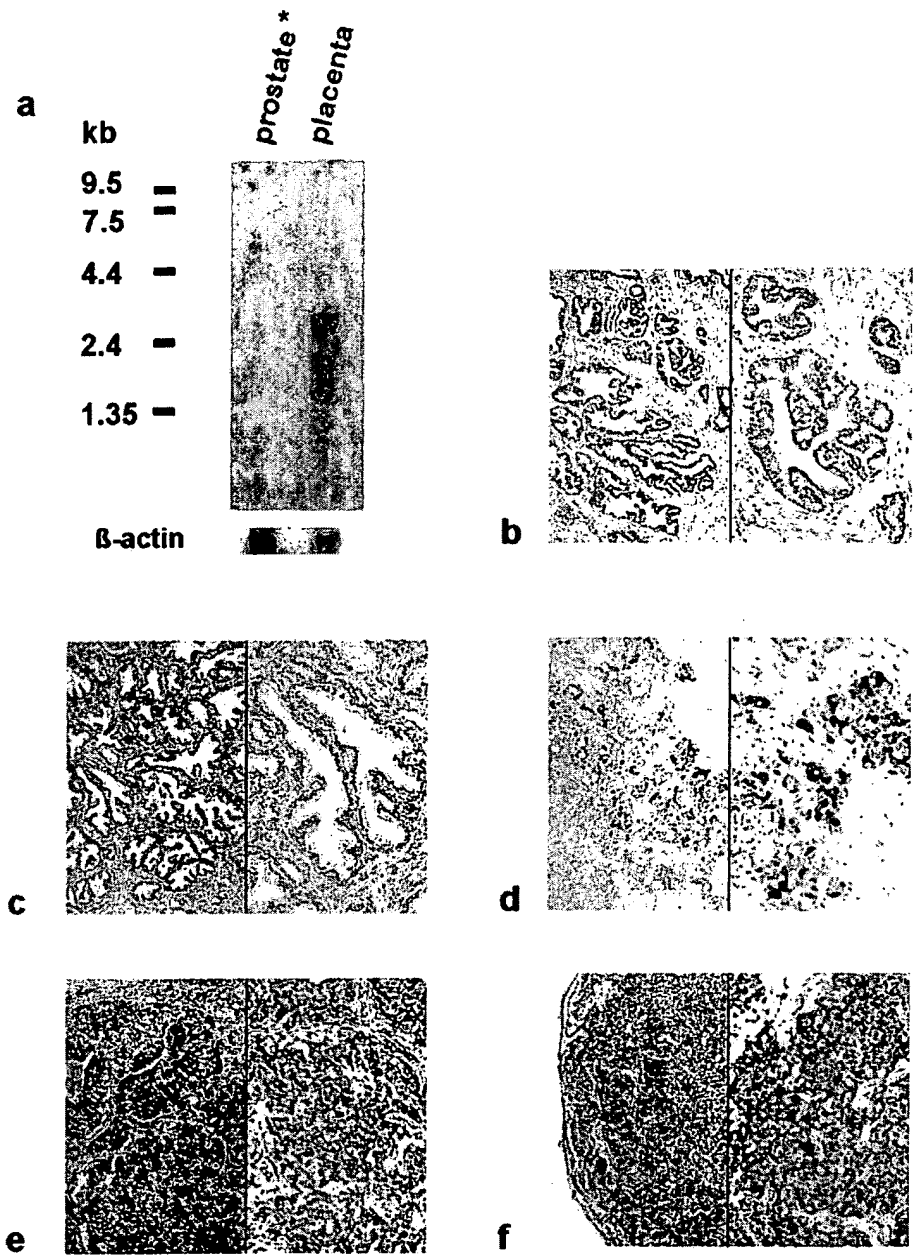

FIG. 5. **CaT-L is expressed in malignant lesions of the prostate but not in benign prostate tissues.** *a*, autoradiogram of blot hybridization analysis using poly(A)$^+$ RNA isolated from human placenta and prostate tissue obtained from 20 patients with benign prostate hyperplasia and without clinical and pathological evidence of malignancy (*, *upper panel*). CaT-L transcripts are present in placenta but, in contrast to Fig. 2*a*, are absent in prostate (*lower panel*, signals after hybridization of human β-actin cDNA as control to the same filters). The absence of CaT-L mRNA expression in normal adult prostate tissue (*b*) and benign prostatic hyperplasia (*c*) was confirmed by *in situ* hybridization analyses. Original magnifications are as follows: × 25 (*left*) and × 100 (*right*). Primary prostatic adenocarcinoma (Gleason score: 3 + 4 = 7) with extraprostatic extension (pT3a) reveals high steady state levels of CaT-L mRNA in subsets of tumor cells (*d*). Extensive CaT-L mRNA expression is detected in lymph node metastasis (*e*) and hormone refractory, recurrent lesions (*f*). Original magnifications are as follows: × 25 (*left*) and × 100 (*right*).

ognition site for the restriction enzyme *Bsp*1286I (Fig. 3*b*). Accordingly, genomic DNA isolated from blood cells of 12 healthy male human individuals was used as template to amplify the 458-bp DNA fragment, and the amplified DNAs were then incubated in the presence of *Bsp*1286I. In 11 out of 12 individuals the expected DNA fragments of the CaT-Lb variant could be identified, whereas one individual contained both a and b variants (Fig. 3*c*). In summary, these findings suggest that the two CaT-L variants may be due to a coupled polymorphism of one gene locus. By using a monochromosomal hybrid mapping panel, this locus was assigned to human chromosome 7 (data not shown).

CaT-L Is a Ca^{2+}-selective Cation Channel—To characterize the electrophysiological properties of CaT-L, CaT-L and GFP were co-expressed in HEK cells using the dicistronic expression vector pdiCaT-L. Whereas only small background currents were observed under control conditions (GFP alone), large inwardly rectifying currents could be recorded in CaT-L-transfected HEK cells after establishing the whole-cell configuration (Fig. 4, *a–e*), indicating that CaT-L forms constitutively active ion channels. Switching the holding potential from the initial −40 to +70 mV, currents increased dramatically in size (Fig. 4, *a* and *e*). This increase in current size with a change in holding potential was not observed for sodium currents (at zero extracellular divalent ions) and indicates that CaT-L may be partially inactivated by intracellular Ca^{2+}. For the following experiments voltage ramps were applied from a holding potential of +70 mV. Although the initial characterization of CaT-L currents was reminiscent of currents mediated by ECaC (33–35), the sequence differences led us to a more detailed investigation of CaT-L selectivity. CaT-L-specific currents were completely abolished following removal of external Ca^{2+} (Fig. 4, *a* and *c*) but slightly increased when external Na^+ was removed (summarized in Fig. 4*e*). The ion exchange experiments and the inwardly rectifying current-voltage relationship with the rather positive reversal potential (E_{rev}) provide strong evidence that CaT-L forms Ca^{2+}-selective ion channels (Fig. 4, *a*, *c*, and *e*). The Ca^{2+} selectivity, as defined by the E_{rev}, becomes even more evident (Fig. 4*c*, *inset*) if the background current is subtracted (background current defined as the remaining current

in the absence of Ca^{2+}). The slight but consistent increase of current size in the absence of Na^+ (Fig. 4*e*) is largely due to a local perfusion effect as perfusion of unaltered bath solution (*puff* in Fig. 4*a*) revealed a similar increase in current size and could indicate an activation mechanism partially mediated by shape changes.

A feature of non-voltage-operated Ca^{2+}-selective ion channels is their ability to conduct Na^+ only if all external divalent cations, namely Ca^{2+} and Mg^{2+}, are removed from the extracellular solution (34–36). To test whether CaT-L channels conform with this phenomenon, normal bath solution was switched to a solution containing no divalent cations with 1 mM EGTA added. As can be seen in Fig. 4, *b, d,* and *e*, CaT-L channels can now conduct very large Na^+ currents. Interestingly, immediately after the solution change, the current size first becomes smaller (Fig. 4*b*) before increasing rapidly, indicating that the pore may initially still be blocked by Ca^{2+} suggesting an anomalous mole fraction behavior. Inactivation of CaT-L currents is mediated in part by binding of Ca^{2+}/Calmodulin (37). Interestingly, this inactivation can be counteracted by phosphorylation of the calmodulin-binding site of CaT-L by protein kinase C (37).

The high Ca^{2+} selectivity of CaT-L channels together with its spontaneous activity leads to the assumption that the resting $[Ca^{2+}]_i$ of CaT-L-transfected cells should be rather high and strongly dependent on the extracellular Ca^{2+} concentration ($[Ca^{2+}]_o$). This prediction was tested in fura-2-loaded CaT-L-transfected HEK cells. In the presence of 1 mM $[Ca^{2+}]_o$, $[Ca^{2+}]_i$ in CaT-L-expressing cells was typically above 200 nM (Fig. 4*f*), whereas in non-transfected control cells or in cells expressing GFP alone, $[Ca^{2+}]_i$ was less than 100 nM. Following removal of extracellular Ca^{2+}, the $[Ca^{2+}]_i$ of CaT-L-expressing cells decreased, whereas readdition of 1 mM Ca^{2+} to the bath led to a significant rise of $[Ca^{2+}]_i$ in CaT-L-transfected cells but not in control cells. Thus, the measurements of $[Ca^{2+}]_i$ are in very good agreement with the electrophysiological recordings, making CaT-L an excellent candidate as a selective Ca^{2+} uptake channel in tissue where it is usually expressed.

Differential Expression of CaT-L Transcripts in Benign and Malignant Prostate Tissue—CaT-L transcripts are abundantly expressed in human prostate as shown by Northern blot analysis using a commercially available human multitissue RNA blot (Fig. 2*a*). To characterize further CaT-L expression, we prepared poly(A)$^+$ RNA from prostate tissues obtained from patients with histologically proven benign prostate hyperplasia. Northern blot analysis with poly(A)$^+$ RNA extracted from benign prostate tissue and human placenta showed CaT-L expression in the latter but failed to demonstrate any CaT-L mRNA in benign prostate tissue (Fig. 5*a*). This observation was confirmed by *in situ* hybridization analysis performed in tissue sections. We were unable to demonstrate detectable levels of CaT-L mRNA in normal prostate tissue (Fig. 5*b*) and benign prostatic hyperplasia (Fig. 5*c*), and the high grade prostatic intraepithelial lesions were investigated. Conversely, high steady state levels of CaT-L mRNA were detectable in primary prostatic adenocarcinoma (Fig. 5*d*). Thus, we can conclude that the commercially available RNA blot contains mRNA from prostate cancer patients, although this has not been specified by the manufacturer. In primary prostate adenocarcinoma the most significant levels of CaT-L mRNA were detected in high grade (primary Gleason grades 4 and 5) tumors with extraprostatic extension (pT3a/b) ranging from 10 to 30% of positive tumor cells (Fig. 5, *c, e,* and *g*). Conversely, in the organ-confined primary Gleason grade 3 tumor, no levels of CaT-L mRNA were detectable. All lymph node metastases (Fig. 5*e*, $n = 5$) and recurrent lesions (Fig. 5*f*, $n = 5$) examined revealed CaT-L expression in 10–60% of tumor cells and 10–55% of positive tumor cells, respectively. This indicates that the presence of CaT-L in human prostate cancer is rather a late event in tumor progression.

DISCUSSION

The present study has identified CaT-L as a novel Ca^{2+}-selective cation channel that is highly expressed in the human placenta, pancreatic acinar cells, salivary glands (Fig. 2), and in malignant prostatic lesions but not in healthy and benign prostate tissues (Fig. 5). Human CaT-like shares 75 and 77% amino acid sequence identity with rabbit and human ECaC, respectively, and the cation permeation properties of the recombinant CaT-L channel resemble those of ECaC (33–35). CaT-L is unlikely to represent the human version of CaT1 as its expression is undetectable in the small intestine and colon, tissues where CaT1 is abundantly expressed. If, however, CaT-L is the human version of rat CaT1, a second gene product appears to be required for Ca^{2+} uptake in human small intestine and colon attributed to CaT1 in rat small intestine and colon. Most interesting, the CaT-L gene, like the human ECaC gene, is localized on human chromosome 7.

In the trophoblasts and syncytiotrophoblasts of the human placenta, CaT-L channels might be involved in transcellular Ca^{2+} transport (38), supplying the fetal circulation with Ca^{2+} from the maternal blood. This transcellular Ca^{2+} transport includes Ca^{2+} influx from maternal plasma across the microvillus plasma membrane into the trophoblasts, Ca^{2+} translocation across the cytosol of the trophoblast cell, and Ca^{2+} efflux from cytosol across the fetal-facing membrane of the trophoblast and entry into the fetal circulation. The Ca^{2+} efflux might be due to the activity of a high affinity Ca^{2+} ATPase identified in the fetal-facing plasma membrane of trophoblasts (39). Ca^{2+} uptake could be accomplished by CaT-L in a similar way as it has been suggested for ECaC in the kidney (9) and CaT1 in the intestine (10).

In pancreatic acinar cells, the activation of exocytotic secretion of digestive enzymes primarily depends on release of Ca^{2+} from stores in the endoplasmic reticulum (40). Exocytosis can be triggered by hormones and neurotransmitters via intracellular messengers such as inositol 1,4,5-trisphosphate, cyclic adenosine 5′-diphosphate-ribose, and NAADP (41). When the cytosolic Ca^{2+} concentration rises, the plasma membrane Ca^{2+}-ATPase pump is invariably activated to extrude Ca^{2+}, and in the absence of compensatory Ca^{2+} entry from the extracellular space, cells would inevitably run out of stored Ca^{2+}. The molecular structures of the channels responsible for Ca^{2+} entry are not known, but Ca^{2+}-selective and non-selective cation influx pathways have been described (42, 43). It will be interesting to study the contribution of CaT-L to these pathways and its role in Ca^{2+} secretion coupling in pancreatic acinar cells.

The most striking feature of CaT-L expression is its complete absence in healthy and benign prostate tissue but its presence at high steady state levels in malignant prostatic lesions (Fig. 5). Prostate cancer is the most commonly diagnosed malignancy in men and is the second leading cause of cancer-related death in Western countries (44). When organ-confined at the time of diagnosis, prostate cancer can be cured by radical prostatectomy. Unfortunately, more than 50% of cancers that are considered clinically confined prior to surgery show extracapsular extension upon pathological analysis and thus represent a high risk of progression (45). In fact, locally advanced cancer is still a fatal disease for which presently no curative treatment is available. There is a great need for new molecular markers predicting tumor progression and the clinical outcome. The observation that CaT-L is undetectable in most of

normal human tissue including the prostate, but present at high levels in locally advanced, metastatic, and recurrent prostatic lesions suggests that CaT-L is a promising marker for the molecular staging and detection of prostate cancer. Interestingly, up-regulation of CaT-L expression has not yet observed in other malignancies such as pancreatic carcinoma (data not shown), arguing against CaT-L being a general marker of cell proliferation. The high levels of CaT-L expression in subsets of tumor cells in advanced stages of the disease suggests a specific function of these cells. It will be of interest to determine the regulating impact of these cells and of the polymorphic variants of the CaT-L protein on the process of tumor progression and hormone therapy failure. Furthermore, the function of CaT-L as Ca^{2+}-selective ion channels may offer novel therapeutic strategies interfering with the uptake of Ca^{2+} and its not yet established downstream events in prostatic cancer cells.

Acknowledgments—We thank Dr. Stephan Philipp for providing the pdi vector; Karin Wolske, Isabell Hunsicker, and Martin Simon Thomas for excellent technical assistance; Drs. U. Zwergel and M. Ziegler for providing us with the tissue samples; and Dr. Markus Hoth for helpful discussion.

REFERENCES

1. Weinreich, F., and Jentsch, T. J. (2000) *Curr. Opin. Neurobiol.* **10,** 409–415
2. Ashcroft, F. M. (1999) *Ion Channels and Disease,* p. 352, Academic Press, London
3. Scott, K., and Zuker, C. (1998) *Curr. Opin. Neurobiol.* **8,** 383–388
4. Colbert, H. A., Smith, T. L., and Bargmann, C. I. (1997) *J. Neurosci.* **17,** 8259–8269
5. Walker, R. G., Willingham, A. T., and Zuker, C. S. (2000) *Science* **287,** 2229–2234
6. Caterina, M. J., Schumacher, M. A., Tominaga, M., Rosen, T. A., Levine, J. D., and Julius, D. (1997) *Nature* **389,** 816–824
7. Caterina, M. J., Rosen, T. A., Tominaga, M., Brake, A. J., and Julius, D. (1999) *Nature* **398,** 436–441
8. Putney, J. W. J., and McKay, R. R. (1999) *BioEssays* **21,** 38–46
9. Hoenderop, J. G., van der Kemp, A., Hartog, A., van de Graaf, S., van Os, C., Willems, P. H., and Bindels, R. J. (1999) *J. Biol. Chem.* **274,** 8375–8378
10. Peng, J. B., Chen, X. Z., Berger, U. V., Vassilev, P. M., Tsukaguchi, H., Brown, E. M., and Hediger, M. A. (1999) *J. Biol. Chem.* **274,** 22739–22746
11. Jaquemar, D., Schenker, T., and Trueb, B. (1999) *J. Biol. Chem.* **274,** 7325–7333
12. Duncan, L. M., Deeds, J., Hunter, J., Shao, J., Holmgren, L. M., Woolf, E. A., Tepper, R. I., and Shyjan, A. W. (1998) *Cancer Res.* **58,** 1515–1520
13. Hoenderop, J. G., Hartog, A., Stuiver, M., Doucet, A., Willems, P. H., and Bindels, R. J. (2000) *J. Am. Soc. Nephrol.* **11,** 1171–1178
14. Wissenbach, U., Schroth, G., Philipp, S., and Flockerzi, V. (1998) *FEBS Lett.* **429,** 61–66
15. Prasher, D. C., Eckenrode, V. K., Ward, W. W., Prendergast, F. G., and Cormier, M. J. (1992) *Gene (Amst.)* **111,** 229–233
16. Kozak, M. (1987) *J. Mol. Biol.* **196,** 947–950
17. Niwa, H., Yamamura, K., and Miyazaki, J. (1991) *Gene (Amst.)* **108,** 193–199
18. Kim, D. G., Kang, H. M., Jang, S. K., and Shin, H. S. (1992) *Mol. Cell. Biol.* **12,** 3636–3643
19. Heim, R., Cubitt, A. B., and Tsien, R. Y. (1995) *Nature* **373,** 663–664
20. Philipp, S., Cavalié, A., Freichel, M., Wissenbach, U., Zimmer, S., Trost, C., Marquart, A., Murakami, M., and Flockerzi, V. (1996) *EMBO J.* **15,** 6166–6171
21. Philipp, S., Wissenbach, U., and Flockerzi, V. (2000) in *Calcium Signaling* (Putney, J. W. J., ed) pp. 321–342, CRC Press, Inc., Boca Raton, FL
22. Drwinga, H. L., Toji, L. H., Kim, C. H., Greene, A. E., and Mulivor, R. A. (1993) *Genomics* **16,** 311–314
23. Dubois, B. L., and Naylor, S. L. (1993) *Genomics* **16,** 315–319
24. Garcia, D. E., Cavalié, A., and Lux, H. D. (1994) *J. Neurosci.* **14,** 545–553
25. Bonkhoff, H., Fixemer, T., Hunsicker, I., and Remberger, K. (1999) *Am. J. Pathol.* **155,** 641–647
26. Saitou, N., and Nei, M. (1987) *Mol. Biol. Evol.* **4,** 406–425
27. Thompson, J. D., Higgins, D. G., and Gibson, T. J. (1994) *Nucleic Acids Res.* **22,** 4673–4680
28. Needleman, S. B., and Wunsch, C. D. (1970) *J. Mol. Biol.* **48,** 443–453
29. Altschul, S. F., Gish, W., Miller, W., Myers, E. W., and Lipman, D. J. (1990) *J. Mol. Biol.* **215,** 403–410
30. Harteneck, C., Plant, T. D., and Schultz, G. (2000) *Trends Neurosci.* **4,** 159–166
31. Lux, S. E., John, K. M., and Bennett, V. (1990) *Nature* **344,** 36–42
32. Müller, D., Hoenderop, J. G., Meij, I. C., van den Heuvel, L. P., Knoers, N. V., den Hollander, A. I., Eggert, P., Garcia-Nieto, V., Claverie-Martin, F., and Bindels, R. J. (2000) *Genomics* **67,** 48–53
33. Hoenderop, J. G., van der, K. A., Hartog, A., van, O. C., Willems, P. H., and Bindels, R. J. (1999) *Biochem. Biophys. Res. Commun.* **261,** 488–492
34. Vennekens, R., Hoenderop, J. G., Prenen, J., Stuiver, M., Willems, P. H., Droogmans, G., Nilius, B., and Bindels, R. J. (2000) *J. Biol. Chem.* **275,** 3963–3969
35. Nilius, B., Vennekens, R., Prenen, J., Hoenderop, J. G., Bindels, R. J., and Droogmans, G. (2000) *J. Physiol. (Lond.)* **527,** 239–248
36. Hoth, M., and Penner, R. (1993) *J. Physiol. (Lond.)* **465,** 359–386
37. Niemeyer, B. A., Bergs, C., Wissenbach, U., Flockerzi, V., and Trost, C. (2001) *Proc. Natl. Acad. Sci.* **6,** 3600–3605
38. Care, A. D. (1991) *J. Dev. Physiol.* **15,** 253–257
39. Fisher, G. J., Kelley, L. K., and Smith, C. H. (1987) *Am. J. Physiol.* **252,** C38–C46
40. Kasai, H., and Augustine, G. J. (1990) *Nature* **348,** 735–738
41. Petersen, O. H., Burdakov, D., and Tepikin, A. V. (1999) *Eur. J. Cell Biol.* **78,** 221–223
42. Krause, E., Pfeiffer, F., Schmid, A., and Schulz, I. (1996) *J. Biol. Chem.* **271,** 32523–32528
43. Camello, C., Pariente, J. A., Salido, G. M., and Camello, P. J. (1999) *J. Physiol. (Lond.)* **516,** 399–408
44. Landis, S. H., Murray, T., Bolden, S., and Wingo, P. A. (1999) *CA-Cancer J. Clin.* **49,** 8–31
45. Scardino, P. T., Weaver, R., and Hudson, M. A. (1992) *Hum. Pathol.* **23,** 211–222
46. Kyte, J., and Doolittle, R. F. (1982) *J. Mol. Biol.* **157,** 105–132
47. Suzuki, M., Sato, J., Kutsuwada, K., Ooki, G., and Imai, M. (1999) *J. Biol. Chem.* **274,** 6330–6335
48. Kanzaki, M., Zhang, Y. Q., Mashima, H., Li, L., Shibata, H., and Kojima, I. (1999) *Cell Biol.* **1,** 165–170

Store depletion and store-operated Ca^{2+} current in human prostate cancer LNCaP cells: involvement in apoptosis

Roman Skryma, Pascal Mariot, Xuefen Le Bourhis*, Fabien Van Coppenolle, Yaroslav Shuba, Fabien Vanden Abeele, Guillaume Legrand, Sandrine Humez, Benoni Boilly* and Natalia Prevarskaya

*Laboratoire de Physiologie Cellulaire, INSERM EPI-9938 and *Laboratoire de Biologie du Développement, USTL, Villeneuve d'Ascq, France*

(Received 31 January 2000; accepted after revision 18 May 2000)

1. In the present study, we investigated the mechanisms involved in the induction of apoptosis by the Ca^{2+}-ATPase inhibitor thapsigargin (TG), in androgen-sensitive human prostate cancer LNCaP cells.

2. Exposure of fura-2-loaded LNCaP cells to TG in the presence of extracellular calcium produced an increase in intracellular Ca^{2+}, the first phase of which was associated with depletion of intracellular stores and the second one with consecutive extracellular Ca^{2+} entry through plasma membrane, store-operated Ca^{2+} channels (SOCs).

3. For the first time we have identified and characterized the SOC-mediated membrane current (I_{store}) in prostate cells using whole-cell, cell-attached, and perforated patch-clamp techniques, combined with fura-2 microspectrofluorimetric and Ca^{2+}-imaging measurements.

4. I_{store} in LNCaP cells lacked voltage-dependent gating and displayed an inwardly rectifying current–voltage relationship. The unitary conductance of SOCs with 80 mM Ca^{2+} as a charge carrier was estimated at $3{\cdot}2 \pm 0{\cdot}4$ pS. The channel has a high selectivity for Ca^{2+} over monovalent cations and is inhibited by Ni^{2+} (0·5–3 mM) and La^{3+} (1 μM).

5. Treatment of LNCaP cells with TG (0·1 μM) induced apoptosis as judged from morphological changes. Decreasing extracellular free Ca^{2+} to 200 nM or adding 0·5 mM Ni^{2+} enhanced TG-induced apoptosis.

6. The ability of TG to induce apoptosis was not reduced by loading the cells with intracellular Ca^{2+} chelator (BAPTA-AM).

7. These results indicate that in androgen-sensitive prostate cancer cells the depletion of intracellular Ca^{2+} stores may trigger apoptosis but that there is no requirement for the activation of store-activated Ca^{2+} current and sustained Ca^{2+} entry in induction and development of programmed cell death.

Prostate cancer is the second highest cause of cancer death in men (Woolf *et al.* 1995; Parker *et al.* 1997). Androgen withdrawal therapy is commonly used to delay the progression of the disease (Montironi *et al.* 1994). However, prostate cancer under hormonal ablation therapy will in most cases exhibit androgen-independent characteristics and the tumours will continue to progress. The androgen-insensitive prostate cancer cells are characterized by a very low proliferation rate that renders the typical chemotherapy agents ineffective. For this reason, targeting programmed cell death, or apoptosis, may be particularly relevant for prostate cancer therapy.

It has now been established that Ca^{2+} ions are major players in an intracellular signalling system that translates extracellular stimuli into the regulation and control of cellular events leading to programmed cell death (for a review see McConkey & Orrenius, 1997; see also Dowd, 1995; Berridge *et al.* 1998). Increases in intracellular Ca^{2+} concentration ($[Ca^{2+}]_i$) have been shown to trigger apoptosis (Martikainen *et al.* 1991; Juin *et al.* 1998) and numerous apoptosis inducers increase $[Ca^{2+}]_i$ (McConkey *et al.* 1989; Spielberg *et al.* 1991). However, the precise mechanism(s) by which Ca^{2+} ions trigger apoptosis remain poorly understood. Ca^{2+} stores are intracellular compartments characterized by their high intraluminal Ca^{2+} content and their participation in the regulation of $[Ca^{2+}]_i$ through rapid Ca^{2+} accumulation and release (Gill *et al.* 1996; Berridge, 1997). The depletion of Ca^{2+} stores induces a 'Ca^{2+}-refilling mechanism', a plasma membrane Ca^{2+} entry initially called capacitative Ca^{2+} influx by Putney (1986, 1990) or store-operated Ca^{2+} current (I_{store}).

This mechanism has been demonstrated in a variety of non-excitable cells (for review see Parekh & Penner, 1997). Store-operated Ca^{2+} channels (SOCs) have been shown to be involved in controlling many important physiological and physiopathological functions: secretion, gene transcription, cell cycle, proliferation and also apoptosis (Parekh & Penner, 1995; Fanger *et al.* 1995; Berridge, 1995*a*; McConkey & Orrenius, 1997; Santella, 1998). While the implication of Ca^{2+} ions in the induction of apoptosis is now generally accepted, the data concerning the role of store-operated current in this process are rather contradictory and confusing. Two hypotheses have been proposed. The first assumes that apoptosis may be triggered by endoplasmic reticulum (ER) calcium pool depletion without any requirement for the cytosolic Ca^{2+} elevation due to store-operated Ca^{2+} entry (He *et al.* 1997; Bian *et al.* 1997). Moreover, according to this hypothesis the capacitative Ca^{2+} current may be important for optimal ER pool filling and apoptosis inhibition. The second hypothesis, on the contrary, assumes that a sustained elevation in cytosolic Ca^{2+} to a critical level is the initiator of apoptosis (Dowd *et al.* 1992; Furuya *et al.* 1994; Wang *et al.* 1999).

This last hypothesis is based on experiments where apoptosis was induced by the sarco-endoplasmic reticulum Ca^{2+}-ATPase (SERCA pump) inhibitor thapsigargin (TG) in androgen-insensitive human prostate cancer cells from the TSU-Pr1, DU-145 and PC-3 cell lines (Furuya *et al.* 1994; Wang *et al.* 1999). However, nothing is known about apoptosis-inducing Ca^{2+} signalling in androgen-sensitive prostate cancer cells, where the androgen receptor plays a critical role in regulating growth and differentiation. The study of Ca^{2+}-regulating mechanisms involved in apoptosis in androgen-dependent human prostate cancer cells could be of great importance as it was shown by Gong *et al.* (1995) that, in such cells, intracellular calcium is a potent regulator of androgen receptor gene expression. It has been found in this work that the calcium ionophore A23187 and thapsigargin down-regulate steady-state androgen receptor mRNA levels. On the other hand, androgen depletion is known to induce apoptosis in androgen-sensitive cancer cells and this mechanism involves Ca^{2+} signals (Isaacs *et al.* 1992). The transition of prostate cancer cells from androgen sensitivity to androgen insensitivity may also involve modifications in Ca^{2+} homeostasis and, probably, in the functioning of store-operated channels. Membrane current initiated by these channels, assumed to play an essential role in cancer cell apoptosis, has never been characterized using patch-clamp techniques in both androgen-sensitive and -insensitive prostate cells. In view of the fact that abnormalities in this current may give rise to human disorders, it is important to understand how this current is regulated and how it affects prostate cell behaviour.

In this work we identify the mechanism by which thapsigargin induces apoptosis in androgen-sensitive human prostate cancer LNCaP cells. We characterize for the first time the store-operated Ca^{2+} current in prostate cancer cells, using patch-clamp and fluorimetric (fura-2) single-cell techniques. We also show that the depletion of intracellular Ca^{2+} stores in androgen-sensitive prostate cancer cells may trigger apoptosis without the activation of a store-activated Ca^{2+} current or sustained Ca^{2+} entry. Our results provide new information on the link between Ca^{2+} pools and apoptosis of cancer cells, suggesting evidence for a potentially important signalling pathway involved in the transition from hormone-sensitive to hormone-insensitive prostate cancer.

METHODS

Cell lines

LNCaP cells from the American Type Culture Collection were grown in RPMI 1640 (Biowhittaker, Fontenay sous Bois, France) supplemented with 5 mM L-glutamine (Sigma, L'Isle d'Abeau, France) and 10% fetal bovine serum (Seromed, Poly-Labo, Strasbourg, France). The culture medium also contained 50 000 IU l^{-1} penicillin and 50 mg l^{-1} streptomycin. Cells were routinely grown in 50 ml flasks (Nunc) and kept at 37 °C in a humidified incubator in an air–CO_2 (95%–5%) atmosphere. For electrophysiological experiments, the cells were subcultured in Petri dishes (Nunc) coated with polyornithine (5 mg l^{-1}, Sigma) and used after 4–6 days.

Recording solutions

Bath Ringer solution contained (mM): 140 NaCl, 5 KCl, 2 $CaCl_2$, 2 $MgCl_2$, 0·3 Na_2HPO_4, 0·4 KH_2PO_4, 4 $NaHCO_3$, 5 glucose and 10 Hepes (pH 7·3 ± 0·01 with NaOH). In perforated-patch experiments, the recording pipette was filled with an artificial intracellular saline containing (mM): 55 CsCl, 70 Cs_2SO_4, 7 $MgCl_2$, 1 $CaCl_2$, 5 D-glucose and 10 Hepes (pH 7·2 with CsOH) with nystatin (200 μg ml^{-1}). In whole-cell experiments, the recording pipette was filled with an artificial intracellular saline containing (mM): 140 CsCl, 2 $MgCl_2$, 1 $CaCl_2$, 10 EGTA and 5 Hepes (pH 7·3 ± 0·01 with CsOH); osmolarity 290 mosmol l^{-1}. In cell-attached experiments, the pipette solution contained 80 mM $CaCl_2$ as a charge carrier plus (mM): TEA-Cl 30, glucose 5, Hepes 10 and 4,4′-diisothiocyanostilbene-2,2′-disulphonic acid (DIDS) 0·1 (pH 7·3 with TEA-OH). The presence in the pipette of the K^+ channel blocker TEA and the Cl^- channel blocker DIDS ensured maximal suppression of potentially contaminating K^+ and Cl^- single-channel activities. All experiments were performed at room temperature (20–22 °C).

Electrophysiological recording

The electrodes were pulled on a PIP 5 (HEKA, Germany) puller in two stages from borosilicate glass capillaries (1·5 mm in diameter; BBL, WPI, USA) to a tip diameter of 1·5–2·0 μm. The cultures were viewed under phase contrast with an Axiovert 135 (Zeiss, Germany) inverted microscope. Electrodes were positioned with List-Medical (Germany) micromanipulators. Grounding was achieved through a silver chloride-coated silver wire inserted into an agar bridge.

Perforated-patch recordings were performed with 200 μg ml^{-1} nystatin in the pipette, which was first back-filled with normal Ringer solution to allow reliable seal formation. Series resistance had a steady value of 20–100 MΩ. Perforated-patch and whole-cell recordings were carried out using an Axopatch-200B amplifier (Axon Instruments). Stimulus control, as well as data acquisition and processing were carried out with a PC computer (IBM), fitted with a Digidata 1200 series interface, using pCLAMP 6 software

(Axon Instruments, interface and software). The activity of single, store-dependent, plasma membrane Ca^{2+} channels was recorded in the cell-attached configuration using a HEKA PC-9 amplifier. The currents in response to voltage-clamp pulses were low-pass filtered at 1·5 kHz and digitized at 10 kHz. Under such filtering conditions the root mean square noise, σ, was 0·09 pA. The single-channel data were analysed using PulseFit and Origin 5 software. The techniques have previously been described in detail (Skryma *et al.* 1994; Prevarskaya *et al.* 1995).

Data and statistical analysis

Results were expressed as means ± standard deviation where appropriate. Each experiment was repeated several times. Student's *t* test was used for statistical comparison among means and differences, with $P < 0·05$ considered significant.

Fluorescence measurements of $[Ca^{2+}]_i$ with fura-2

For fura-2 measurements, cells were excited alternately at 340 and 380 nm. Emitted fluorescence was long-pass filtered at 510 nm, captured and analysed by a photomultiplier-based system (Photon Technologies International Ltd, Princeton, NJ, USA). $[Ca^{2+}]_i$ was calculated from the ratio of the emitted fluorescence, excited by 340 and 380 nm light, using the Grynkiewicz, Poenie & Tsien equation (Grynkiewicz *et al.* 1985). For microfluorimetric measurements, cells were grown on glass coverslips for at least 3 days before the experiment, loaded for 30 min with the acetoxymethyl ester derivative of the dye (5 μM fura-2 AM), and subsequently washed three times with a dye-free solution.

Determination of apoptosis

Cells were seeded in 8-chamber culture slides (Lab-Tek) in RPMI medium containing 10% fetal calf serum. After 24 h, cells were treated with Ni^{2+} or thapsigargin for varying periods of time. For morphological analysis, at the end of the treatment, cells were fixed with ice-cold methanol for 10 min and washed twice with phosphate-buffered saline (PBS). Cells were then stained with 5 μg ml^{-1} Hoescht 33258 for 10 min at room temperature and mounted in glycergel (DAKO). Nuclear morphology was displayed on an Olympus BH-2 fluorescence microscope (405–435 nm). The percentage of apoptotic cells was determined by counting at least 500 cells in random fields. Apoptosis was also detected by the TUNEL technique (terminal deoxynucleotide transferase-mediated dUTP–biotin nick-end labelling) using an apoptosis detection kit (Boehringer Mannheim). Following the TUNEL reaction, which detects strand breaks, cells were counterstained with 0·1% Methyl Green for 10 min. The free calcium concentration was assayed in solutions used for apoptosis experiments using the fura-2 fluorescence equipment described above. The fluorescence of culture medium containing no added calcium was measured, as was that of chelated serum with EGTA at various concentrations (0·1 and 1 mM) with 5 μM fura-2 pentapotassium salt. Free calcium concentration was found to be 200 and 20 nM in the presence of 0·1 and 1 mM EGTA, respectively. Using serial dilutions, we assumed that the free calcium contamination in the culture medium containing no added calcium and chelated serum was around 5–10 μM. The free calcium concentration of the Ringer solution used for calcium measurements was 1 μM with no added $CaCl_2$ and no EGTA.

It should be noted that the incubation with the high doses (more than 1 mM) of Ni^{2+} was toxic for LNCaP cells (the percentage of cells incorporating Trypan Blue was enhanced by 20 ± 5% after incubation with 1 mM Ni^{2+} for 24 h). As 0·5 mM Ni^{2+} inhibited I_{store} but was not toxic in long-term experiments this concentration was selected as a standard dose for all studies of apoptosis.

Chemicals

All chemicals were bought from Sigma except for fura-2 AM, fura-2 pentapotassium salt, SK&F 96365 and thapsigargin, which were purchased from Calbiochem.

RESULTS

SERCA pump inhibitors induce a biphasic Ca^{2+} rise in LNCaP cells

The $[Ca^{2+}]_i$ resting level of LNCaP cells in a solution containing 2 mM $CaCl_2$ was about 81 ± 7 nM ($n = 103$) and remained stable during the recording for up to 60 min.

A common means of discharging the Ca^{2+} stores is to inhibit SERCA pump activity (Premack *et al.* 1994; Parekh & Penner, 1996). Potent, selective Ca^{2+} pump inhibitors such as thapsigargin (Thastrup *et al.* 1990) or cyclopiazonic acid (CPA; Mason *et al.* 1991) deplete intracellular Ca^{2+} pools and concomitantly promote a sustained capacitative Ca^{2+} entry (Huang & Putney, 1998). This makes Ca^{2+} pump inhibitors useful tools for studying controlled intracellular calcium changes and their consequences in cell physiology.

Exposure of fura-2-loaded LNCaP cells to 0·1 μM thapsigargin in the presence of 2 mM extracellular calcium produced a large initial increase in intracellular Ca^{2+} as a

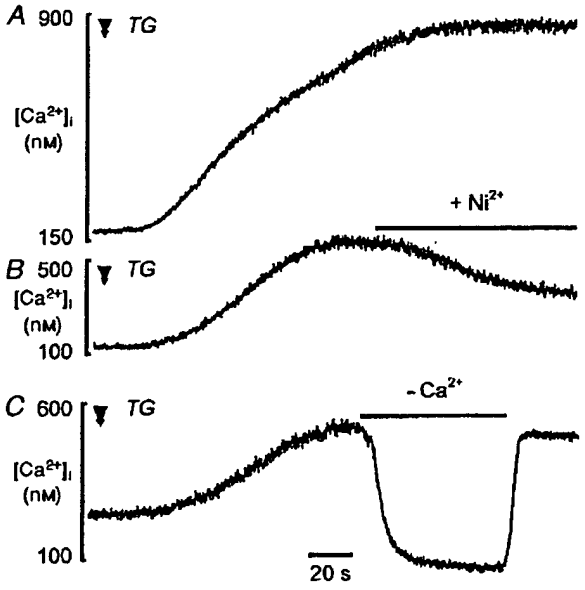

Figure 1. Stimulation of Ca^{2+} influx by thapsigargin in LNCaP cells

A, thapsigargin (0·1 μM) induces an increase in Ca^{2+} in LNCaP cells and stimulates Ca^{2+} release with consecutive Ca^{2+} entry. *B*, the action of thapsigargin (0·1 μM) in Ca^{2+}-containing medium in the presence of Ni^{2+} (3 mM). *C*, dependence of thapsigargin-induced Ca^{2+} influx on extracellular Ca^{2+}. Removing Ca^{2+} from the external medium (measured free Ca^{2+} in these conditions was 1 μM) blocks thapsigargin-stimulated Ca^{2+} entry. Thapsigargin (0·1 μM) was added at the time indicated by arrows. Testing solutions were applied from a puffing pipette during the periods indicated by bars.

result of the depletion of intracellular stores (Fig. 1*A*). This was followed by a sustained plateau, corresponding to a Ca^{2+} influx. This depletion-activated Ca^{2+} entry was confirmed by the fact that 3 mM Ni^{2+} (Fig. 1*B*) and 1 μM La^{3+} (data not shown) blocked the sustained Ca^{2+} rise. Decreasing extracellular free Ca^{2+} concentration to 1 μM by removing $CaCl_2$ from the bath also suppressed Ca^{2+} entry while reintroducing extracellular Ca^{2+} restored Ca^{2+} (Fig. 1*C*).

To ensure that the effects of thapsigargin resulted from its action on intracellular Ca^{2+}-ATPase, we also examined the effects of CPA, a structurally unrelated agent that similarly inhibits the SERCA pump. CPA (10 μM) produced similar effects on $[Ca^{2+}]_i$ to those of thapsigargin, also inducing an initial Ca^{2+} mobilization followed by Ca^{2+} entry (not shown, $n = 11$).

Depletion of intracellular Ca^{2+} stores activates a Ca^{2+} current through store-operated channels

We used the perforated-patch recording technique combined with $[Ca^{2+}]_i$ measurement to compare the kinetics of the $[Ca^{2+}]_i$ increase induced by TG, and the development of the I_{store} Ca^{2+} current. As illustrated in Fig. 2, within 15 ± 6 s, TG stimulated an initial $[Ca^{2+}]_i$ increase due to the mobilization of Ca^{2+} from intracellular stores. An inward current appeared within 25 ± 5 s after TG application ($n = 11$). Decreasing extracellular free Ca^{2+} concentration to 1 μM by removing $CaCl_2$ from the bath inhibited the second phase of the $[Ca^{2+}]_i$ increase induced by TG and the corresponding inward current (Fig. 2*A*, $n = 7$). When Ca^{2+} was added again the sustained plateau was restored and the Ca^{2+} current was induced. I_{store} was also blocked by Ni^{2+} in the range of 0·5–3 mM. However, the rate of blockade was concentration dependent; 3 mM Ni^{2+} completely inhibited the current within 1–2 min whereas 10–15 min were required to completely inhibit the current with 0·5 mM Ni^{2+}. Figure 2*B* demonstrates the effect of TG on $[Ca^{2+}]_i$ and I_{store} in cells incubated in 0·5 mM Ni^{2+} during 15 min where only Ca^{2+} mobilization from intracellular stores was observed without any stimulation of store-operated current. Moreover, when Ni^{2+} was present in the extracellular solution, TG only induced an initial Ca^{2+} rise due to Ca^{2+} mobilization, but I_{store} was not stimulated ($n = 9$, Fig. 2*B*). Likewise, TG induced a monophasic increase in $[Ca^{2+}]_i$ under conditions when extracellular Ca^{2+} was removed from the bath solution (not shown, $n = 7$).

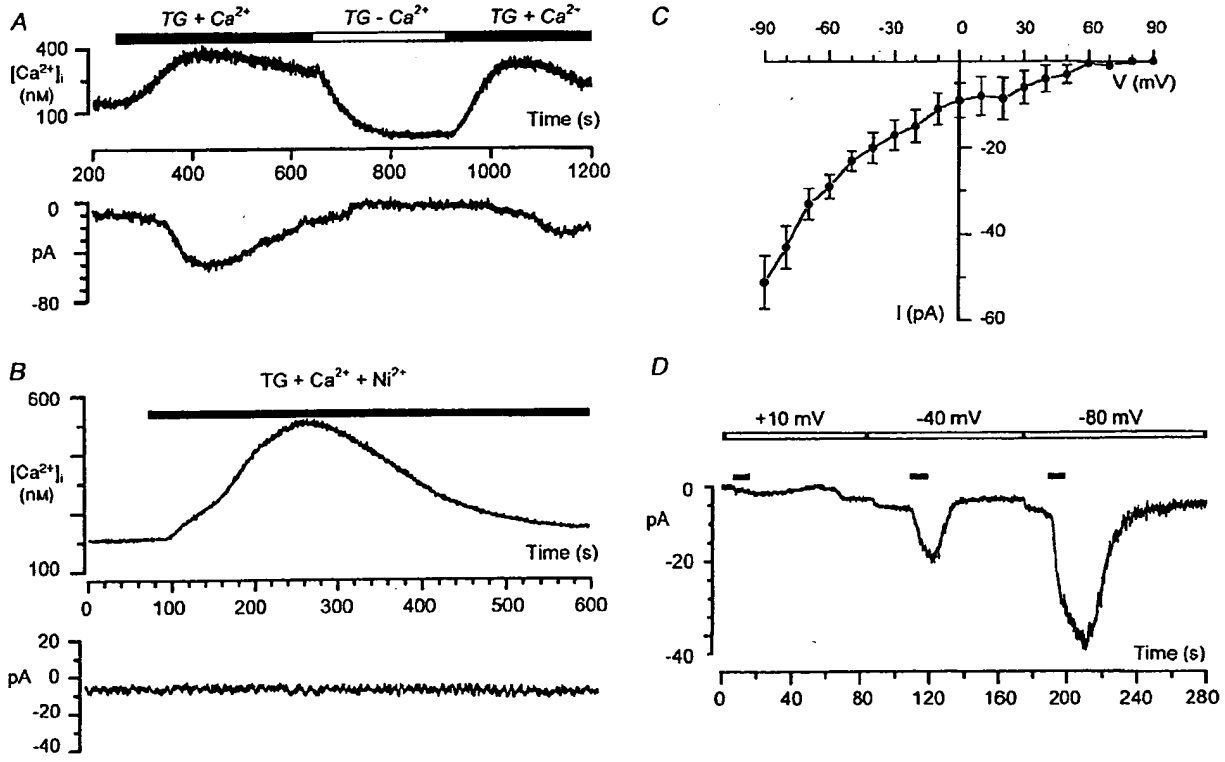

Figure 2. Patch-clamp recordings of store-operated Ca^{2+} current in LNCaP cells

A and *B*, combined perforated-patch and microspectrofluorimetric single-cell recordings of the thapsigargin-activated store-operated Ca^{2+} current at a holding potential of −80 mV. *A*, reversible blockade of Ca^{2+} current by removing Ca^{2+} from external medium (measured free Ca^{2+}, 1 μM). *B*, thapsigargin induces Ca^{2+} mobilization but does not induce store-operated Ca^{2+} current in the presence of 0·5 mM Ni^{2+}. *C*, current–voltage relationship of the store-operated Ca^{2+} current (current is inwardly rectifying and not activated by depolarization). *D*, whole-cell patch-clamp recordings of store-operated Ca^{2+} current at different holding membrane potentials. The horizontal filled bars indicate the episodes of 22 mM $CaCl_2$ application.

We used the whole-cell patch-clamp technique to study the voltage dependence of I_{store} in LNCaP cells. Ca^{2+} stores were emptied by incubating cells with 0·1 μM TG for 15 min in the low free Ca^{2+} (1 μM) bath solution while dialysing the interior of the cell with a strongly buffered Ca^{2+} solution (see Methods). I_{store} was elicited by adding 22 mM $CaCl_2$ to the bath at different holding membrane potentials. An example of such an experiment and its current–voltage (I–V) relationship are shown in Fig. 2*C* and *D*. The store-operated calcium channels in LNCaP cells were non-conducting at very depolarized potentials. In contrast, the current amplitude increased following membrane hyperpolarization and the I–V relationship displayed an inward rectification (Fig. 2*C*).

Changing external Na^+ (replaced by choline) had no significant effect on I_{store} in both whole-cell ($n = 5$) and perforated-patch experiments ($n = 3$). In all cells studied ($n = 7$, perforated-patch combined with fura-2 experiments) I_{store} was also insensitive to one of the suggested capacitative Ca^{2+} current inhibitors, SK&F 96365 (100 μM).

The activity of single store-operated Ca^{2+} channels

The cell-attached patch-clamp configuration was used to study the unitary SOC activity in LNCaP cells. In the presence of 0·1 μM TG in the Ca^{2+}-free bath solution and 80 mM $CaCl_2$ in the pipette, under conditions that ensured inhibition of all membrane currents except those of Ca^{2+}, we recorded a unitary activity in an inward direction that had a resolvable amplitude only at potentials more negative than the resting potential of the cell. In order to examine this type of activity at a broad range of membrane potentials and at the same time measure its I–V relationship, we employed a complex pulse protocol consisting of two steady levels of hyper- and depolarizing potentials connected to each other with a voltage ramp (V_r). The pulse protocol together with the single-channel traces are shown in Fig. 3*A*. In order to construct the I–V relationship, we thoroughly inspected each trace and used the cursor procedure to select those portions of the traces in response to voltage ramps that contained openings of only one channel (overlapping openings and closed states were discarded). Single-channel amplitudes corresponding to each ramp voltage were averaged, then the resulting curve was smoothed and placed in the I–V coordinates (Fig. 3*B*). The resultant I–V plot showed strong rectification in the inward direction. The currents at potentials close to and more positive than the resting potential were beyond the resolution limit, therefore the slope conductance was determined by the linear fit of the I–V plot at potentials of −40 to −120 mV (relative to V_r) where unitary amplitudes could be adequately resolved. This linear fit produced a slope conductance value of 3·2 ± 0·4 pS ($n = 5$).

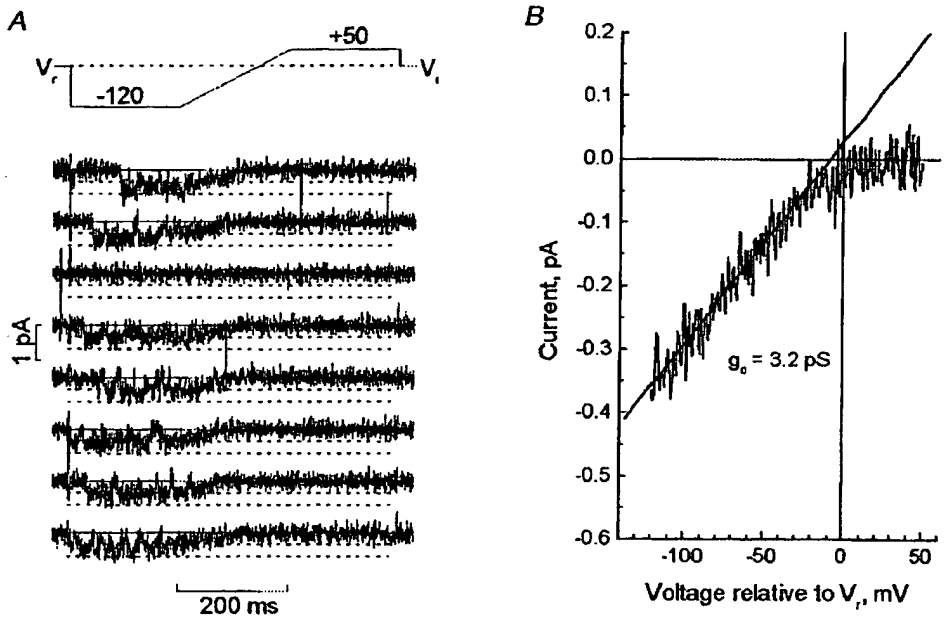

Figure 3. The activity of single store-dependent Ca^{2+} channels

A, single-channel recordings obtained in response to the consecutive application of voltage-clamp pulses (shown in the upper panel, 10 s interpulse interval) to the cell-attached patch in TG-treated LNCaP cells; superimposed continuous lines indicate zero current levels; downward deflection corresponds to the inward current. The recordings presented probably reflect the activity of two store-dependent Ca^{2+} channels. Dotted lines indicate two levels of single-channel amplitudes of −0·35 and −0·7 pA. *B*, the I–V relationship of the single store-dependent Ca^{2+} channel; the I–V plot was constructed from the ramp portions of single-channel recordings by selecting the parts corresponding to the opening of one channel (overlapping openings and closed states were discarded) with subsequent averaging and digital smoothing of the resulting curve to reduce noise; superimposed linear fit provides the value of the slope conductance (g_o) of 3·2 pS.

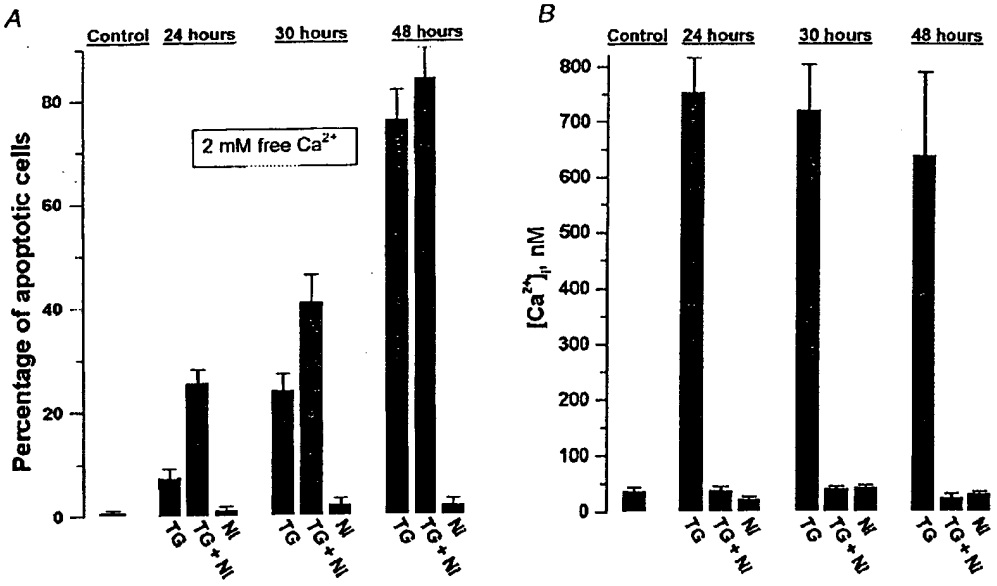

Figure 4. Temporal changes in apoptosis and in the cytosolic Ca^{2+} concentration of the LNCaP cells under physiological conditions of 2 mM extracellular free Ca^{2+}

A, temporal changes in apoptosis of the LNCaP cells (estimated by the number of apoptotic cells) treated with 0·1 μM TG, 0·5 mM Ni^{2+} or 0·1 μM TG combined with 0·5 mM Ni^{2+}. *B*, temporal changes in cytosolic Ca^{2+} concentration of the LNCaP cells treated with 0·1 μM TG, 0·5 mM Ni^{2+} or 0·1 μM TG combined with 0·5 mM Ni^{2+}.

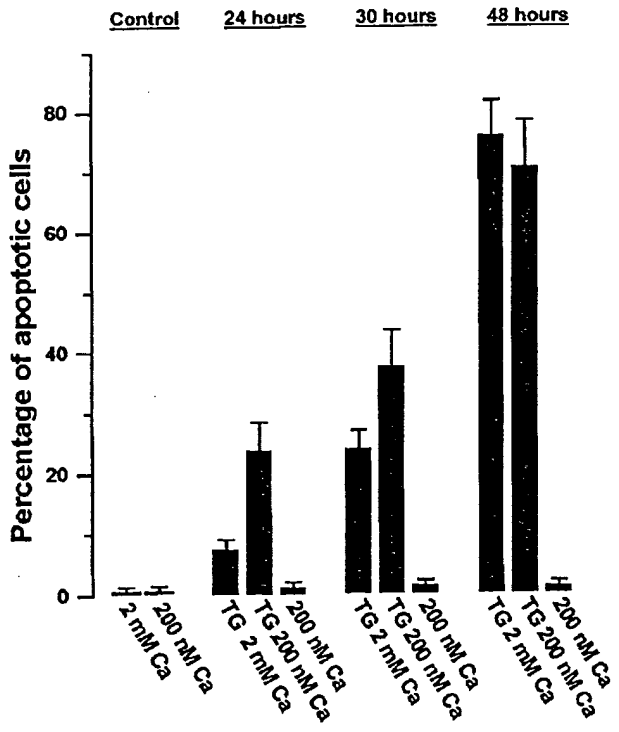

Figure 5. Temporal changes in the apoptosis of LNCaP cells under conditions of low extracellular free Ca^{2+}

Cells were treated with 0·1 μM TG in 2 mM free Ca^{2+}, with 0·1 μM TG in 200 nM free Ca^{2+} or with 200 nM free Ca^{2+} medium.

The following lines of evidence support our notion that the unitary activity described thus far is associated with the activation of single store-dependent, plasma membrane Ca^{2+} channels. (i) This activity was only observed in TG-treated cells; no similar activity was found in the cells under normal conditions. (ii) The activity shows strong inward rectification, typical of Ca^{2+}-selective channels. (iii) Neither K^+ (Skryma *et al.* 1997, 1999) nor Cl^- (Y. M. Shuba, unpublished observation) channels known to be present in LNCaP cells would be capable of producing a similar type of activity under these experimental conditions used. (iv) SOC has no similarity to the TG-independent Ca^{2+}-permeable 23 pS cation channel recently reported by Gutiérrez *et al.* (1999) in LNCaP cells.

Thapsigargin induces apoptosis in LNCaP cells

Hoescht staining was used to determine apoptosis induced by TG treatment. Under control conditions, in the absence of TG, the percentage of apoptotic cells was less than 1%. Typical apoptotic features induced by treatment with 0·1 μM TG for 24 h are shown in Fig. 6*C*. TG-induced apoptosis was also detected by the TUNEL technique (Fig. 7*C*). TG induced apoptosis in a time-dependent manner (Fig. 4*A*), with 7, 24 and 77% of cells reaching apoptosis at 24, 30 and 48 h, respectively.

Sustained elevation of cytosolic Ca^{2+} due to SOC activation is not required for induction of apoptosis by thapsigargin

As it has previously been reported that I_{store} activation, leading to a sustained increase in cytosolic Ca^{2+}, is required for TG-induced apoptosis in androgen-insensitive prostate

cancer cells (Furuya *et al.* 1994), we tested this hypothesis in androgen-sensitive prostate cancer LNCaP cells.

To determine whether the I_{store} in LNCaP cells is important in apoptosis induction by TG, we examined the ability of TG to induce apoptosis under different experimental conditions. In patch-clamp experiments, I_{store} was completely abolished by 0·5 mM Ni^{2+} (Fig. 2*B*). According to the hypothesis stated above, TG-induced apoptosis should decrease in cells treated with 0·5 mM Ni^{2+}. Unexpectedly, TG-induced apoptosis was significantly potentiated by treatment with 0·5 mM Ni^{2+} (Fig. 4*A*) whereas cell treatment with 0·5 mM Ni^{2+} alone did not induce apoptosis in LNCaP cells (Figs 4*A*, 6*B* and 7*B*). This enhancement of cell death was mostly visible after 24 and 30 h (25 *vs.* 7% and 41 *vs.* 24% of apoptotic cells for TG + Ni^{2+} and TG at 24 and 30 h, respectively). It therefore seems that Ni^{2+} does not enhance cell death any further after 48 h treatment (84 *vs.* 77% of apoptotic cells for TG + Ni^{2+} and TG, respectively). Apparently, blocking the store-operated Ca^{2+} current facilitates and accelerates TG-induced apoptosis. Figure 6*D* shows the apoptotic features of LNCaP cells after combined treatment with TG and Ni^{2+} for 24 h. These results were also confirmed by the TUNEL technique. Figure 7 shows the apoptosis detection in LNCaP cells treated with TG (Fig. 7*C*) and with TG combined with Ni^{2+} (Fig. 7*D*) for 24 h. To assess how $[Ca^{2+}]_i$ is affected by these apoptosis-inducing conditions, we compared cytoplasmic Ca^{2+} levels in LNCaP cells after 24, 30 and 48 h treatment with TG, Ni^{2+} and TG combined with Ni^{2+}. $[Ca^{2+}]_i$ remained at high levels throughout the 48 h, and even longer when cells were treated with TG alone, while the $[Ca^{2+}]_i$ level in cells treated with Ni^{2+} or TG combined with Ni^{2+} was almost the same as that of the control (Fig. 4*B*). This indicates that a sustained high level of $[Ca^{2+}]_i$ is not required for induction of apoptosis by TG and its subsequent development.

To confirm that blocking Ca^{2+} influx potentiates rather than inhibits TG-induced apoptosis, we then assessed the influence of decreasing the extracellular Ca^{2+} concentration. The Ca^{2+}-deprived medium contained no added Ca^{2+} and dialysed serum was used to remove Ca^{2+} contaminants (as well as other low molecular weight species) in addition to 0·1 mM EGTA to buffer the free calcium concentration in the extracellular solution (see Methods). This gave a Ca^{2+} concentration of 200 nM. As shown in Fig. 5, the Ca^{2+}-deprived medium potentiated the apoptosis induced by TG in a time-dependent manner without having any action on its own. The potentiation of TG-induced apoptosis due to

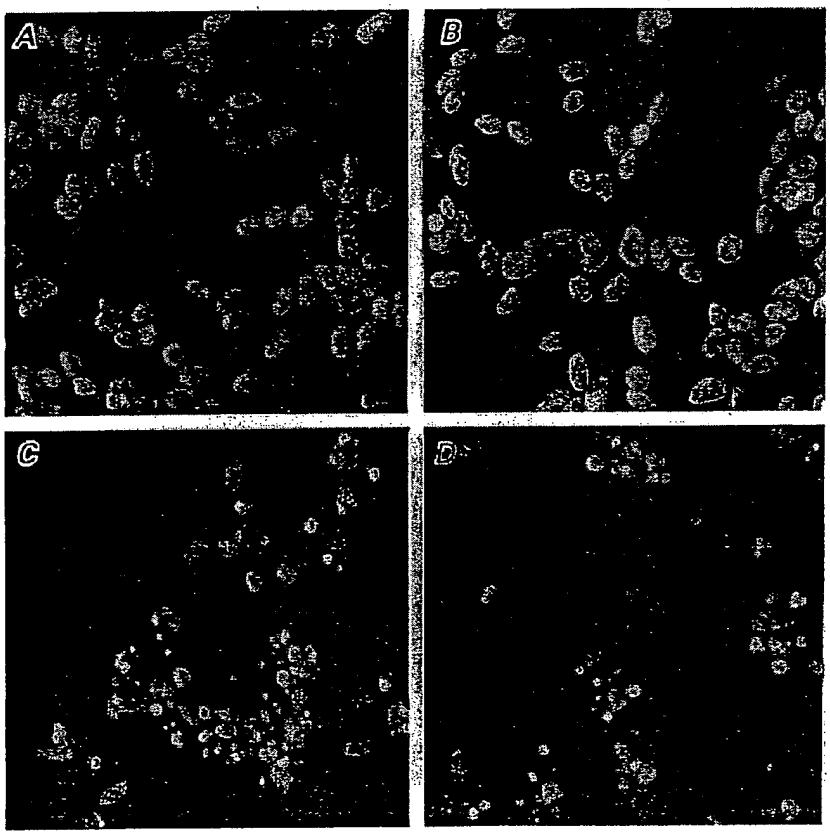

Figure 6. LNCaP prostate cells (staining with 5 μg ml^{-1} Hoescht) undergoing apoptosis due to treatment with thapsigargin

A, control cells; *B*, cells treated with 0·5 mM Ni^{2+} (24 h); *C*, cells treated with 0·1 μM TG (24 h); *D*, cells treated with 0·1 μM TG + 0·5 mM Ni^{2+} (24 h).

decreasing the extracellular calcium was similar to that caused by nickel. Indeed, we observed that TG-induced apoptosis was enhanced by 340% (34 h) and 170% (30 h) by a Ca^{2+}-deprived solution compared with 310% (24 h) and 160% (30 h) by nickel. Reduction to even lower Ca^{2+} levels with 1 mM EGTA (giving 20 nM free Ca^{2+}) in the external medium also led to an enhancement of TG-induced apoptosis. However, in this condition, the Ca^{2+}-deprived medium had an apoptotic action on its own (20, 28 and 88% of apoptotic cells at 24, 30 and 48 h, respectively; data not shown). The effects of Ni^{2+} and low extracellular Ca^{2+} were really due to enhancement of TG-induced cell apoptosis and not due to necrosis. This was confirmed by an increase in the morphological indicators of apoptosis, i.e. the extent of internucleosomal degradation and DNA ladder formation (data not shown). Furthermore, the percentage of cells excluding Trypan Blue was not affected by incubation with 0·5 mM Ni^{2+} or 200 nM free Ca^{2+} medium for more than 72 h.

Transient $[Ca^{2+}]_i$ increase due to depletion of Ca^{2+} stores is not responsible for apoptosis induction by thapsigargin

As thapsigargin is still capable of inducing a rise in $[Ca^{2+}]_i$ in the absence of extracellular Ca^{2+}, due to a passive leak of Ca^{2+} through the ER membrane, we checked whether this initial transient increase in $[Ca^{2+}]_i$ was involved in apoptosis induction. To eliminate the transient rise in $[Ca^{2+}]_i$, LNCaP cells were incubated for 20 min in the presence of 50 μM BAPTA-AM, an intracellular Ca^{2+} chelator, and in the 200 nM free Ca^{2+} medium (with 0·1 mM EGTA). This procedure resulted in sufficient intracellular Ca^{2+} buffering to completely eliminate the transient rise in $[Ca^{2+}]_i$ that occurred when thapsigargin was added to a Ca^{2+}-free medium (not shown). In BAPTA-loaded cells, $[Ca^{2+}]_i$ was 69 ± 9 nM. $[Ca^{2+}]_i$ was 65 ± 7 nM 150 s after TG addition, a concentration not different from that before TG addition. BAPTA-AM treatment for 20 min without TG did not induce apoptosis in LNCaP cells (< 0·1% of apoptotic cells in control after 48 h and < 0·1% of apoptotic cells after 48 h following 20 min incubation with BAPTA-AM). The cells were then treated with 0·1 μM TG for 48 h and the percentage of apoptotic cells was compared with that of cells not loaded with BAPTA. The ability of TG to induce apoptosis in LNCaP cells was not reduced by BAPTA loading in these conditions (70 ± 5% apoptotic cells in BAPTA-loaded, TG-treated cells, as compared with 71 ± 8% in TG-treated cells in the 200 nM free Ca^{2+} medium).

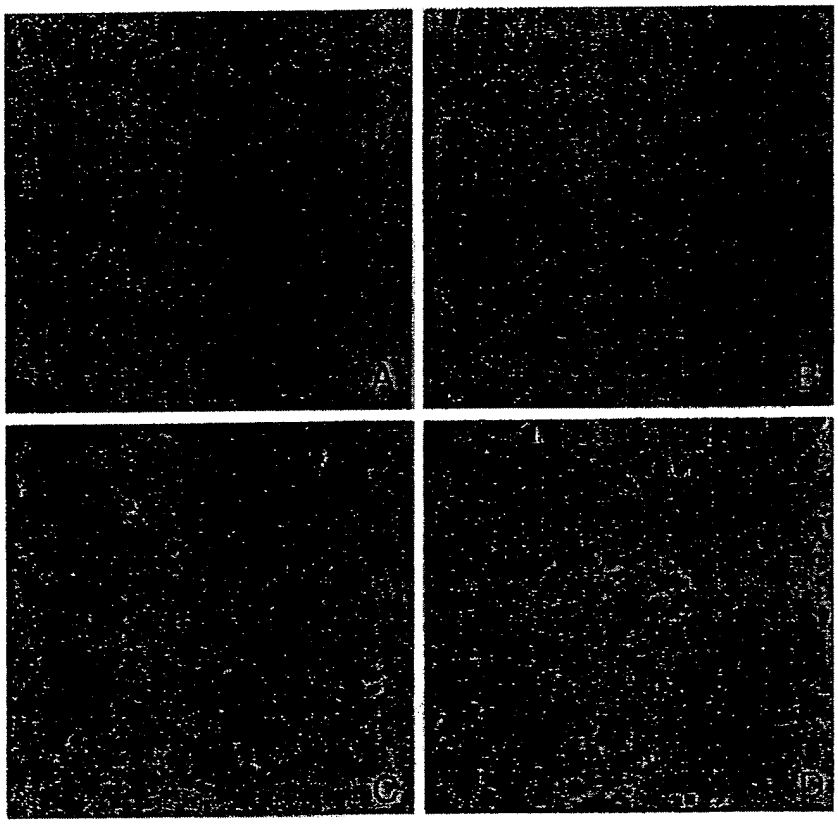

Figure 7. Thapsigargin-induced apoptosis detection in LNCaP prostate cells using the TUNEL technique

A, control cells; *B*, cells treated with 0·5 mM Ni^{2+} (24 h); *C*, cells treated with 0·1 μM TG (24 h); *D*, cells treated with 0·1 μM TG + 0·5 mM Ni^{2+} (24 h).

DISCUSSION

The present study demonstrates that emptying intracellular Ca^{2+} stores by SERCA pump inhibitors stimulates a Ca^{2+} current, I_{store}, through specific store-operated channels (SOCs), in androgen-sensitive human prostate cancer LNCaP cells. These channels are activated by intracellular store depletion, and had not previously been identified and characterized in prostate cells.

The presence of store-operated Ca^{2+} entry has been documented in a large variety of cells, mainly on the basis of measurements of intracellular Ca^{2+} levels after store depletion by thapsigargin. The first electrophysiological demonstration of a store-operated Ca^{2+} current was carried out in mast cells by Hoth & Penner (1992), who called it Ca^{2+} release-activated current (I_{CRAC}). I_{CRAC} is now the best-characterized store-operated Ca^{2+} current. It is known to be activated by depleting intracellular Ca^{2+} stores and has the highest selectivity for Ca^{2+} over other cations (Hoth & Penner, 1992; Zweifach & Lewis, 1993; Berridge, 1995*b*). Recent studies using patch-clamp techniques have now clearly established the existence of a number of store-operated Ca^{2+} currents in several non-excitable cell types, differentiated by their unitary conductance, selectivity and pharmacology (for review see Parekh & Penner, 1997). Regardless of some differences in channel properties, store-operated channels form a family of channels characterized by several specific, common features. The first of these properties consists of current activation by emptying the intracellular calcium stores, using a variety of procedures. In our experiments, I_{store} was identified by emptying intracellular stores using TG. As in basophilic leukaemia (RBL) cells, or Jurkat T cells, I_{store} in LNCaP cells appears to be the critical Ca^{2+} influx pathway as LNCaP cells do not have voltage-activated Ca^{2+} channels (Skryma *et al.* 1997, 1999). The second important property of I_{store} is its characteristic voltage dependence. I_{store} could be considered as a voltage-independent Ca^{2+} current, as it is not gated by membrane voltage changes (Zweifach & Lewis, 1993; Hoth & Penner, 1993). However, once it has been activated by store depletion, I_{store} increases when the membrane potential shifts toward negative values. The current–voltage relationship also shows a pronounced inward rectification at negative voltages (Zweifach & Lewis, 1993; Hoth & Penner, 1993). The I_{store} reversal potential was above +50 mV, as expected for selective Ca^{2+} currents. Changing external Na^+ had no significant effect on I_{store} in LNCaP cells, demonstrating that Na^+ does not permeate the channel in the presence of external Ca^{2+}. I_{store} was inhibited by Ni^{2+} and La^{3+}, thus corresponding to the typical pharmacological profile of store-operated currents in other cells (Schlegel *et al.* 1993; Grudt *et al.* 1996). SK&F 96365, one of the proposed inhibitors of capacitative Ca^{2+} current, did not inhibit I_{store} in LNCaP cells. However, blocking the Ca^{2+} current with this inhibitor is not evidence for capacitative current as it can also block other channels in similar concentrations (Franzius *et al.* 1994).

The unitary conductance of the I_{store} channel was identified as approximately 3·2 pS, which is rather large in comparison with classical I_{CRAC} single-channel conductance, which is usually under 1 pS (Zweifach & Lewis, 1993; Parekh & Penner, 1997). Large single-channel conductances of 2 and 11 pS were also observed for store-operated currents in A431 epidermal cells (Lückhoff & Clapham, 1994) and endothelial cells (Vaca & Kunze, 1995), respectively. However, in our experiments, as in other cell models (Lückhoff & Clapham, 1994), the *I–V* relationship for store-operated channels is non-linear. For a non-linear *I–V* relationship, the slope conductance is a function of potential. When comparing values obtained in different cells it is, therefore, necessary to consider not only specific ionic conditions but also the range of membrane potentials at which they were determined. This makes separating store-operated channels by their single-channel conductance quite a challenging task. Thus the properties of SOC in human cancer prostate LNCaP cells suggest that it belongs to the 'store-operated' channel family, but it may be not the same as classical CRAC.

Our study provides the first direct demonstration and characterization of a store-operated current in prostate cells. SOC characterization could be of great interest in prostate cancer studies as these channels were suggested to be the target of a Ca^{2+}-influx inhibitor, which has been found, in clinical trials, to slow down the growth of certain aggressive cancer cells (Kohn *et al.* 1996). We studied the role of SOCs in TG-induced apoptosis in androgen-sensitive prostate cancer LNCaP cells. TG induces apoptosis in many cell types (Furuya *et al.* 1994; Gill *et al.* 1996; He *et al.* 1997; Bian *et al.* 1997). Based on the changes in Ca^{2+} homeostasis induced by TG, three hypotheses can be proposed to explain the apoptosis induction mechanism. Apoptosis is induced by: (i) a transient increase in $[Ca^{2+}]_i$ due to a passive leak of Ca^{2+} through the ER membrane, (ii) Ca^{2+} pool depletion, or (iii) a sustained rise in cytosolic Ca^{2+} secondary to Ca^{2+} entry through I_{store} channels. In this report we show that neither the transient nor the sustained increase in $[Ca^{2+}]_i$ is required for induction of apoptosis by TG. Our results show first that a sustained increase in $[Ca^{2+}]_i$ via I_{store} activation is not required for TG to induce apoptosis in LNCaP cells because I_{store} inhibition by the 200 nM free Ca^{2+} medium or 0·5 mM Ni^{2+} did not abolish TG-induced apoptosis whereas the TG-increased cytosolic Ca^{2+} concentration was reduced to control values by the incubation in 200 nM free Ca^{2+} or 0·5 mM Ni^{2+}-containing medium. Under these conditions, however, a transient rise in $[Ca^{2+}]_i$ can still occur due to calcium mobilization from internal stores. We strongly buffered $[Ca^{2+}]_i$ by preincubating cells with the Ca^{2+} chelator BAPTA-AM to eliminate the transient rise in $[Ca^{2+}]_i$, while the sustained rise was abolished by the absence of external calcium. This did not inhibit apoptosis induced by TG, suggesting that the transient increase in $[Ca^{2+}]_i$ is not responsible for apoptosis induction. These results, where cytosolic Ca^{2+} is strongly buffered using BAPTA-AM, also exclude another possible consequence of ER depletion that might induce apoptosis: mitochondrial calcium overloading

(Berridge *et al.* 1998; Green & Reed, 1998). These data are consistent with the findings of others on lymphoid cells (Berridge, 1995*a*; Bian *et al.* 1997) and murine hypothalamic cell lines (Wei *et al.* 1998). However, surprisingly, they are in contrast with those described in androgen-insensitive prostate cancer cells (Furuya *et al.* 1994). In these cells, as in thymocytes (Jiang *et al.* 1998), TG-induced apoptosis was inhibited by preincubating cells with BAPTA-AM, or by overexpressing the cytosolic Ca^{2+}-binding protein calbindin. On the basis of these results, a sustained increase in cytosolic Ca^{2+}, mediated by a store-operated Ca^{2+} current, was considered to play a role in apoptosis induction by TG (Furuya *et al.* 1994).

Our results therefore suggest that Ca^{2+} pool depletion, and not an increase in cytosolic Ca^{2+}, induces apoptotic cell death in androgen-sensitive human prostate cancer cells. In addition, our data show that TG-induced apoptosis was enhanced (see Figs 4*A* and 5) by 0·5 mM Ni^{2+} and a low external free Ca^{2+} concentration (200 nM free Ca^{2+}). Therefore, blocking capacitative Ca^{2+} entry potentiates apoptosis induced by TG. This reinforces the hypothesis that Ca^{2+} pool depletion is involved in apoptosis, since an increase in cytosolic Ca^{2+} due to capacitative Ca^{2+} entry (inhibited by Ni^{2+}) would be required for optimal ER pool filling and apoptosis inhibition. It should be noted that decreasing external calcium to very low levels using 1 mM EGTA (20 nM free Ca^{2+}) led to apoptosis on its own. This is certainly due to the inversion of the Ca^{2+} concentration gradient in comparison to physiological conditions (the intracellular Ca^{2+} concentration of LNCaP cells is usually about 100 nM). The intracellular Ca^{2+} stores are depleted in response to the decrease in cytosolic Ca^{2+} concentration (in turn induced by stimulation of the Ca^{2+} pump of the plasma membrane by low extracellular Ca^{2+}). This calcium gradient hypothesis may also be confirmed by the fact that, under low external calcium conditions (200 nM), where values are, however, higher than the intracellular Ca^{2+} concentration (100 nM), apoptosis was not observed in the absence of TG (< 1 % of apoptotic cells at 48 h). Similarly, this does not occur with Ni^{2+} because the Ca^{2+} gradient is not perturbed.

Our data are in agreement with those of Distelhorst and colleagues (He *et al.* 1997) on WEH17.2 lymphoma cells. These authors suggested that ER calcium pool depletion by TG could trigger apoptosis and that overexpression of the Bcl-2 anti-apoptotic protein, which anchors to intracellular membranes, maintains Ca^{2+} homeostasis within the ER, thereby inhibiting apoptosis induction by TG.

The exact mechanism by which calcium pool depletion induces apoptosis is not known. The high levels of Ca^{2+} within the lumen of the ER are essential not only for Ca^{2+} signal transduction, but also for protein synthesis and processing, and cell division (Sambrook, 1990; Koch, 1990; Kuznetsov *et al.* 1992; Gill *et al.* 1996; Jiang *et al.* 1998). Three potential mechanisms by which ER depletion might contribute to apoptosis have been proposed (He *et al.* 1997): (i) depletion of the ER Ca^{2+} pool might destabilize the Ca^{2+}–protein gel and its associated membrane, leading to vesiculation and the formation of apoptotic blebs; (ii) disruption of protein processing and transport within the ER may contribute to TG-induced apoptosis; (iii) TG-induced ER Ca^{2+} pool depletion releases an endonuclease into the nucleus responsible for DNA fragmentation. Thus the decline in ER calcium levels leads to the activation of stress signals that switch on the genes associated with death. Although the importance of intraluminal ER Ca^{2+} storage in apoptosis appears to be evident, other mechanisms depending on extracellular, cytosolic, mitochondrial or nuclear Ca^{2+} have been shown to contribute to apoptosis in a variety of cell models (Dowd, 1995; Marin *et al.* 1996; McConkey & Orrenius, 1997). Therefore, the general applicability of the store-depletion hypothesis is doubtful and the relationship between intracellular Ca^{2+} stores, Bcl-2 and apoptosis may be cell specific.

The reasons why the differences between androgen-dependent and androgen-independent prostate cancer cells are associated with changes in Ca^{2+} store-dependent mechanisms involved in apoptosis remain intriguing. It is known that such progression is also associated with expression of the intracellular membrane protein Bcl-2 (Raffo *et al.* 1995; Chaudhary *et al.* 1999). Bcl-2 expression modulates intracellular signalling and preserves the integrity of the ER Ca^{2+} pool in cells exposed to various apoptosis-inducing stimuli, including cytotoxic Ca^{2+} ionophores, TG and reactive oxygen species (Disthelhorst *et al.* 1996; He *et al.* 1997). Moreover, it has been shown that Bcl-2 preserves the ER Ca^{2+} store via an upregulation of calcium pump SERCA gene expression. Bcl-2 may possibly interact with this pump as well (Kuo *et al.* 1998). Interestingly, the androgen-insensitive DU-145 cells do not express Bcl-2, but rather Bcl-X(L) (Shirahama *et al.* 1997), which is poorly expressed in LNCaP cells. Wang *et al.* (1999) have shown that apoptosis induction by TG in DU-145 cells requires an increase in cytoplasmic Ca^{2+} since it activates the Ca^{2+}-activated protein phosphatase calcineurin that was found to dephosphorylate BAD (proapoptotic member of Bcl-2 family), thus enhancing BAD heterodimerization with Bcl-X(L) (but not with Bcl-2) and promoting apoptosis. Another Ca^{2+}-regulating protein, calreticulin (Krause & Michalak, 1997), has been identified in prostate cells (Zhu & Wang, 1999). The expression of this highly conserved intracellular Ca^{2+}-binding protein in the lumen of the endoplasmic reticulum is regulated by androgen (Zhu *et al.* 1998). The downregulation of calreticulin by androgen ablation correlates with apoptosis and the upregulation of calreticulin by androgen replacement in castrated rats correlates with proliferation and differentiation of epithelial cells in the prostate (Zhu *et al.* 1998; Zhu & Wang, 1999). The induction of calreticulin by androgen in prostate organ culture partially resists protein synthesis inhibition,

suggesting that calreticulin is a direct androgen-response gene (Zhu *et al.* 1998). Furthermore, Mery *et al.* (1996) have shown in a mouse L fibroblast cell line that overexpression of calreticulin increases intracellular Ca^{2+} storage and decreases store-operated Ca^{2+} current suggesting an active involvement of calreticulin in intracellular Ca^{2+} pool refilling regulation. Thus, as calreticulin is a major intracellular Ca^{2+}-binding protein involved in Ca^{2+} homeostasis and is regulated by androgens, it could be a promising candidate for mediating androgen regulation of intracellular calcium levels in prostate cells. Thus the differences in Ca^{2+}-dependent apoptosis induction between androgen-dependent and androgen-independent prostate cancer cells may be explained by the differential expression of apoptosis-regulating proteins (Bcl-2, Bcl-X(L), calreticulin).

In summary, we have characterized the Ca^{2+}-regulated mechanisms involved in thapsigargin-induced apoptosis in androgen-sensitive human prostate cancer LNCaP cells. We suggest that a decrease in ER calcium is the major factor in apoptosis induction in these cells; however, direct measurement of the Ca^{2+} concentration in ER lumen would be required to confirm this statement. In contrast to the situation in androgen-insensitive prostate cancer cells, the activation of I_{store}, responsible for ER refilling, and increasing cytosolic Ca^{2+} are not required for TG-induced apoptosis. Further studies are needed to identify the precise Ca^{2+}-regulated mechanisms involved in the progression of prostate cancer cells from androgen dependence to androgen independence.

Berridge, M. J. (1995*a*). Calcium signalling and cell proliferation. *Bioessays* **17**, 491–500.

Berridge, M. J. (1995*b*). Capacitative calcium entry. *Biochemical Journal* **312**, 1–11.

Berridge, M. J. (1997). Elementary and global aspects of calcium signalling. *Journal of Physiology* **499**, 291–306.

Berridge, M. J., Bootman, M. D. & Lipp, P. (1998). Calcium – a life and death signal. *Nature* **935**, 645–648.

Bian, X., Hughes, F. M. Jr, Huang, Y., Cidlowski, J. A. & Putney, J. W. Jr (1997). Roles of cytoplasmic Ca^{2+} and intracellular Ca^{2+} stores in induction and suppression of apoptosis in S49 cells. *American Journal of Physiology* **272**, C1241–1249.

Chaudhary, K. S., Abel, P. D. & Lalani, E. N. (1999). Role of the bcl-2 gene family in prostate cancer progression and its implications for therapeutic intervention. *Environmental Health Perspectives* **107**, 49–57.

Disthelhorst, C. W., Lam, M. & McCormick, T. S. (1996). Bcl-2 inhibits hydrogen peroxide-induced ER Ca^{2+} pool depletion. *Oncogene* **12**, 2051–2055.

Dowd, D. R. (1995). Calcium regulation of apoptosis. *Advances in Second Messenger and Phosphoprotein Research* **30**, 255–279.

Dowd, D. R., McDonald, P. N., Komm, B. S., Haussler, M. R. & Miesfeld, R. (1992). Stable expression of the calbindin-D28K complementary DNA interferes with the apoptotic pathway in lymphocytes. *Molecular Endocrinology* **6**, 1843–1848.

Fanger, C. M., Hoth, M., Crabtree, G. R. & Lewis, R. S. (1995). Characterization of T cell mutants with defects in capacitative calcium entry: genetic evidence for the physiological roles of CRAC channels. *Journal of Cellular Biology* **131**, 655–667.

Franzius, D., Hoth, M. & Penner, R. (1994). Non-specific effects of calcium entry antagonists in mast cells. *Pflügers Archiv* **428**, 433–438.

Furuya, Y., Lundmo, P., Short, A. D., Gill, D. L. & Isaacs, J. T. (1994). The role of calcium, pH, and cell proliferation in the programmed (apoptotic) death of androgen-independent prostatic cancer cells induced by thapsigargin. *Cancer Research* **54**, 6167–6175.

Gill, D. L., Waldron, R. T., Rys-Sikora, K. E., Ufret-Vincenty, C. A., Graber, M. N., Favre, C. J. & Alfonso, A. (1996). Calcium pools, calcium entry, and cell growth. *Bioscience Reports* **16**, 139–157.

Gong, Y., Blok, L. J., Perry, J. E., Lindzeys, J. K. & Tindall, D. J. (1995). Calcium regulation of androgen receptor expression in the human prostate cancer cell line LNCaP. *Endocrinology* **136**, 2172–2178.

Green, D. R. & Reed, J. C. (1998). Mitochondria and apoptosis. *Apoptosis* **281**, 1309–1316.

Grudt, T. J., Usowicz, M. M. & Henderson, G. (1996). Ca^{2+} entry following store depletion in SH-SY5Y neuroblastoma cells. *Molecular Brain Research* **36**, 93–100.

Grynkiewicz, G., Poenie, M. & Tsien, R. Y. (1985). A new generation of Ca^{2+} indicators with greatly improved fluorescence properties. *Journal of Biological Chemistry* **260**, 3440–3450.

Gutiérrez, A. A., Arias J. M., Garcia L., Mas-Oliva, J. & Guerrero-Hernandez, A. (1999). Activation of a Ca^{2+}-permeable cation channel by two different inducers of apoptosis in a human prostatic cancer cell line. *Journal of Physiology* **517**, 95–107.

He, H., Lam, M., McCormick, T. S. & Distelhorst, C. W. (1997). Maintenance of calcium homeostasis in the endoplasmic reticulum by bcl-2. *Journal of Cellular Biology* **138**, 1219–1228.

Hoth, M. & Penner, R. (1992). Depletion of intracellular calcium stores activates a calcium current in mast cells. *Nature* **355**, 353–356.

Hoth, M. & Penner, R. (1993). Calcium release-activated calcium current in rat mast cells. *Journal of Physiology* **465**, 359–386.

Huang, Y. & Putney, J. W. (1998). Relationship between intracellular calcium store depletion and calcium release-activated calcium current in a mast cell line (RBL-1). *Journal of Biological Chemistry* **273**, 19554–19559.

Isaacs, J. T., Lundmo, P. I., Berges, R., Martikainen, P., Kyprianou, N. & English, H. F. (1992). Androgen regulation of programmed death of normal and malignant prostatic cells. *Journal of Andrology* **13**, 457–464.

Jiang, S., Chow, S. C., Nicotera, P. & Orremius, S. (1998). Intracellular Ca^{2+} signals activate apoptosis in thymocytes: studies using the Ca^{2+}-ATPase inhibitor thapsigargin. *Experimental Cellular Research* **212**, 84–92.

Juin, P., Pelletier, M., Oliver, L., Tremblais, K., Grégoire, M., Meflah, K. & Vallette, F. M. (1998). Induction of a caspase-3-like activity by calcium in normal cytosolic extracts triggers nuclear apoptosis in a cell-free system. *Journal of Biological Chemistry* **273**, 17559–17564.

Koch, G. L. E. (1990). The endoplasmic reticulum and calcium storage. *Bioessays* **12**, 527–531.

KOHN, E. C., REED, E., SAROSY, G., CHRISTIAN, M., LINK, C. J., COLE, K., FIGG, W. D., DAVIS, P. A., JACO GOLDSPIEL, B. & LIOTTA, L. A. (1996). Clinical investigation of a cyanotic calcium influx inhibitor in patients with refractory cancers. *Cancer Research* **56**, 569–573.

KRAUSE, K. H. & MICHALAK, M. (1997). Calreticulin. *Cell* **88**, 439–443.

KUO, T. H., KIM, H. R. C., ZHU, L., YU, Y., LIN, H. M. & TSANG, W. (1998). Modulation of endoplasmic reticulum calcium pump by bcl-2. *Oncogen* **17**, 1903–1910.

KUZNETSOV, G., BROSTROM, M. A. & BROSTROM, C. O. (1992). Role of endoplasmic reticular calcium in oligosaccharide processing of alpha 1-antitrypsin. *Journal of Biological Chemistry* **268**, 2001–2008.

LÜCKHOFF, A. & CLAPHAM, D. E. (1994). Calcium channels activated by depletion of internal calcium stores in A431 cells. *Biophysical Journal* **67**, 177–182.

MCCONKEY, D. J., NICOTERA, P., HARTZELL, P., BELLOMS, G., WYLLIE, A. M. & ORREMIUS, S. (1989). Glucocorticoids activate a suicide process in thymocytes through an elevation of cytosolic Ca^{2+} concentration. *Archives of Biochemistry and Biophysics* **269**, 365–370.

MCCONKEY, D. J. & ORRENIUS, S. (1997). The role of calcium in the regulation of apoptosis. *Biochemical and Biophysical Research Communications* **239**, 357–366.

MARIN, M. C., FERNANDEZ, A., BICK, R. J., BRISBAY, S., BUJA, L. M., SNUGGS, M., MCCONKEY, D. J., VON ESCHENBACH, A. C., KEATING, M. J. & MCDONNELL, T. J. (1996). Apoptosis suppression by bcl-2 is correlated with the regulation of nuclear and cytosolic Ca^{2+}. *Oncogen* **12**, 2259–2266.

MARTIKAINEN, P., KYPRIANOU, N., TUCKER, R. W. & ISAACS, J. T. (1991). Programmed death of nonproliferating androgen independent prostatic cancer cells. *Cancer Research* **51**, 4693–4700.

MASON, M. J., GARCIA-RODRIGUEZ, C. & GRINSTEIN, S. (1991). Coupling between intracellular Ca^{2+} stores and the Ca^{2+} permeability of the plasma membrane. Comparison of the effects of thapsigargin, 2,5-di-(tert-butyl)-1,4-hydroquinone, and cyclopiazonic acid in rat thymic lymphocytes. *Journal of Biological Chemistry* **266**, 20856–20862.

MERY, L., MESAELI, N., MICHALAK, M., OPAS, M., LEW, D. P. & KRAUSE, K. H. (1996). Overexpression of calreticulin increases intracellular Ca^{2+} storage and decreases store-operated Ca^{2+} influx. *Journal of Biological Chemistry* **271**, 9332–9339.

MONTIRONI, R., MAGI-GALLUZZI, C., MUZZUNIGRO, G., PRETE, E., POLITO, M. & FABRIS, G. (1994). Effects of combination endocrine treatment on normal prostate, prostatic intraepithelial neoplasia, and prostatic adenocarcinoma. *Journal of Clinical Pathology* **47**, 906–913.

PAREKH, A. B. & PENNER, R. (1995). Activation of store-operated calcium influx at resting $InsP_3$ levels by sensitization of the $InsP_3$ receptor in rat basophilic leukaemia cells. *Journal of Physiology* **489**, 377–382.

PAREKH, A. B. & PENNER, R. (1996). Regulation of store-operated calcium currents in mast cells. *Organellar Ion Channels and Transporters* **51**, 231–239.

PAREKH, A. B. & PENNER, R. (1997). Store depletion and calcium influx. *Physiological Reviews* **77**, 901–929.

PARKER, S. L., TONG, T., BALDEN, S. & WINGO, P. A. (1997). Cancer statistics. *CA Cancer Journal for Clinicians* **47**, 5–27.

PREMACK, B. A., MCDONALD, T. V. & GARDNER, P. (1994). Activation of Ca^{2+} current in Jurkat T cells following the depletion of Ca^{2+} stores by microsomal Ca^{2+}-ATPase inhibitors. *Journal of Immunology* **152**, 5226–5240.

PREVARSKAYA, N., SKRYMA, R., VACHER, P., DANIEL, N., DJIANE, J. & DUFY, B. (1995). Rôle of tyrosine phosphorylation in potassium channel activation. *Journal of Biological Chemistry* **270**, 24292–24299.

PUTNEY, J. W. JR (1986). A model for receptor-regulated calcium entry. *Cell Calcium* **7**, 1–12.

PUTNEY, J. W. JR (1990). Capacitative calcium entry revisited. *Cell Calcium* **11**, 611–624.

RAFFO, A. J., PERLMAN, H., CHEN, M. W., DAY, M. L., STREITMAN, J. S. & BUTTYAN, R. (1995). Overexpression of bcl-2 protects prostate cancer cells from apoptosis *in vitro* and confers resistance to androgen depletion *in vivo*. *Cancer Research* **55**, 4438–4445.

SAMBROOK, J. F. (1990). The involvement of calcium in transport of secretary proteins from the endoplasmic reticulum. *Cell* **61**, 197–199.

SANTELLA, L. (1998). The role of calcium in the cell cycle: facts and hypotheses. *Biochemical and Biophysical Research Communications* **244**, 317–324.

SCHLEGEL, W., MOLLARD, P., DEMAUREX, N., THELER, J. M., CHIAVAROLI, C., GUÉRINEAU, N., VACHER, P., MAYR, G., KRAUSE, K. H., WOLLHEIM, C. B. & LEW P. D. (1993). Calcium signalling: comparison of the role of Ca^{2+} influx in excitable endocrine and non-excitable myeloid cells. *Advances in Second Messenger and Phosphoprotein Research* **28**, 142–152.

SHIRAHAMA, T., SAKAKURA, C., SWEENEY, E. A., OZAWA, M., TAKEMOTO, M., NISHIYAMA, K., OHI, Y. & IGARASHI, Y. (1997). Sphingosine induces apoptosis in androgen-independent human prostatic carcinoma DU-145 cells by suppression of bcl-X(L) gene expression. *FEBS Letters* **407**, 97–100.

SKRYMA, R., PREVARSKAYA, N., VACHER, P. & DUFY, B. (1994). Voltage-dependent ionic conductances in Chinese hamster ovary cells. *American Journal of Physiology* **267**, 544–553.

SKRYMA, R. N., PREVARSKAYA, N. B., DUFY-BARBE, L., ODESSA, M. F., AUDIN, J. & DUFY, B. (1997). Potassium conductance in the androgen-sensitive prostate cancer cell line, LNCaP: involvement in cell proliferation. *The Prostate* **33**, 112–122.

SKRYMA, R. N., VAN COPPENOLLE, F., DUFY-BARBE, L., DUFY, B. & PREVARSKAYA, N. (1999). Characterization of Ca^{2+}-inhibited potassium channels in the LNCaP human prostate cancer cell line. *Receptors and Channels* **6**, 241–253.

SPIELBERG, H., JUNE, C. H., BLAIR O. C., NYSTROM-ROSANDER, C., CEREB, N. & DEEG, H. J. (1991). UV irradiation of lymphocytes triggers an increase in intracellular Ca^{2+} and prevents lectin-stimulated Ca^{2+} mobilization: evidence for UV- and nifedipine-sensitive Ca^{2+} channels. *Experimental Hematology* **19**, 742–748.

THASTRUP, O., CULLEN, P. J., DROBAK, B. K., HANLEY, M. R. & DAWSON, A. P. (1990). Thapsigargin a tumor promoter discharges intracellular Ca^{2+} stores by specific inhibition of the endoplasmic reticulum Ca^{2+}-ATPase. *Proceedings of the National Academy of Sciences of the USA* **87**, 2466–2470.

VACA, L. & KUNZE, D. L. (1995). Depletion of intracellular Ca^{2+} stores activates a Ca^{2+}-selective channel in vascular endothelium. *American Journal of Physiology* **269**, C733–738.

WANG, H.-G., PATHAN, N., ETHELL, I. M., KRAJEWSKI, S., YAMAGUCHI, Y., SHIBASAKI, F., MCKEON, F., BOBO, T., FRANKE, T. F. & REED, J. C. (1999). Ca^{2+}-induced apoptosis through calcineurin dephosphorylation of BAD. *Science* **284**, 339–343.

WEI, H., WEI, W., BREDESEN, D. E. & PERRY, D. C. (1998). Bcl-2 protects against apoptosis in neuronal cell line caused by thapsigargin-induced depletion of intracellular calcium stores. *Journal of Neurochemistry* **70**, 2305–2314.

Woolf, S. H. (1995). Screening for prostate cancer with prostate specific antigen. An examination of the evidence. *New England Journal of Medicine* **333**, 1401–1405.

Zhu, N. & Wang, Z. (1999). Calreticulin expression is associated with androgen regulation of the sensitivity to calcium ionophore-induced apoptosis in LNCaP prostate cancer cells. *Cancer Research* **59**, 1896–1902.

Zhu, N., Pewitt, E. B., Cai, X., Cohn, E. B., Lang, S., Chen, R. & Wangs, Z. (1998). Calreticulin: an intracellular Ca^{2+}-binding protein abundantly expressed and regulated by androgen in prostatic epithelial cells. *Endocrinology* **139**, 4337–4344.

Zweifach, A. & Lewis, R. S. (1993). Mitogen-regulated Ca^{2+} current of T lymphocytes is activated by depletion of intracellular Ca^{2+} stores. *Proceedings of the National Academy of Sciences of the USA* **90**, 6295–6299.

Acknowledgements

The authors gratefully acknowledge the technical assistance of Isabelle Servant and Isabelle Spadone. This work was supported by grants from INSERM, Ministère de l'Education Nationale, ARC (Association pour la Recherche Contre le Cancer), Ligue Nationale Contre le Cancer, ARTP (Association pour le Recherche sur les Tumeurs de la Prostate), France. Y. Shuba was supported by INSERM and University of Science and Technology of Lille International Cooperation Programs.

R. Skryma and P. Mariot contributed equally to this work.

Corresponding author

N. Prevarskaya: Laboratoire de Physiologie Cellulaire, INSERM EPI-9938, USTL, Bâtiment SN3, 59655 Villeneuve d'Ascq Cedex, France.

Email: phycel@pop.univ-lille1.fr

Author's permanent address

Y. Shuba: Bogomoletz Institute of Physiology, Bogomoletz Street, 4, Kiev, Ukraine.

The Prostate 19:299–311 (1991)

Effect of Calcium and Calcium Antagonists on ^{45}Ca Influx and Cellular Growth of Human Prostatic Tumor Cells

Satish Batra, Lars D. Popper, and Beryl Hartley-Asp

Departments of Obstetrics and Gynecology (S.B.) and Pharmacology (S.B., L.D.P.), University of Lund, and Kabi Pharmacia Therapeutics AB (B.H.-A., S.B.), Lund, Sweden

Calcium and calmodulin play significant roles in DNA synthesis and cell proliferation. In this work the effects of verapamil, trifluoperazine, and tamoxifen on ^{45}Ca uptake and cell growth in human prostatic tumor cells (DU 145) and human fibroblast cells (1 BR) were studied. Although the maximum proliferation was achieved at a concentration of around 2 mM $CaCl_2$ in both DU 145 and 1 BR, growth of DU 145 cells was considerably greater than 1 BR at all calcium concentrations (0.1–4 mM). Calcium uptake experiments, using ^{45}Ca, revealed that the unstimulated ^{45}Ca uptake in 1 BR fibroblasts was 4–5 times higher than in DU 145 cancer cells. Depolarization with high extracellular K caused a 2–3-fold increase in ^{45}Ca influx in 1 BR but only 25–55% increase in DU 145 cells. Verapamil caused a significant inhibition of cell growth with an IC_{50} value of 55 μM. Verapamil paradoxically increased ^{45}Ca uptake in both unstimulated and K-stimulated DU 145 cells. Whereas unstimulated ^{45}Ca uptake could be blocked by very low concentrations of lathanum (10 μM), much higher concentrations (1–10 mM) were required to completely block uptake in K-depolarized cells. Both trifluoperazine and tamoxifen also inhibited cell proliferation with an IC_{50} concentration of approximately 5 μM. These drugs, had, however, no effect on ^{45}Ca uptake either in unstimulated or depolarized cells. The results suggest that voltage-gated calcium channels exist in both DU 145 cancer cells and fibroblasts. However, verapamil, in contrast to 1 BR, failed to block these channels in DU 145 cells. The mechanism of antiproliferative action of verapamil may be related to the observed, although paradoxical, increase in cellular calcium. The effect of trifluoperazine and tamoxifen does not involve changes in transmembrane calcium movements but could be mediated by their inhibition of calmodulin-mediated reactions within the cell.

Key words: calcium channels, cell proliferation, verapamil, tamoxifen

INTRODUCTION

Cell calcium metabolism is intimately involved in the regulation of many biological and biochemical activities. Data from several recent studies have shown that calcium and/or calmodulin play significant roles in DNA synthesis and cell proliferation [1–4]. During the pre-replicative stage of the cell cycle at the G_1/S border the calmodulin level is increased and at anaphase initiation the intracellular ionic calcium is increased [5]. This G1/S increase can be inhibited by calmodulin antagonists,

Received for publication January 7, 1991; accepted April 23, 1991.

Address reprint requests to Dr. S. Batra, Kabi Pharmacia Therapeutics AB, Scheelevägen 22, S-223 63 Lund, Sweden.

causing a block in DNA synthesis [1,6–8]. It has also been reported that calmodulin levels are significantly elevated in exponentially growing transformed cells [9,10]. In addition, the levels of calcium and/or calmodulin are increased in hepatomas [11–13] and in human mammary tumor tissue [14]. Thus, prolonged abnormally high levels of calcium and/or calmodulin may lead to a bypass of critical steps during cell proliferation. This biochemical abnormality may be linked to the relatively autonomous cell growth associated with cancer [2,8].

Available information on the degree of dependence of cancer cell proliferation on extracellular calcium is fragmentary and contradictory [4,15–17]. The weight of the evidence favours the argument that the requirement for extracellular calcium for growth of cancer cells is not as critical as that of normal cells [18,19]. In contrast to the requirement of calcium for cell growth, a sudden increase in intracellular, particularly intranuclear calcium, and the resulting increase in endonucleases appears to be an early event in programmed cell death [20,21].

In addition to the basic importance of intracellular calcium ion concentration in the regulation of cell growth and cell death, recent observations on the reversal of multidrug resistance to chemotherapeutic agents by certain calcium channel blockers has aroused considerable interest. One basis for chemoresistance within a given tumor cell resides with the ability of that cell to extrude cytotoxic compounds via an active mechanism, thereby effectively reducing the available intracellular drug concentration [22].

Verapamil, and similar substances that have been shown to reverse multidrug resistance, may retard active outward transport of drug [22–24], may increase oxygen and ATP utilization [25], may reduce intracellular pH [26], and may interfere with calcium-regulating mechanisms [27,28]. However, in cancer cells there are no clear-cut data showing the effects of these agents on the entry of extracellular calcium in unstimulated cells or during the activation of the so-called voltage-dependent calcium channels. In a preliminary study we found that verapamil paradoxically caused an increase in cellular calcium in prostatic cancer cells [29].

In order to delineate these various mechanisms in the present study, we have examined the effects of some calcium channel blockers and calmodulin inhibitors on both cell growth and ^{45}Ca influx in human prostatic tumor cells. Sensitivity to extracellular calcium was also examined in normal human fibroblasts for comparison. Although epithelial cells from normal human prostate would have been the most appropriate control cell type for DU 145 cells, unfortunately they do not readily proliferate in culture.

MATERIALS AND METHODS

Chemicals

$^{45}CaCl_2$ (10 mCi/ml, 15–50 mCi/mg) was purchased from New England Nuclear (Boston, MA). Verapamil and nifedipine were gifts from Knoll and Bayer Pharmaceuticals (Ludwigshafen and Eiberfeld, Germany), respectively. Trifluoperazine, tamoxifen, and lanthanum chloride were purchased from Sigma Chemical Co. (St. Louis, MO). Whereas verapamil and trifluoperazine were dissolved in Hanks' balanced salt solution (BSS) (Grand Island Biological Co., Grand Island, NY) tamoxifen and nifedipine were dissolved in ethanol at 5 or 10 mM, respectively, and

then diluted in Hanks' BSS. The final concentration of ethanol (0.05%) present in assays had no effect on ^{45}Ca uptake or cell proliferation.

Cell Lines

The established cell lines used in this work were DU 145, a cell line derived from a lesion in the brain of a patient with widespread metastatic carcinoma of the prostate, and 1 BR, a fibroblast cell line derived from a skin biopsy of a normal male. The cell line DU 145 was kindly donated by Dr. D Mickey, Duke University (USA), and 1 BR by Dr. A Lehman, University of Sussex (UK). The 1 BR cells were grown as monolayer cultures in minimum essential medium (MEM) and DU 145 in RPMI 1640 medium containing 10% fetal calf serum, penicillin (50 units/ml), streptomycin (50 μg/ml), and 2 mM L-glutamine (GIBCO, Grand Island, NY). The cells were incubated at 37°C in 95% air/5% CO_2 in a humidified chamber. The culture medium was changed every 2 days.

Cell Growth Experiments and Cytotoxicity

Experiments were conducted to study the optimal concentration of calcium for the growth of DU 145 and 1 BR cells and the antiproliferative effects of verapamil, nifedipine, trifluoperazine, tamoxifen, and lanthanum on DU 145 cells. Cell cultures were plated on day 0 in 60-mm Petri dishes (Falcon No. F3002, Falcon Plastics) at a density of 10^5 cells/dish in 3 ml of medium. Twenty-four hours later, when cells had attached, medium was changed and test compounds at various concentrations were added to replicate dishes. Culture media with or without test substance were changed every second day and experiments concluded on day 7. To test the calcium requirement, cells were incubated in calcium-free MEM (GIBCO, Grand Island, NY) containing 10% dialyzed calcium-free fetal calf serum (GIBCO, Grand Island, NY). Various concentrations of calcium chloride were then added to the medium. Cells from triplicate cultures for each treatment were harvested by trypsinization and dispersed into single cell suspension with calcium- and magnesium-free Hanks' BSS. Cell viability was determined by adding trypan blue (final concentration 0.25%) and duplicate samples from each culture were counted in a hemocytometer.

Calcium Influx and Uptake

Following incubation in ^{45}Ca containing buffered solutions, the net uptake of calcium into the cells was estimated by measuring the ^{45}Ca content of the cells. The uptake was measured by a modification of the method of Messing et al. [30]. DU 145 and 1 BR cells were plated onto polylysine-coated, 60 mm plastic culture dishes at $0.5–1 \times 10^6$ cells/dish and used 3–4 days later. The last change of culture medium was 12–15 h prior to the experiment. After sucking off the growth medium, the cells, attached to the bottom of the plate, were washed once with 3 ml of nonradioactive calcium- and magnesium-free Hanks' BSS. The cells were then pre-incubated at 25°C for 20 min in 3 ml of Na-HEPES buffer containing (mM) NaCl (135); KCl (4.6); $MgCl_2$ (1.2); $CaCl_2$ (1.5); glucose (11); and HEPES (10) adjusted to pH 7.4, which had been bubbled with 100% O_2 for 30 min. To assay ^{45}Ca uptake and to determine the amount of calcium accumulated, pre-incubation buffer was aspirated and cells were incubated in 3 ml normal Na-HEPES incubation buffer (4.6 mM KCl) or cells were depolarized in K-HEPES buffer containing a high concentration of KCl (80 mM), with a trace of ^{45}Ca (0.5 μCi/ml). Cells were incubated at 25°C for 1 min to

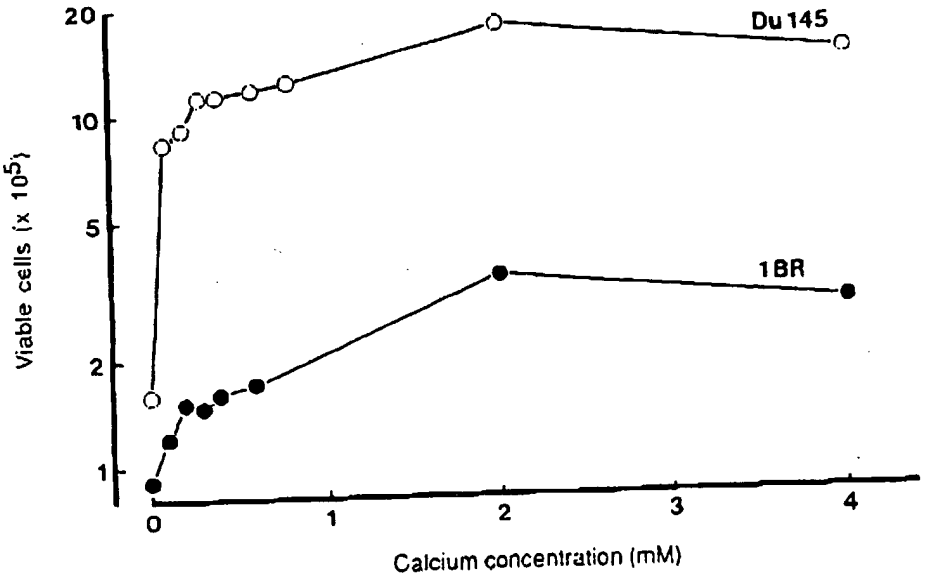

Fig. 1. Effect of different concentrations of $CaCl_2$ on the growth of DU 145 human prostatic tumor cells and 1 BR human fibroblast cells depicted in a semi-log plot. Cells (1×10^5), 24 h after plating, were washed and refed with 3 ml calcium-free MEM containing 10% dialyzed calcium-free fetal calf serum. Various concentrations of $CaCl_2$ were then added. Cells were grown for 7 days with or without $CaCl_2$ in the medium, and viable cells were counted. Data shown are mean values from two separate experiments which showed less than 10% variation.

estimate calcium influx or 20 min to measure calcium uptake. They were then washed 3 times with 3 ml of ice-cold (2°C) La-HEPES buffer containing (mM) NaCl (135); KCl (4.6); $MgCl_2$ (1.2); $LaCl_3$ (10); glucose (11); and HEPES (10) (pH 7.4). Washing with ice-cold $LaCl_3$-containing solution ensured inhibition of efflux and/or active extrusion of intracellular calcium as well as removal of any surface-bound calcium [31]. After the third wash, 2 ml of 0.5 N NaOH was added to each plate and left overnight to digest the cells. Aliquots (1 ml) of the digested cells were counted in a liquid scintillation spectrophotometer (Packard). Stimulated ^{45}Ca uptake was defined as the difference between uptake in 80 mM KCl (K-HEPES) and 4.6 mM KCl (Na-HEPES) buffer or the difference between uptake in the presence and absence of drugs. In some experiments ^{45}Ca was present in the growth medium throughout the whole period (7 days) and cellular calcium measured thereafter. Appropriate blanks were included in each case to account for any binding to cell culture plates.

Protein in cell digest was determined by the method of Peterson [32] using bovine serum albumin (Fraction V, Sigma Chemical Co., St. Louis, MO) as standard.

RESULTS

The data in Figure 1 show the effect of different concentrations of calcium on cell growth. The 1 BR cells grew poorly when calcium concentration was ≤0.6 mM. A considerable increase in cell growth was found between 0.6–2 mM $CaCl_2$, and the

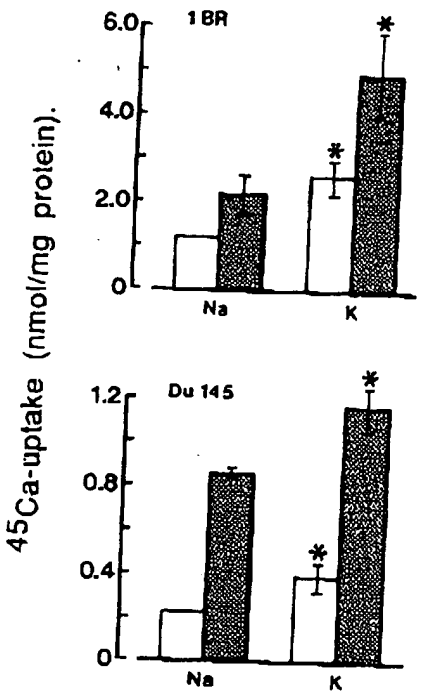

Fig. 2. Uptake of ^{45}Ca in DU 145 cancer cells and 1BR fibroblast cells, incubated in normal (Na) or in high potassium (K) depolarizing solution. ^{45}Ca uptake was measured after 1 min (□) and 20 min (▨). The results shown are means ±SE of three separate experiments performed in duplicate ($^{*}P < 0.05$).

cell count remained fairly constant in medium containing up to 4 mM $CaCl_2$. Compared to 1 BR the growth response of DU 145 cells was much greater at low calcium concentrations, maximum proliferation being achieved with 2 mM $CaCl_2$. The calculated EC_{50} for DU 145 cells and 1 BR fibroblasts was 0.12 mM and 0.66 mM calcium, respectively. Preliminary data on the time course of ^{45}Ca uptake showed that the uptake doubled from 1 to 20 min incubation and increased little thereafter—~20% in the next 20 min in both DU 145 cancer cells and 1 BR fibroblasts. Therefore, in the present experiments on ^{45}Ca uptake we obtained data after 1 and 20 min incubations.

In order to see whether voltage-dependent membrane calcium channels existed in these cells, ^{45}Ca influx was measured in a normal and high-potassium solution. High-potassium (80 mM KCl) solution was used to depolarize cell membranes. The data in Figure 2 clearly showed that calcium uptake in unstimulated polarized DU 145 cancer cells (Na) was 4–5 times lower than in 1 BR fibroblasts. Depolarization (K) caused a 2–3-fold increase in ^{45}Ca influx in 1 BR cells but only a 25–55% increase in DU 145 cancer cells. Further data were obtained only on DU 145 cells.

The data in Figure 3 show the effect of different concentrations of verapamil on the growth of DU 145 cells. Verapamil caused a significant inhibition of cell growth with an IC_{50} (concentration causing 50% inhibition of growth) of 55 μM. In some experiments the cells were exposed t the highest concentration (100 μM) of ve-

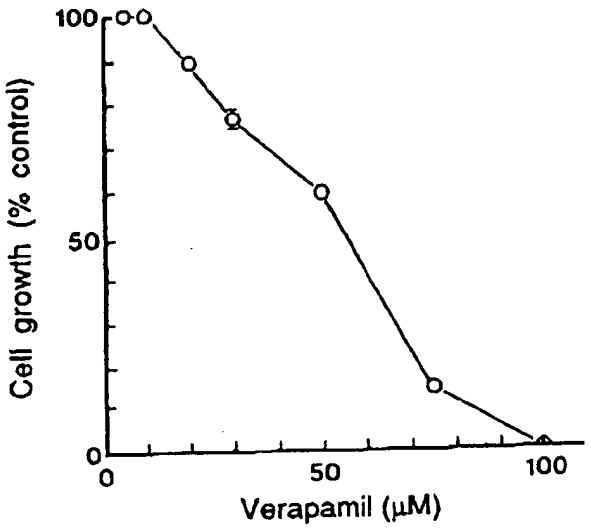

Fig. 3. Effect of different concentrations of verapamil (VPM) on the growth of DU 145 cells. Cells were plated 24 h previously at 10^5 cells in 3 ml medium. Cells were then grown in media containing various concentrations of verapamil, and viable cells were counted after 7 days. Data shown are mean values ± SE from three separate experiments performed in duplicate.

rapamil for 48 h, followed by a drug-free period of 4 days, and counted. It was found that the cell viability was over 90%, indicating that the effect of verapamil was reversible.

The effect of verapamil on ^{45}Ca uptake in DU 145 cells is illustrated in Figure 4. Verapamil caused an increase in ^{45}Ca uptake in both unstimulated and K-stimulated cells, with the largest change occurring in unstimulated (Na) cells. Verapamil inhibited K-stimulated ^{45}Ca uptake in fibroblasts by 45% but had no effect on unstimulated cells (data not shown). When ^{45}Ca was present in the growth medium continuously and measured in DU 145 cells after 7 days, the uptake in the presence of verapamil (75 μM) was doubled compared to that in control (Fig. 5). At lower concentrations (up to 30 μM), however, calcium uptake in these experiments was not elevated. Nifedipine, which is 10–20 times more potent as a calcium channel blocker than verapamil [33], had at a concentration of 10 μM no effect on ^{45}Ca influx or on cell growth in DU 145 cells (data not shown).

Low concentrations of lanthanum (10 μM) almost completely blocked ^{45}Ca influx in unstimulated (Na) DU 145 but had only a marginal effect on depolarized (K) cells (Fig. 6). Higher concentrations (1–10 mM) of lanthanum were required to completely block ^{45}Ca in depolarized DU 145 cells. Cell proliferation was also inhibited to about 50% by 1 mM lanthanum (data not shown).

Effects of the calmodulin inhibitors trifluoperazine and tamoxifen on cell growth and ^{45}Ca uptake in DU 145 cancer cells are shown in Figure 7 and 8, respectively. Both tamoxifen and trifluoperazine inhibited cell proliferation in a dose-dependent fashion with an IC_{50} concentration of approximately 5 μM for both drugs. These drugs had, however, no effect on ^{45}Ca influx either in unstimulated (Na) or depolarized (K) cells (Fig. 8).

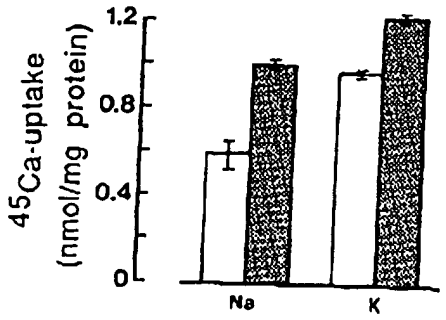

Fig. 4. Uptake of ^{45}Ca in DU 145 cells in normal (Na) and in high-potassium (K) depolarizing solution in the presence (▣) or absence (□) of 100 μM verapamil (VPM). Cells were incubated for 20 min. Data shown are mean values ± SD from two separate experiments performed in duplicate.

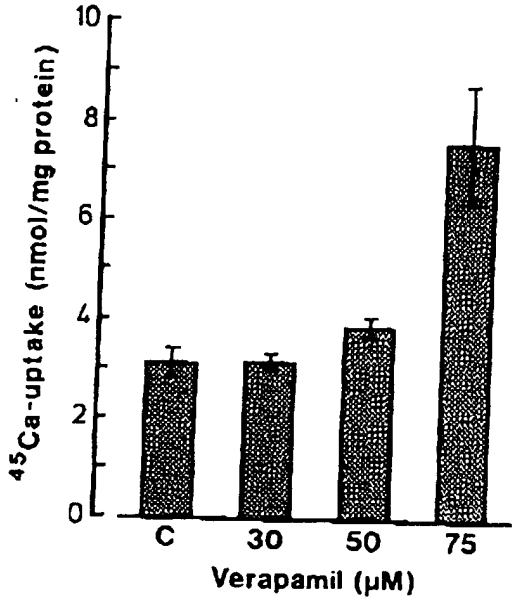

Fig. 5. Effect of verapamil on ^{45}Ca uptake in DU 145 cancer cells. Cells were plated 24 h previously at 10^5 cells in 3 ml medium. Cells were then grown in media containing various concentrations of verapamil with trace of ^{45}Ca. Cells were grown for 7 days and viable cells were counted. Data shown are mean values ± SE of three separate experiments, each performed in duplicate.

DISCUSSION

The present data clearly showed that the presence of calcium was essential for the growth of DU 145 human prostate cancer cells and of 1 BR human fibroblasts. Four to five times as many viable DU 145 cells as fibroblasts can be maintained in low calcium-supplemented medium. These data suggest that even small amounts of calcium, often present as a contaminant in the incubation medium, would be sufficient to support growth of cancer cells, which may explain the data in the literature

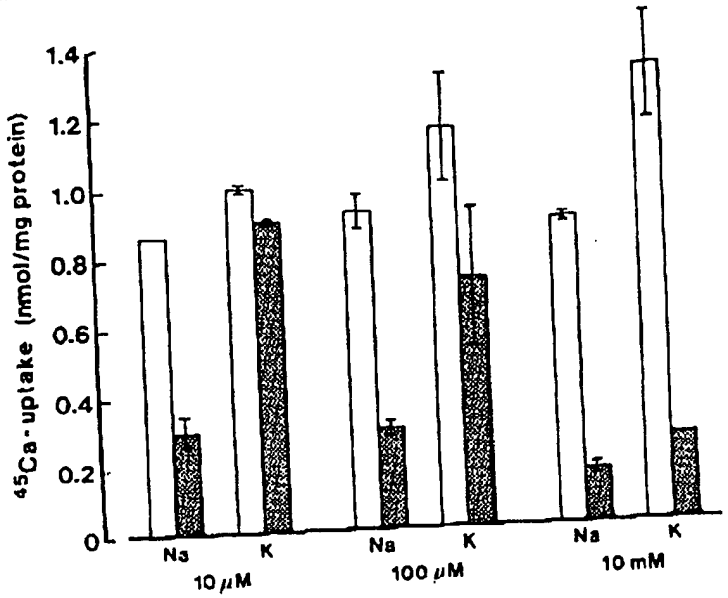

Fig. 6. Uptake of ^{45}Ca in DU 145 cancer cells in normal (Na) and in high-potassium (K) depolarizing solution in the absence (□) or presence (▨) of 10 μM, 100 μM, and 10 mM lanthanum. Cells were incubated for 20 min. The results shown are mean values ± SD from 2–3 separate experiments performed in duplicate.

claiming independence of cancer cell proliferation from extracellular calcium [34]. The much lower calcium uptake in DU 145 cancer cells compared to 1 BR fibroblasts (Fig. 2) is consistent with the higher sensitivity of DU 145 cell proliferation to extracellular Ca as compared to fibroblasts. These data are also in general agreement with previous observations showing a lower requirement for extracellular calcium for the proliferation of cancer cells than that of normal cells [8] and are essentially in agreement with the recent data of Chan [35] on ovarian cancer cells.

Verapamil, which is known to block the entry of calcium through potential-dependent channels, inhibited cell proliferation, although the concentration for total growth inhibition in the present work (100 μM) was almost tenfold higher than that which blocks calcium influx in excitable cells [36]. Our data are in agreement with the recent findings in brain tumor cells where the IC_{50} for growth inhibition ranged between 25 and 50 μM verapamil. These authors also showed decreased DNA-, RNA-, and protein synthesis accompanying cytotoxicity [37]. The data showing an increase in ^{45}Ca influx upon K-depolarization suggest that voltage-dependent calcium channels exist in DU 145 cancer cells. These channels could be blocked by verapamil in fibroblasts but, paradoxically, not in cancer cells.

An unexpected observation in the present study was that verapamil increased ^{45}Ca uptake in DU 145 cells both in unstimulated and depolarized cells, but more particularly in the former. To our knowledge this has not been reported previously in cancer cells. Very recently, however, Zaidi et al. [38] reported that in rat osteoclasts, verapamil at low micromolar concentrations did not block the entry of calcium, but

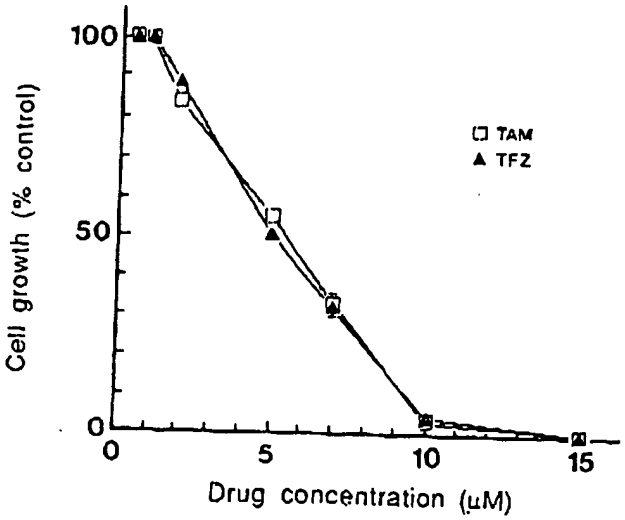

Fig. 7. Effect of different concentrations of trifluoperazine (TFZ) and tamoxifen (TAM) on the growth of human DU 145 cancer cells. Cells were plated 24 h previously at 10^5 cells in 3 ml medium. Cells were then grown in media containing various concentration of trifluoperazine or tamoxifen. Cells were grown for 7 days and viable cells were counted. Data shown are mean values ± SE from three separate experiments performed in duplicate for each drug.

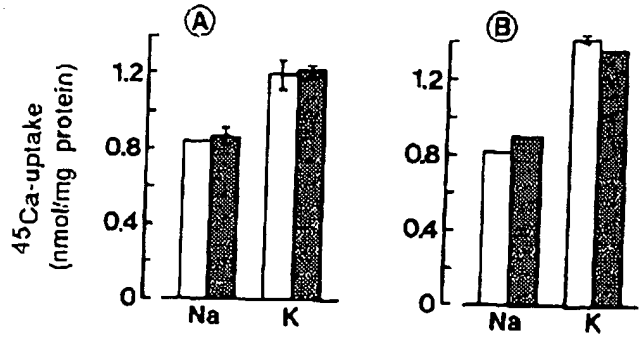

Fig. 8. Uptake of ^{45}Ca in DU 145 cells in normal (Na) and in high-potassium (K) depolarizing solution in the presence (▩) or absence (□) of 10 μM tamoxifen (A) or trifluoperazine (B). Cells were incubated for 20 min. The results shown are mean values ± SD from two separate experiments in duplicate for each drug.

at very high concentrations (300 μM or above) it led to a rapid and sustained elevation of intracellular calcium. Furthermore, they found that the effect of verapamil was specific for osteoclasts since it was not observed in macrophages and lymphocytes. Although in the present study we found an increase in cellular calcium by verapamil in DU 145 cancer cells, this was observed at much lower concentrations (75 μM) of verapamil than that observed in osteoclasts by Zaidi et al. [38]. It is conceivable therefore that the growth-inhibitory effect of verapamil on tumor cells may be related to the increase in cellular calcium which was quite substantial in

unstimulated (polarized) cells (Fig. 4). Since the verapamil-stimulated increase in calcium itself causes toxicity, it is reasonable to think that addition of verapamil makes drug-resistant cells more sensitive to therapy.

It has previously been suggested that an increase in cellular calcium is the final common pathway in cell death [39]. Orrenius et al. [40] have recently presented data showing that an increase in nuclear calcium preceded cell death. They suggested that an increase in the activity of calcium-activated endonucleases was an underlying mechanism. Interestingly, activation of Ca^{2+}-Mg^{2+}-dependent endonucleases appears to be one of the mechanisms for programmed cell death in the prostate [20,21]. This would be compatible with our observation of an increase in calcium uptake by verapamil and the reduction in DU 145 cell survival. The lack of effect of low concentrations (up to 30 μM), which inhibited cell proliferation, on calcium uptake could be explained by assuming that although no change in total cellular calcium was detected in these cells by the present method, nuclear calcium was elevated. Support for this assumption can be found in the recent data of Nicotera et al. [41] showing a very considerable increase in intranuclear calcium with a relatively small increment in extranuclear calcium. Answers to some of these questions could possibly be obtained by carrying out experiments at different extracellular calcium concentrations as well as by measuring the subcellular distribution of calcium in the presence of verapamil. Studies of this nature are in progress in our laboratory.

Our data demonstrating the inability of verapamil to inhibit K-stimulated calcium influx in DU 145 cells may also be explained by a possible dual effect of verapamil on calcium influx. The increase in calcium influx caused by verapamil may have partly masked the inhibition by verapamil of accelerated entry of calcium through voltage-dependent channels, which is consistent with a less than complete additivity observed in the presence of both verapamil and potassium. This could suggest the existence of a separate channel in DU 145 cells, through which calcium enters upon incubation with verapamil, which probably is voltage independent. Alternatively, verapamil might have an inhibitory effect on energy-dependent calcium extrusion by the membrane calcium ATP-ase pump.

Lanthanum has previously been shown to block both passive diffusion and channel-activated ^{45}Ca influx in cardiac and smooth muscle cells [42,43]. In the present studies lanthanum was also found to block both passive entry and accelerated influx of ^{45}Ca upon K-stimulation in DU 145 cells, although much higher concentrations were required to block the latter. This indicates that although voltage-dependent calcium channels in DU 145 cells could not be blocked by the classical organic calcium channel blockers such as verapamil and nifedipine, they were sensitive to lanthanum block.

Trifluoperazine, a calmodulin antagonist, and tamoxifen, which is now also known to interfere with calmodulin-mediated action in the cell besides being an antiestrogen, inhibited cell growth without any inhibition of ^{45}Ca influx in the present study. The observation is compatible with the suggestion for a role of calmodulin in cell proliferation. Although competition with the intracellular estrogen receptor is the general accepted mode of action of tamoxifen, recent reports on several other interesting pharmacological effects of tamoxifen have been published. Evidence has been presented that indicates that tamoxifen is a calmodulin antagonist [44], a calcium channel blocking agent [45], an inhibitor of protein kinase C [46], and more recently even to be an histaminic and cholinergic antagonist [47,48]. It therefore appears that

in addition to interference by tamoxifen in the normal processing of intracellular events triggered by estrogen, this drug may interact with cell membrane components. This is compatible with recent evidence showing the specific binding of tamoxifen in isolated microsomal fractions [49]. Although tamoxifen in the present experiments did not affect ^{45}Ca uptake, the growth-inhibitory effect could result from a combination of the above-mentioned actions of this drug.

Collective data on both trifluoperazine and tamoxifen would suggest that the effect of both these drugs was probably a result of their action within the cell. Both drugs might act through the inhibition of calmodulin-stimulated enzymatic reactions essential for cell proliferation.

In conclusion, the present data show that verapamil, a calcium channel blocker, and trifluoperazine and tamoxifen, calmodulin antagonists, can by themselves cause inhibition of cell growth of prostatic tumor cells. These agents, however, do not act via an inhibition of the entry of extracellular calcium in these cancer cells. In fact, the paradoxical increase in cellular calcium that was found after verapamil treatment of DU 145 cells could be a mechanism underlying its antiproliferative action. Whether this is operative in all tumor cells or is more specific for prostatic cancer cells remains to be explored.

ACKNOWLEDGMENTS

We thank Monica Heidenholm for technical assistance, and Maria Dahlberg and Annica Andersson for typing the manuscript. This work was supported by grants from the Swedish Cancer Society (2978-B91-01XAB) and the medical faculty, University of Lund.

REFERENCES

1. Chafouleas JG, Bolton WE, Hidaka H, Boyd AE, Means AR: Calmodulin and the cell cycle: Involvement in regulation of cell-cycle progression. Cell 18:41–50, 1982.
2. Durham ACH, Walton JM: Calcium ions and the control of proliferation in normal and cancer cells. Biosci Rep 2:15–30, 1982.
3. Means AR: Molecular mechanisms of action of calmodulin. Recent Prog Horm Res 44:223–262, 1988.
4. Parsons PG, Musk P, Goss PD, Leah J: Effects of calcium depletion on human cells in vitro and the anomalous behavior of the human melanoma cell line MM170. Cancer Res 43:2081–2087, 1983.
5. Tombes RM, Borisy GB: Intracellular free calcium and mitosis in mammalian cells: anaphase onset is calcium modulated, but is not triggered by a brief transient. J Cell Biol 109:627–636, 1989.
6. Criss WE, Kakiuchi S: Calcium: Calmodulin and cancer. Fed Proc 41:2289–2291, 1982.
7. Sasaki Y, Hidaka H: Calmodulin and cell proliferation. Biochem Biophys Res Common 104:451–456, 1982
8. Whitfield JF, Boynton AL, MacManus JP, Rixon RH, Sikorska M, Tsang B, Walker PR, Swierenga SHH: The roles of calcium and cyclic AMP in cell proliferation. Ann NY Acad Sci 339:216–240, 1980.
9. Chafouleas JG, Pardue RL, Brinkley BR, Dedman JR, Means AR: Regulation of intracellular levels of calmodulin and tubulin in normal and transformed cells. Proc Natl Acad Sci USA 78:996–1000, 1981.
10. Watterson DM, Van Eldik LJ, Smith RE, Vanaman TC: Calcium dependent regulatory protein of cyclic nucleotide metabolism in normal and transformed chicken embryo fibroblasts. Proc Natl Acad Sci USA 73:2711–2715, 1976.
11. Hickie RA, Kalant H: Calcium and magnesium content of rat liver in Morris hepatoma 5123 tc. Cancer Res 27:1053–1057, 1967.

12. MacManus JP, Braceland BM, Rixon RH, Whitfield JF, Morris HP: An increase in calmodulin during growth of normal and cancerous liver in vivo. FEBS Lett 133:99–102, 1981.
13. Wei JW, Morris HP, Hickie RA: Positive correlation between calmodulin content and hepatoma growth rates. Cancer Res 42:2571–2574, 1982.
14. Anghileri LJ, Miller ES, Robinette J, Prasad KN, Lagerborg VA: Calcium metabolism in tumors: its relationship with chromium complex accumulation II. Calcium, magnesium and phosphorus in human and animal tumors. Oncology 25:193–209, 1971.
15. Okazaki T, Mochizuki T, Tashima M, Sawada H, Uchino H: Role of intracellular calcium ion in human promyelocytic leukemia HL-60 cell differentiation. Cancer Res 46:6059–6063, 1986.
16. Shirakawa F, Yamashita U, Oda S, Chiba S, Eto S, Suzuki H: Calcium dependency in the growth of adult T cell leukemia cells in vitro. Cancer Res 46:658–661, 1986.
17. Yoneda T, Kitamura M, Ogawa T, Aya SI, Sakuda M: Control of VX2 carcinoma cell growth in culture by calcium, calmodulin, and prostaglandins. Cancer Res 45:398–405, 1985.
18. Swierenga SHH, Auersperg N, Wong KS: Effect of calcium deprivation on the proliferation and ultrastructure of cultured human carcinoma cells. Cancer Res 43:6012–6020, 1983.
19. Chan TCK, Howell SB: The effects of calcium, W7, WS, and a phorbol ester on human ovarian carcinoma cell growth. Fed Proc 45:450A, 1986.
20. Kyprianou N, English HF, Isaacs T: Activation of a Ca^{2+}-Mg^{2+}-dependent endonuclease as an early event in castration-induced prostatic cell death. The Prostate 13:103–117, 1988.
21. Kyprianou N, Isaacs JT: Activation of programmed cell death in the rat ventral prostate after castration. Endocrinology 122:552–553, 1988.
22. Gottesman MM, Pastan I: Resistance to multiple chemotherapeutic agents in human cancer cells. TIPS 9:54–58, 1988.
23. Kessel D, Wilberding C: Anthracycline resistance in P388 murine leukemia and its circumvention by calcium antagonists. Cancer Res 45:1687–1691, 1985.
24. Tsuruo T, Iida H, Tsukagoshi S, Sukursi Y: Potentiation of vincristine and adriamycin effects in human hemopoietic tumor cell lines by calcium antagonists and calmodulin inhibitors. Cancer Res 434:2267–2272, 1983.
25. Broxterman HJ, Pinedo HM, Kuiper CM, Kaptein LCM, Schuurhuis GJ, Lankelma J: Induction by verapamil of a rapid increase in ATP consumption in multidrug-resistant tumor cells. FASEB J 2:2278–2282, 1988.
26. Hiskias G, Keizer HJ: Increased cytosolic pH in multidrug resistant human lung tumor cells: Effect of verapamil. JNCI 81:706–709, 1989.
27. Anghileri LJ, Crone-Escanye MC, Robert J: Antitumor activity of Gallium and Lanthanum: Role of cation-cell membrane interaction. Anticancer Res 7:1205–1208, 1987.
28. Simpson WG: The calcium channel blocker verapamil and cancer chemotherapy. Cell Calcium 6:449–467, 1985.
29. Popper LD, Batra S: The kinetics of calcium uptake and the effect of calcium antagonists on ^{45}Ca influx and cellular growth in cancer cell lines. Cancer Chemother Pharmacol 24:83A, 1989.
30. Messing R, Carpenter CL, Greenberg DA: Mechanism of calcium channel inhibition by phenytoin comparison with classical calcium channel antagonists. J Pharmacol Exp Ther 235:407–441, 1985
31. Batra S: Uptake and energy-dependent extrusion of calcium in the rat uterus. Acta Physiol Scand 114:447–452, 1982.
32. Peterson GL: A simplification of the protein assay method of Lowry et al. which is more generally acceptable. Anal Biochem 83:346–356, 1979.
33. Kenakin TP, Beek D: The activity of nifedipine, diltiazem, verapamil, and lidoflazine in isolated tissues: An approach to the determination of calcium channel blocking activity. Drug Dev Res 5:347–358, 1985.
34. Swierenga SHH, Whitfield JF, Boynton AL, MacManus JP, Rixon RH, Sikorska M, Tsang BK, Walker PR: Regulation of proliferation of normal and neoplastic rat liver cells by calcium and cyclic AMP. Ann NY Acad Sci 349:294–311, 1980.
35. Chan TCK: Calcium-independent growth of human ovarian carcinoma cells. J Cell Physiol 141: 461–466, 1989.
36. Batra S: Characterization of (^3H)-nitrendipine binding to uterine smooth muscle plasma membrane and its relevance to inhibition of calcium entry. Br J Pharmacol 85:767–774, 1985.
37. Schmidt WF, Huber KR, Ettinger RS, Neuberg RW: Antiproliferative effect of verapamil alone on brain tumor cells in vitro. Cancer Res 48:3617–3621, 1988.
38. Zaidi M. Paradoxi. 167:807–
39. Schanne pathway.
40. Orrenius Pharmac
41. Nicotera free Ca^{2+}
42. Frank SJ: Publishin
43. Godfrain J Physiol
44. Lam HYF Biochem
45. Lipton A: Chemothe
46. O'Brian C Cancer Re
47. Batra S: In channel bl
48. Kroegar H. Commun
49. Watts CRW in MCF-7

The Prostate 33:112–122 (1997)

Potassium Conductance in the Androgen-Sensitive Prostate Cancer Cell Line, LNCaP: Involvement in Cell Proliferation

Roman N. Skryma, Natalia B. Prevarskaya, Luce Dufy-Barbe, Marie F. Odessa, Jacques Audin, and Bernard Dufy*

Laboratory of Neurophysiology, University of Bordeaux II, Bordeaux, France

BACKGROUND. Very little is known about the expression of ion channels in prostate cells (both normal and malignant), and their possible role in physiological and pathological functions. We therefore studied ion conductances and their role in the proliferation of LNCaP cells, an androgen-sensitive human prostate cancer cell line.

METHODS. We applied patch-clamp recording techniques for electrophysiological studies, and ^{3}H-thymidine incorporation and protein content assays for cell growth studies.

RESULTS. Only one type of voltage-dependent ion conductance, a potassium K^+ conductance, was identified. This current, which was depressed by a rise in intracellular Ca^{2+}, had a high sensitivity to tetraethylammonium (TEA) (with half-block at 2 mM) and was also inhibited by 2 nM α-dendrotoxin (DTX) and 20 nM mast-cell degranulating peptide (MCDP). K^+ channel inhibitors inhibited [^{3}H]thymidine incorporation and protein content, in a dose-dependent fashion, indicating that K^+ channels are involved in cell growth.

CONCLUSIONS. We conclude from our findings that the human cancer prostate cell line LNCaP has a new type of K^+ channel, likely to play an essential role in the physiology of these cells and, more specifically, in cell proliferation. *Prostate 33:112–122, 1997.*

KEY WORDS: **LNCaP cells; K^+ channels; patch clamp; proliferation**

INTRODUCTION

LNCaP is an androgen-sensitive human prostate cancer cell line, derived from a lymph node of a subject with metastatic carcinoma of the prostate [1]. The growth of these cells, like prostate glandular cells, is extremely sensitive to androgens [2–5]. For this reason, the LNCaP cell line has been extensively studied and used as a model for studies of prostate cancer cell growth [6–8]. Control of prostate cancer cell proliferation is believed to depend on both external (hormones and growth factors) and internal signals that modify the activity of cell cycle proteins [9–12]. However, it is not clear which intracellular transduction mechanism from the cell surface to the nucleus mediates these processes. Several second-messenger pathways have already been shown to be implicated in the regulation of prostate cell proliferation: the protein kinase A (PKA)-dependent pathway [13,14], the protein kinase C (PKC)-dependent pathway [15], and the calcium-calmodulin kinase-dependent pathway [16]. In various cell models, membrane ion channels have been shown to be involved in these second-messenger transduction pathways [17,18]. Ion channels have also been thought to play an important role in the regulation of growth and proliferation. A number of studies have shown that the mechanisms promoting the cell proliferation and tumorization processes often involve

Roman N. Skryma and Natalia B. Prevarskaya are now at the Laboratoire de Physiologie cellulaire, Université des Sciences et Technologie de Lille, Flandre-Artois (Lille I), Cité Scientifique (Bat. 3N), 59655 Villeneuve-D'Ascq Cedex, France.

*Correspondence to: Bernard Duffy, Laboratoire de Neurophysiologie, CNRS UMR 5543, Université de Bordeaux II, 146 rue Léo Saignat, 33076 Bordeaux Cedex, France.

Received 11 July 1996; Accepted 28 October 1996

the activation of voltage- and/or calcium-activated potassium K^+ channels. Most of these studies were performed on T-lymphocytes, where K^+ channels may play a role in the triggering and/or support of mitogen-induced proliferation [19–23]. Potassium channel blockers not only block lymphocyte voltage-gated potassium currents, but also inhibit mitogen-stimulated proliferation in long-term cell culture [21]. Experiments on other cell types have also implicated potassium channels in mitogenic responses [24]. Functional voltage-dependent potassium channels are necessary for the normal proliferation of brown fat cells in culture [25]. The incidence of a 23-pS potassium channel is correlated to the rate of cell proliferation in breast carcinoma cells [26], while delayed rectifier potassium channels are involved in the control of melanoma cell proliferation [27]. It has also been suggested that K^+ channels are significant in cell transformation by oncogene products: in mammalian fibroblasts, ras oncogene expression is associated with the appearance of a Ca^{2+}-activated K^+ current [28], and the oncogene product pp60 v-src profoundly modulates K^+ channel properties [29]. The signal transduction between ion channel stimulation and gene expression involves a series of specific serine-threonine and tyrosine kinases [30,31]. We have recently shown that K^+ channels are constitutively associated with JAK2 tyrosine kinase [32], known to be implicated in the proliferation and tumorization processes [33].

In prostate cells (both normal and malignant), the expression of ion channels, and their possible role in physiological and pathological functions, including proliferation, apoptosis, secretion, differentiation, and tumorization, have never been investigated. We present here the first electrophysiological study of androgen-sensitive prostate cancer cells, of the LNCaP line, using the patch-clamp recording technique. We show that these cells express voltage-activated Ca^{2+}-dependent K^+ channels but not voltage-dependent Ca^{2+} channels. We also show that these voltage-sensitive K^+ channels are involved in the control of LNCaP cell proliferation.

MATERIALS AND METHODS

Chemicals

Tetraethylammonium (TEA), α-dendrotoxin (DTX), and mast-cell degranulating peptide (MDCP) were obtained from Sigma Chemical Co. (L'Isle d'Abeau, France). Charybdotoxin (CTX) and iberiotoxin (IBTX) were obtained from Latoxan (Rosans, France).

Cell Culture

LNCaP cells from the American Type Culture Collection (Rockville, MD) were grown in RPMI 1640 (Biowhittaker, Fontenay sous Bois, France) supplemented with 5 mM L-glutamine (Sigma Chemical Co.) and 10% fetal bovine serum (Seromed, Poly-Labo, Strasbourg, France). The culture medium also contained 50,000 IU/l penicillin and 50 mg/l streptomycin. Cells were routinely grown in 50-ml flasks (Nunc, Poly-Labo) and kept at 37°C in a humidified incubator in an air/Co_2 (95%/5%) atmosphere.

Cells were subcultured in petri dishes (Nunc) or round glass coverslips coated with poly-ornithine (5 mg/l; Sigma Chemical Co.) for electrophysiology or microspectrofluorimetry, respectively. They were used after 4–6 days.

Electrophysiological Recording

The whole-cell, cell-attached, inside-out, and outside-out modes of the patch technique were employed. The electrodes were pulled on an L/U-3P (List-Medical, Darmstad, Germany) puller in two stages from borosilicate glass capillaries (Clark, Pangbourne Readings, UK) (1.5 mm in diameter) to a tip diameter of 1.5–2.0 μm. Patch electrodes were coated with sylgard and then fire-polished. The pipettes had an average resistance of 2–4 MΩ.

Cultures were viewed under phase contrast with a Leitz-Diavert (Leitz, Wetzlar, Germany) inverted microscope. Electrodes were positioned with Leitz micromanipulators. Grounding was achieved through a silver chloride-coated silver wire inserted into an agar bridge (4% agar in electrode solution).

An Axopatch-1D amplifier (Axon Instruments, Foster City, CA) was used for tight-seal, whole-cell, outside-out, inside-out, and cell-attached voltage clamping. Stimulus control and data acquisition and processing were carried out with a PC computer, Tandon AT-80386 (Tandon, Moorpark, CA), fitted with a Labmaster TL-1 interface, using Pclamp 5.5.1 software (Axon Instruments interface and software).

Electrode offset was balanced before forming a giga-seal. Seal resistances were typically in the range of 13–30 GΩ. Leakage and capacitative current subtraction protocols were composed of four hyperpolarizing pulses one fourth of the test pulse size, applied from the holding potential before the test pulses. During data analysis, leak data were scaled and subtracted from the raw data. Series resistances were compensated. Series resistances were calculated before and after compensation. The series resistance averaged 1.15 MΩ and ranged from 0.4–1.7 MΩ. Recordings where series resistance resulted in a 5-mV or greater

error in voltage commands were discarded. Currents were low-pass filtered at 2 kHz (whole-cell) with an 8-pole Bessel filter (−3 dB; Axon Instruments) and digitized at 10 kHz for storage and analysis.

Data Analysis and Statistics

Peak currents in whole-cell recordings were measured using the automatic peak detection function in the Clampan section of the Pclamp software. Late currents measured isochronally were taken before the end of the pulse to avoid capacitative transients spread out by digital filtering.

Single-channel data analysis was performed after elimination of capacity transients and leak current by subtraction of record averages without channel activity from each current record. The openings and closings of the channel were detected using the criterion of a 50% excursion between fully open and fully closed states to determine the occurrence of an opening or closing event, such as crossings of the line at a half distance between zero current level and a level corresponding to the average open channel amplitude. In this way, real current records were put into ideal form by setting all intermediate amplitudes to the level of zero current line or to the level of the average open-channel amplitude. The open probability was calculated as the open-time integral divided by the number of channels in the patch and the duration of the data segment analyzed. The number of channels was estimated by examining the record for multiple openings under conditions of high open probability ($P > 0.75$). Ten-second data segments were analyzed for open probability estimates.

Results are expressed as means ± standard deviation where appropriate. Each experiment was repeated several times. Student's *t*-test was used for statistical comparison among means and differences, with $P < 0.05$ considered significant.

Recording Solutions

For whole-cell voltage clamp studies, the standard extracellular solution contained (in mM): 140 NaCl, 5 KCl, 10 $CaCl_2$, 2 $MgCl_2$, 0.3 Na_2HPO_4, 0.4 KH_2PO_4, 4 $NaHCO_3$, 5 glucose, and 10 HEPES (N-2-hydroxyethylpiperazine-N'-2-ethano-sulfonic acid). The osmolarity of the external salt solution was adjusted to 300–310 mosmol/kg with sucrose, and pH was adjusted to 7.3 ± 0.01 with NaOH. To study ionic selectivity, external KCl was increased to 75 mM and to 150 mM by replacement with equimolar amounts of NaCl. The recording pipette was filled with an artificial intracellular saline containing (in mM): 150 KGlu, 2 $MgCl_2$, 1.1 EGTA (ethyleneglycol bis (b-aminoethyl ether-N,N,N',N'-tetraacetic acid), and 5 HEPES (pH 7.3 ± 0.01 with KOH), osmolarity 290 mosmol/kg.

Free Ca^{2+} concentrations in the range of 10 nM–1 μM for the solutions, applied from the inner side of membrane, were buffered with 1.1 mM EGTA and were calculated using the method of Abercrombie et al. [34]. Calcium concentrations >1 μM were achieved by adding the desired amount of $CaCl_2$.

To allow local drug application to the investigated cell, an additional "pouring" pipette with a tip opening of 10–30 μm was used. This pipette was filled with the same extracellular saline as in the bath, and the drug under investigation was added to it in appropriate concentrations. The pipette was brought close to the investigated cell at a distance of 50–90 μm. All experiments were performed at room temperature (20–22°C).

Microfluorimetric Assay of Cytosolic Ca^{2+}

Intracellular free calcium concentration was measured on individual cells using the fluorescent Ca^{2+} probe indo 1. The method has been previously detailed [35]. Briefly, cells were loaded for 25 min in HBSS (in mM) (142.6 NaCl, 5.6 KCl, 2 $CaCl_2$, 0.8 $MgCl_2$, 5 glucose, and 10 HEPES, pH 7.3, adjusted with NaOH; osmolality was 300 mosmol) containing 5 μM indo-1 acetoxymethylester (indo 1 AM, Sigma Chemical Co.) and 0.02% Pluronic 127 (Molecular Probes, Eugene, OR). The cells were then rinsed three times and placed in HBSS for Ca^{2+} measurements. Test substances were applied to the cells by low-pressure ejection from micropipettes (tip diameter 3–5 μM) positioned 20 μM from the cell membrane.

Indo-1 was excited at 355 nm, and the emitted fluorescence was measured at 405 and 480 nm by separate photometers (Nikon, Paris, France). The voltage signals from the photometers were divided on-line by an analog divider (AD 535, Analog Device, Norwood, MA). After subtraction of the mean background, the F405/F480 ratio was recorded on-line as a voltage trace of a pen recorder (Gould, Paris, France), digitized (TL1-DMA, Interface, Axon Instruments), stored, and analyzed on an IBM PC using Axotape software (version 1-2.0.1, Axon Instruments).

Cell Proliferation Assays

For ^3H-thymidine incorporation and protein assay experiments, the cells were seeded in 24-well plates (Nunc) precoated with poly-ornithine (5 mg/l) at 5×10^4 cells per well. K^+-channel inhibitors were added at given concentrations 2 hr after plating. Each concentration was tested in quadruplicate wells, and experiments were performed at least three times.

^{3}H-thymidine Incorporation Assay

Forty-eight hours after the addition of channel inhibitors, 50 nM of ^{3}H-methyl-thymidine (ICN, Orsay, France, specific activity, 60 Ci/m mole) were added to each well for 24 hr. At the end of this pulse period, the medium was discarded, the cells were rinsed twice in RPMI, and chase was achieved by 2 hr of incubation in 50 μM unlabeled thymidine in RPMI. The chase medium was discarded and the cells were lysed in 0.1 M sodium hydroxyde. The lysis medium was neutralized with 0.1 M hydrochloric acid and transferred into vials containing 6 ml of liquid scintillation counting medium (Ready Safe, Beckman, Gagny, France). The mixture was thoroughly emulsified and counted 24 hr later in a Beckman LS6000IC spectrometer (Beckman Instruments, Fullerton, CA).

Protein Assay

Proteins were measured according to the method of Bradford [36], using the Biorad Protein Assay Reagent (Bio-Rad, Munich, Germany). Briefly, after 72 hr of culture under various conditions, the culture medium was discarded and the cultures were rinsed in phosphate-buffered saline (PBS). The cells were then lysed in 1 ml distilled water, and 100-μl fractions of the cell lysates were added to 2 ml of dye protein reagent diluted in distilled water (20/80). The various samples were thoroughly emulsified, and optical density (OD) was measured at 595 nM.

Detection of Apoptosis

Possible apoptotic cell death after 72 hr of culture in 4 mM TEA was assessed by two methods: 1) an "in situ" cell death assay, where direct immunofluorescence of digoxigenin-labeled genomic DNA in formalin-fixed cell cultures was identified using the Apoptag fluorescence kit (Oncor, Gaithersburg, MD); and 2) electrophoretic analysis of extracted DNA. DNA was extracted from 5×10^6 cells according to Blin and Stafford [37] and electrophoresed on 2% agarose gels in tris-acetate EDTA buffer. The gels were stained with ethidium bromide and photographed.

RESULTS

Passive Membrane Properties

Under whole-cell voltage clamp, the capacitative transient current decayed according to an exponential function, indicating a cell capacitance of 16 ± 3 pF (n = 7). The membrane resting potential of LNCaP cells varied from −30−−70 mV, with an average value of −42 ± 6 mV (n = 11). Increasing the external K^+ concentration from 5 to 50 mM depolarized the cell membrane by approximately 20 mV, showing the contribution of K^+ conductance to the resting potential.

K^+ Conductance Identification

In order to test for the presence of ion conductances in LNCaP cells and simultaneously visualize all voltage-dependent currents, voltage steps of 10 mV were applied, from a holding potential of −80 mV. Pulse duration was 200 msec, and stimulation frequency was 1 pulse every 30 sec. Figure 1A shows a typical recording performed on an LNCaP cell. Only outward conductance was observed at all membrane potentials. Responses to voltage steps were similar, even when all cells were held at −80 mV, irrespective of their previous membrane potential. Outward membrane currents were activated between −40−−30 mV, and this characteristic was independent of the holding potential value. Once this current attained its peak value, it did not inactivate. The current-voltage (I–V) relationship for outward current in a 5-mM external and 150-mM internal K^+ gradient is shown in Figure 1B, demonstrating that the outward current in LNCaP cells displays an outward rectification for large membrane depolarizations.

The reversal potential of the outward current was estimated from the reversal of the tail currents at a [K^+] concentration of 5 mM in the bath (Fig. 1C). The cells were first stepped by a prepulse from −70 mV to a potential which activated the outward current (+30 mV) for 50 msec and then shifted back by a test pulse to various potentials between −120−−10 mV in 10-mV steps for 50 msec. The amplitude of the tail current (measured 10 msec after the beginning of the test pulse minus steady-state current) was plotted against the voltage of the test pulse. This measurement underestimates the actual tail current amplitudes, but can be used to determine the reversal potential of the current [38]. However, it does avoid a possible distortion of the early current phase by the capacitive artifact. In the example shown in Figure 1D, the resulting I–V curve reversed at a potential of −85 mV. The average value of the reversal potential for LNCaP cells was −83.3 ± 2.5 mV (n = 8), close to the calculated potassium equilibrium potential (E_K = −89 mV). As the external K^+ concentration was increased from 5 to 50 mM, the reversal potential of the current shifted to the right, equalizing to 0 mV in a symmetrical K^+ gradient (150 mM external and 150 mM internal), as could be expected from a channel that is mainly permeable to K^+.

When an equimolar concentration of Cs^+ (150 mM) or Na^+ (150 mM) was substituted for K^+ in the pipette solution, the outward conductance was blocked over the whole range of depolarizing steps, confirming the

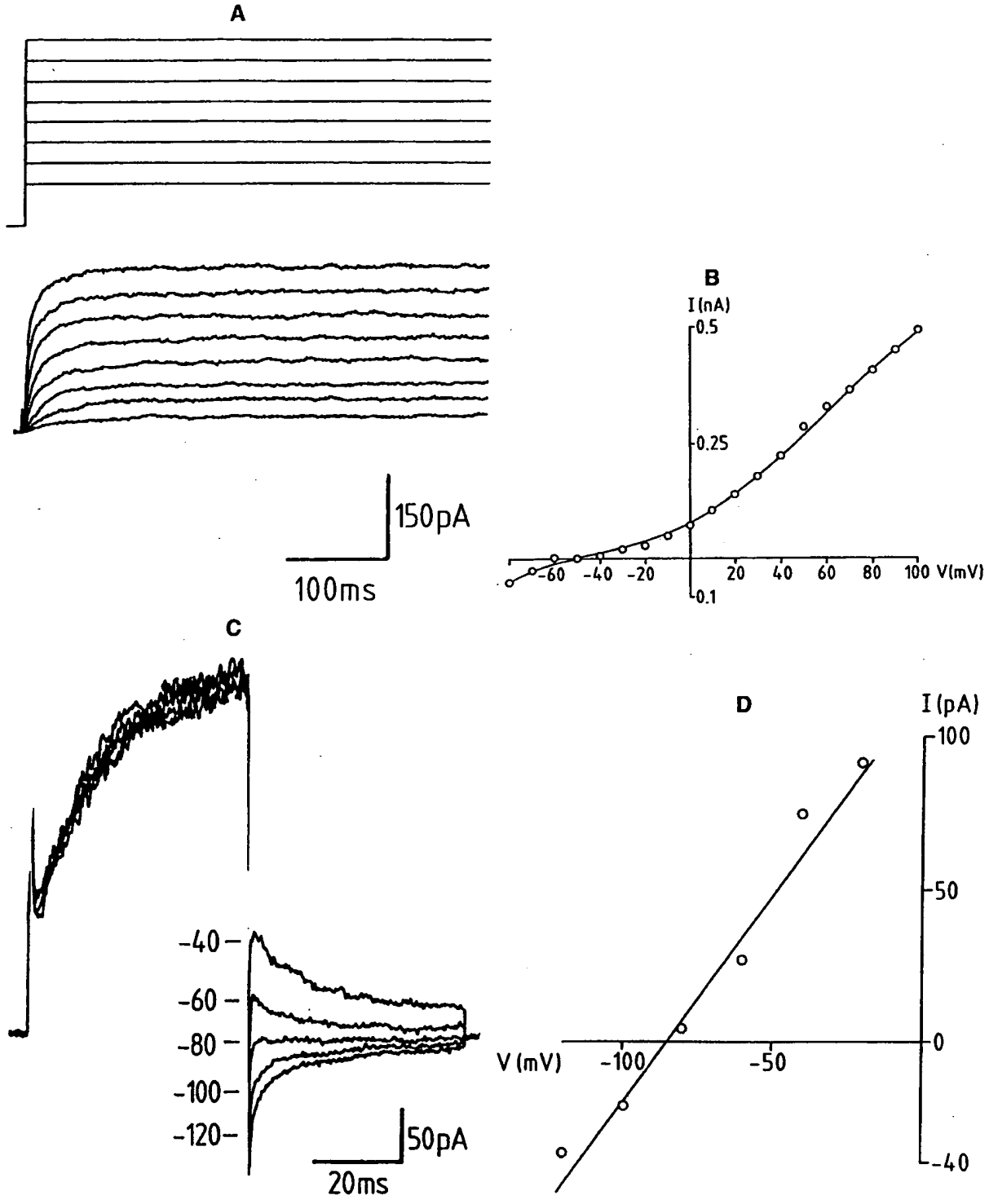

Fig. 1. Voltage-activated K^+ conductance in LNCaP cells. **A:** Voltage command pulses of increasing amplitude were applied from −80–+100 mV (holding potential (Vh) of −80 mV; step duration 200 msec). Upward deflection indicates an outward (K^+) conductance. A downward deflection at the beginning of the voltage step would have indicated an inward (Na^+ or Ca^{2+}) current. **B:** Current-voltage (I–V) relationship of K^+ conductance. **C:** Tail-currents evoked by a double-pulse protocol. The cells were held at −70 mV and stepped by a 50-msec prepulse to +30 mV. The membrane was then repolarized by 50-msec test pulses to the levels indicated. **D:** I–V relationship for tail current (measured 10 msec after onset of test pulse minus steady-state current) from the cell shown in C.

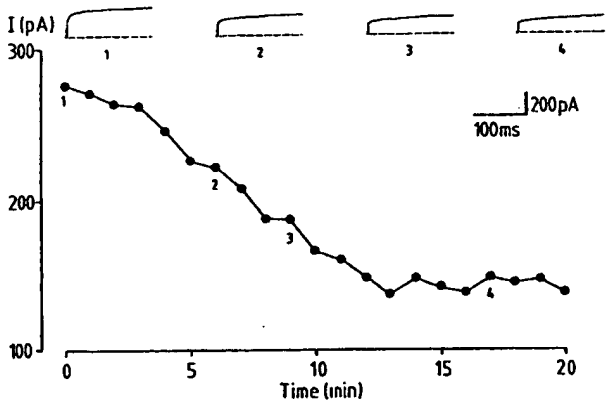

Fig. 2. $[Ca^{2+}]i$ sensitivity of K^+ channel. Time course of the inhibition of K^+ current by 0.2 μM free Ca^{2+} concentration. Plot of K^+ current (I) vs. time and respective original current records (1–4) obtained by 200-msec depolarizing test pulses to +30 mV from holding potential of −70 mV (top).

specificity of outward currents for K^+ ions.

Neither sodium nor calcium voltage-dependent conductances were observed in LNCaP cells under our experimental conditions, in a wide range of membrane potentials.

Ca^{2+} Dependence of K^+ Conductance

The standard pipette solution contained 0.01 μM Ca^{2+} (see Materials and Methods). When the internal free Ca^{2+} concentration was increased to 0.2–1 μM, the amplitude of the K^+ current gradually decreased following rupture of the seal. In control conditions of whole-cell experiments, the K^+ current was almost stable under internal perfusion. No decrease in current (or "run-down") was observed during recordings lasting 20 min or more. Figure 2 shows an example of the time-dependence of the decrease in K^+ current caused by the 0.2-μM free-Ca^{2+} concentration. Within approximately 10 min of perfusion the outward current was almost completely inhibited (n = 5).

Pharmacology of K^+ Channels

We have investigated the sensitivity of K^+ channels in LNCaP cells to various pharmacological K^+ channel blockers. In our experiments, the drugs were applied locally, close to the soma of the cell under study using a 40–50-μm pressure ejection micropipette. Under these conditions, it was assumed that the drug concentration close to the cell membrane (applied at low pressure) was close to the concentration of the solution in the micropipette.

We first studied the effect of a potent K^+ channel blocker, tetraethylammonium (TEA), that had previously been shown to inhibit various types of K^+ channels in different cell models [39,40]. The action of externally applied 4 mM TEA on K^+ currents is shown in Figure 3. The I–V curve was determined before TEA application, and activating voltage steps were then applied at 1-sec intervals as the TEA-containing micropipette was brought close to the cell. A second I–V relationship for K^+ current was determined when the TEA effect was maximal (after 1 min of TEA application) (Fig. 3B). K^+ current decreased within 3 sec of the onset of TEA application, and the effect remained stable until the micropipette was removed. The effect of TEA was reversed by removal of the TEA-containing pipette. As shown in Figure 3B, TEA application did not affect the K^+ current threshold, but reduced the K^+ channel conductance, as shown by the different slopes of the I–V relationships obtained before and during TEA application. The IC_{50} was estimated at 2 mM.

TEA did not affect the internal calcium concentration $[Ca^{2+}]_i$, measured using a microfluorimetric assay with the fluorescent Ca^{2+} probe indo 1, at any of the concentrations used (Fig. 4).

We checked the effect of 4-aminopyridine (4-AP), widely used as a selective inhibitor of transient K^+ currents [38,40]. 4-AP (1 mM) did not affect K^+ conductance in our studies at all membrane potentials.

Several recently characterized toxins have been used to determine the different kinds of potassium channels expressed in a variety of cells [41]. We used several toxins known to inhibit voltage-dependent K^+ channels. Charybdotoxin (CTX) and iberiotoxin (IBTX), inhibitors of Ca^{2+}-activated K^+ channels in several cell models [41–43], had no effect on K^+ channels in LNCaP cells.

Conversely, α-dendrotoxin (DTX), a polypeptide isolated from the venom of the green mamba snake *Dendroaspis angusticeps* [44], dramatically decreased the amplitude of the K^+ current in LNCaP cells in whole-cell recordings. The onset of action of DTX was in the range of 2–10 min and depended on the concentration. Low concentrations of DTX (0.2–0.5 nM) required a longer time (approximately 10 min) for onset of action and induced a smaller reduction in K^+ current. For DTX concentrations in the 2–5-nM range, onset of action was in the range of 3–5 min, and the reduction to half-amplitude current was completed within 8 ± 2 min. Figure 5 gives an example of the time-dependence of 5-nM DTX application for 8 min on the K^+ currents for a depolarizing voltage shift to +50 mV from a holding potential of −70 mV in LNCaP cells. The maximal reduction in K^+ current obtained with DTX (5 nM) was 53 ± 13% (n = 7). After DTX washout, the K^+ current reversed very slowly and did not reach the initial amplitude even after 30 min.

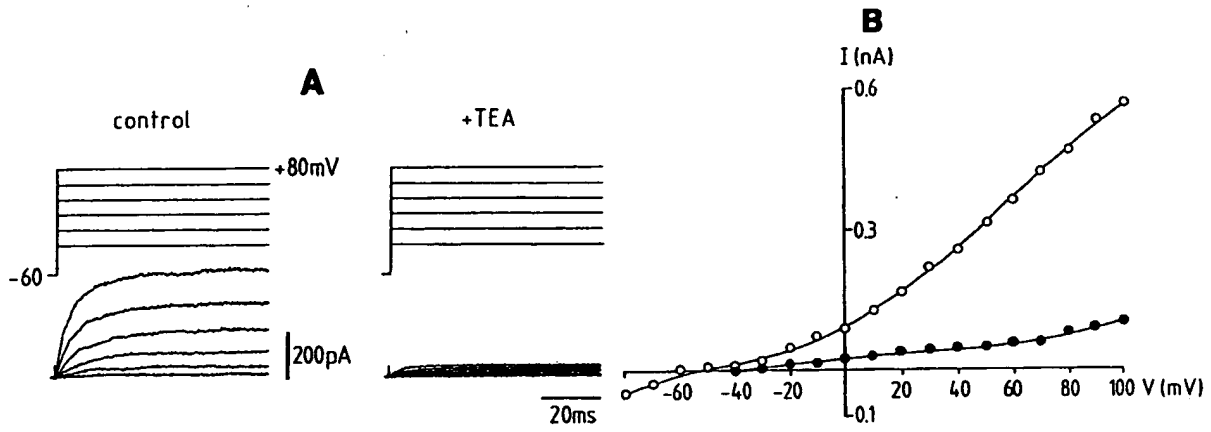

Fig. 3. Effect of TEA on K^+ current. **A:** Example of the effect of 4 mM TEA on K^+ current recorded before TEA application **(left)**, and 1 min after TEA application **(right)**. Voltage command pulses of increasing amplitude were applied from −80–+100 mV (Vh of −80 mV; step duration, 200 msec). **B:** I–V relationships of K^+ conductance before (○) and after (●) TEA application, corresponding to K^+ currents in A.

We also used mast-cell degranulating peptide (MCDP), extracted from bee venom [41], that selectively blocked voltage-activated K^+ currents in several other systems. MCDP inhibited the amplitude of the K^+ current in LNCaP cells with the same slow kinetics as DTX (data not shown). The maximal reduction in K^+ current with MCDP (80 nM) was 55 ± 11% (mean value ± SD, n = 5) for a depolarizing voltage shift +30 mV from the holding potential of −70 mV. When the K^+ current was already inhibited by 5 nM DTX, the subsequent addition of 80 nM MCDP was ineffective (Fig. 5), indicating that these two peptides affect a common set of K^+ channels.

Modulation of Cell Proliferation by Potassium Channel Blockers

In order to determine whether proliferation of LNCaP cells was altered by potassium channel modulators, we used the ^{3}H-thymidine incorporation assay and protein assay.

Figure 6 shows that TEA inhibited [^{3}H] thymidine incorporation in a dose-dependent fashion after 3 days of culture. TEA also significantly inhibited protein content, as shown in Figure 6B. MCDP (at a concentration of 80 nM, which inhibited the half-amplitude of the K^+ current in electrophysiological experiments) also inhibited [^{3}H] thymidine incorporation by 56 ± 6% (n = 5) of controls. As DTX is known to be unstable in long-term experiments (see "Sigma Peptide and Amino Acid Catalog: Handling, Reconstitution and Storage of Peptides," 1992), it was not used in cell proliferation assays. The inhibitory effects appeared to be correlated with K^+ channel inhibition, as 4-AP had no effect on either K^+ channel conductance in electrophysiological studies, nor on ^{3}H-thymidine incorporation nor on protein content (data not shown). Furthermore, alteration in cell-growth kinetics by K^+ channel blockers was not due to cytotoxicity, as the percentage of cells excluding trypan blue was not affected by incubation with the blockers in the range of concentrations used.

K^+ Channel Inhibition and Apoptosis

As tumor-cell populations may simultaneously undergo proliferation and programmed (apoptotic) death, we investigated whether K^+ channel blockers induced apoptosis in LNCaP cells. We used 4 mM TEA, the most effective concentration in inhibiting cell proliferation under our experimental conditions. Gel electrophoresis showed no evidence of the DNA fragmentation characteristic of apoptosis after a 72-hr treatment with TEA. Similarly, the percentage of immunostained cells in the in situ cell-death assay was identical (<2%) in control and TEA-treated populations.

DISCUSSION

Metastatic prostate cancer is one of the most widespread malignant diseases for which no cure has yet been found. Many studies on the proliferation of prostate cells have focused on the effect of steroids and their role at the genomic level. A novel approach aimed at understanding the role of plasma membrane-related events may be of special interest in these tumor cells.

Membrane ion channels of prostate cells had not been characterized until now. A systematic search (via the Medline information system) located two papers, in which the existence of L-type calcium channels in

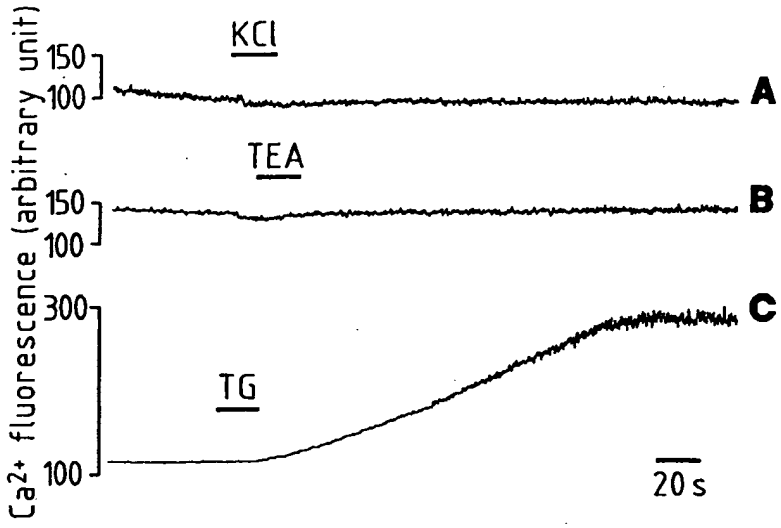

Fig. 4. Intracellular Ca^{2+} measurements in single LNCaP cells by the indo 1 method. Effect of short (20-sec) applications of 30 mM KCl **(A)**, 10 mM TEA **(B)**, and 1 μM thapsigargin **(C)**. The calcium concentration has been expressed in arbitrary units.

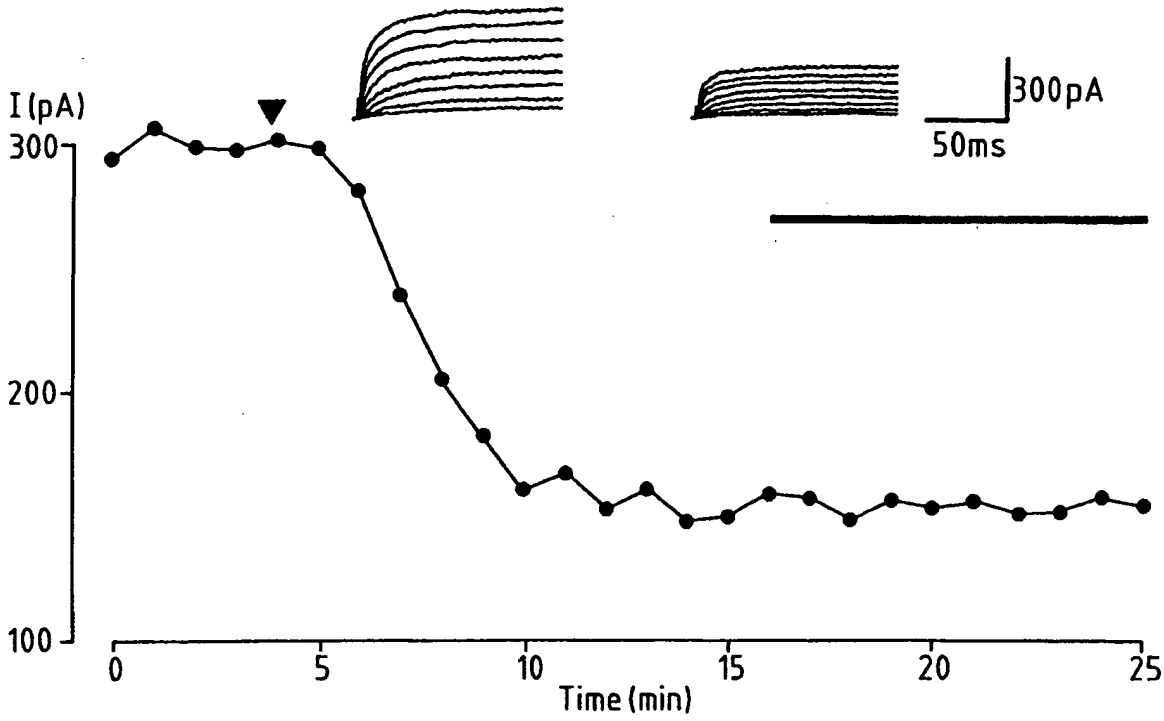

Fig. 5. Effect of DTX and MCDP on K^+ conductance. Time course of the inhibition of K^+ current by 5 nM DTX. **Above:** Current traces obtained by 200-msec test pulses from holding potential of −70 mV to different test potentials for the control solution **(left)** and 10 min after 5-nM DTX application **(right)**. **Below:** Respective plot of K^+ current amplitude vs. time at the membrane potential of +50 mV. ▼, DTX application starting time. Horizontal bar indicates an episode of 80-nM MCPD application.

LNCaP cells [45] and the presence of high-conductance K^+ channels in the prostate carcinoma (PC3) cell line [46] were inferred from only biochemical and pharmacological experiments.

For the first time we have applied the electrophysiological approach and the patch-clamp recording technique to identify directly the ion conductances in LNCaP cells. We found that, in all cells investigated,

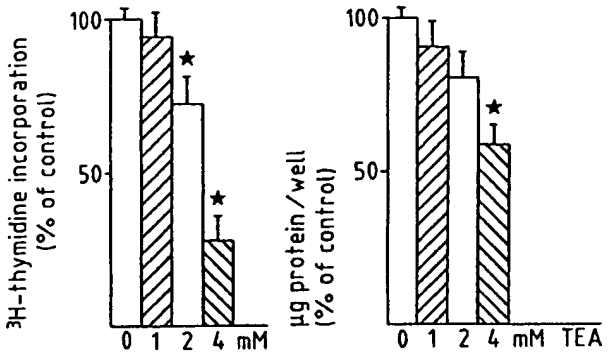

Fig. 6. Synopsis of the modulation of LNCaP cell proliferation by K^+ inhibitors. **Left:** Changes in ^3H thymidine incorporation induced by TEA (left to right: control; 1 mM TEA; 2 mM TEA; 4 mM TEA) (n = 3). **Right:** Effect of TEA on protein content (left to right: control; 1 mM TEA; 2 mM TEA; 4 mM TEA) (n = 3). Means ± SD are depicted. Significant changes ($P < 0.05$) obtained from student's t-test are indicated by asterisks.

only an outward potassium conductance was present. No voltage-dependent calcium conductance of any type, nor any sodium conductance, was observed. LNCaP cells are known to be electrically nonexcitable as they are not capable of producing action potentials in response to depolarizing voltage stimulation. It is, therefore, not surprising that they lack both Na^{2+} and Ca^{2+} voltage-dependent channels. In these cells, potassium conductance seems to play an essential role in the maintenance of cell membrane potential, as the rise in extracellular K^+ ion concentration depolarized the cell membrane.

A specific property of LNCaP-cell K^+ channels is that they are directly and reversibly inhibited by intracellular Ca^{2+}. This rather unusual property of voltage-dependent K^+ channels has also been reported in lymphocytes [47,48] and rat microglial cells [38].

To further characterize the type of voltage-dependent K^+ channels expressed in LNCaP cells, we used several toxins known to specifically inhibit different types of K^+ channels in other cell models. CTX, known to inhibit Ca^{2+}-dependent K^+ channels [43,49], was not capable of inhibiting K^+ channels in LNCaP cells. However, two toxins, DTX and MCDP, that have never been shown to inhibit K^+ channels involved in cell proliferation, markedly decreased the K^+ current amplitude and channel open probability. Inhibition of the K^+ channel by these toxins displayed very slow kinetics and was almost irreversible, in accordance with their previously demonstrated mode of action on noninactivating K^+ current in dorsal-root ganglion neurons [50].

Detailed electrophysiological and pharmacological analysis of K^+ channels in LNCaP cells indicates that we have identified a new type of K^+ conductance, with unique overall properties.

To ascertain if the voltage-activated, Ca-dependent K^+ channel was involved in the modulation of cell proliferation in LNCaP cells, we studied whether incubation of LNCaP cells with K^+-channel inhibitors interfered with cell proliferation. Inhibitors that were effective in depressing K^+ channels in electrophysiological studies were found to markedly reduce the number of metabolically active tumor cells (MTT assay), and to decrease ^3H-thymidine incorporation (^3H-thymidine incorporation assay) and protein content, suggesting a strong antiproliferative action of the drugs. Alteration of cell-growth kinetics by K^+ channel blockers was not due to cytotoxicity, as the percentage of cells excluding trypan blue was not affected by incubation with the blockers in the range of concentrations used in this study. The overall effects of K^+ channel blockers on LNCaP cell proliferation were different from those reported for mitogen-stimulated lymphocytes [20], melanoma cells [27], or breast-cancer cells [26]. These quantitative and qualitative discrepancies may be due to differences in the type of K^+ channel expressed in the various cell populations.

Although it is clear that potassium channels are important for cell growth, the action mechanism of these potassium channel effects remains to be defined. Indeed, several hypotheses may be proposed for the mechanisms by which K^+ channels and their inhibitors affect cell proliferation: 1) K^+ channel modulation results in changes in intracellular K^+ concentration ($[K^+]_i$) which may directly or indirectly influence cell growth [51]. 2) Changes in membrane potential resulting from $[K^+]_i$ modulation may also interfere with mitogenic activity [22]. 3) Furthermore, changes in membrane potential will modify the driving force for the electrogenic transport of Ca^{2+} ions [35] that may affect cell proliferation. This hypothesis is unlikely, as our measurements showed that acute application of TEA, in concentrations similar to those used in patch-clamp experiments, had no effect on intracellular Ca^{2+} concentration. 4) The reduction in cell proliferation may be mediated by possible changes in intracellular pH [52] or cell volume [53] following K^+ channel blockade. 5) Finally, K^+ channel modulation has been shown to alter the expression of several genes, including the early genes c-fos and c-jun [54,55], as well as the Ha-ras oncogene [56]. Thus, K^+ channel blockade may inhibit cell proliferation by acting directly at the gene level. More detailed study is required of the mechanisms involved in signal transduction evoked by K^+-channel modulation in relation to cell proliferation.

In conclusion, LNCaP human prostate cancer cells express K^+ channels, that are likely to play an essential

role in the physiology of these cells and, more specifically, in their proliferation. Additional experiments will be needed to determine if these results can be extended to other prostate cell types, and to further understand how K^+ channels can interfere with the regulatory pathways involved in cell growth and proliferation.

ACKNOWLEDGMENTS

This work was supported by grants from the Association pour la Recherche sur les Tumeurs de la Prostate, P. Fabre Médicament, La Ligue Contre le Cancer, and the Fondation pour la Recherche Médicale. We are grateful to G. Gaurier and D. Varoqueaux for excellent technical assistance.

REFERENCES

1. Horoszewicz JS, Leong SS, Kawinski E, Karr J, Rosenthal H, Chu MT, Mirand EA, Murphy GP: LNCaP model of human prostate carcinoma. Cancer Res 1983;43:1908–1918.
2. Sonnenshein C, Olea N, Pasanen ME, Soto AM: Negative controls of cell proliferation: Human prostate cancers and androgens. Cancer Res 1989;49:3174–3181.
3. Isaacs JT, Lundmo PJ, Berges R, Martikainen P, Kyprianou N, English HF: Androgen regulation of programmed death of normal and malignant prostate cells. J Androl 1992;13:457–464.
4. Furuya Y, Isaacs JT: Differential gene regulation during programmed death (apoptosis) vs. proliferation of prostate glandular cells induced by androgen manipulation. Endocrinology 1993;133:2660–2666.
5. Furuya Y, Lin XS, Walsh JC, Nelson WG, Isaacs JT: Androgen ablation-induced programmed death of prostate glandular cells does not involve recruitment into a defective cell cycle or p53 induction. Endocrinology 1995;136:1898–1906.
6. Connolly JM, Rose DP: Production of epidermal growth factor and transforming growth factor-α by the androgen-responsive LNCaP human prostate cancer cell line. Prostate 1990;16:209–218.
7. Castagnetta LA, Miceli MD, Sorci CMG, Pfeiffer U, Farruggio R, Oliveri G, Calabra M, Carruba G: Growth of LNCaP human prostate cancer cells is stimulated by estradiol via its own receptor. Endocrinology 1995;136:2309–2319.
8. Limonta P, Dondi D, Moretti RM, Maggi R, Motta M: Antiproliferative effects of luteinizing hormone-releasing hormone agonists on the human prostate cancer cell line LNCaP. Endocrinology 1995;75:207–212.
9. Isaacs JT, Moston RA, Markikainen P, Isaacs WB: Growth factors affecting normal and malignant prostate cells. In Schomberg DW (ed.): "Growth Factors in Reproduction," New York: Springer-Verlag, 1991:167–184.
10. Takahashi A, Yamaguchi H, Miyamoto H: Change in K^+ current of HeLa cells with progression of the cell cycle studied by patch-clamp technique. Am J Physiol 1993;265:328–336.
11. Wilson TM, Yu-Lee LY, Kelley MR: Coordinate gene expression of luteinizing hormone-releasing hormone (LHRH) and the LHRH-receptor after prolactin stimulation in the rat NB2 T-cell line: Implications for a role in immunomodulation and cell cycle gene expression. Mol Endocrinol 1995;9:44–53.
12. Colombel M, Olsson CA, Ng PY, Buttyan R: Hormone-regulated apoptosis results from reentry of differentiated prostate cells onto a defective cell cycle. Cancer Res 1992;52:4313–4319.
13. Blok LJ, Hoogerbrugge JW, Themmen AP, Baarends WM, Post M, Grootegoed JA: Transient down-regulation of androgen receptor messenger ribonucleic acid (mRNA) expression in Sertoli cells by follicle-stimulating hormone is followed by up-regulation of androgen receptor mRNA and protein. Endocrinology 1992;131:1343–1349.
14. Lindzey JK, Grossman ME, Kumar MV, Tindall DJ: Regulation of the 5′-flanking region of the mouse androgen receptor gene by cAMP and androgen. Mol Endocrinol 1993;7:1530–1570.
15. Mizokami A, Saiga H, Matsui T, Mita T, Sugita A: Regulation of androgen receptor by androgen and epidermal growth factor in a human prostate cancer cell line, LNCaP. Endocrinol Jpn 1992; 39:235–243.
16. Nakhla AM, Bardin CW, Salomon Y, Mather JP, Janne OA: The actions of calcitonin on the TM3 Leyding cell line and on rat Leyding cell-enriched cultures. J Androl 1989;10:311–320.
17. Levin G, Keren T, Peretz T, Chikvashvili D, Thornhill WB, Lotan I: Regulation of RCK1 currents with a cAMP analog via enhanced protein synthesis and direct channel phosphorylation. J Biol Chem 1995;270:14611–14618.
18. White RF, Lee AB, Shcherbatko AD, Lincoln TM, Schonbrunn A, Armstrong DL: Potassium channel stimulation by natriuretic peptides through cGMP-dependent dephosphorylation. Nature 1993;361:263–266.
19. Mahaut-Smith MP, Mason MJ: Ca^{2+}-activated K^+-channels in rat thymic lymphocytes activation by concanavalin. Am J Physiol 1991;439:513–528.
20. Decoursey TE, Chandy KG, Gupta S, Cahalan MD: Mitogen induction of ion channels in murine T lymphocytes. J Gen Physiol 1987;89:405–420.
21. Lee SC, Sabath DE, Deutsch C, Prystowsky MB: Increased voltage-gated potassium conductance during interleukin-2-stimulated proliferation of a mouse helper T lymphocyte clone. J Cell Biol 1986;102:1200–1208.
22. Freedman BD, Price MA, Deutsch CJ: Evidence for voltage modulation of IL-2 production in mitogen stimulated human peripheral blood lymphocytes. J Immunol 1992;149:3784–3794.
23. Wang YF, Jia H, Walker AM, Cukierman S: K-current mediation of prolactin-induced proliferation of malignant (Nb2) lymphocytes. J Cell Physiol 1992;152:185–189.
24. Wilson GF, Chin SY: Mitogenic factors regulate ion channels in Schwann cells cultured from newborn rat sciatic nerve. J Physiol (Lond) 1993;470:501–520.
25. Pappone PA, Ortiz-Miranda SJ: Blockers of voltage-gated K channels inhibit proliferation of cultured brown fat cells. Am J Physiol 1993;1014–1019.
26. Wegman EA, Young JA, Cook DJ: A 23-pS Ca^{2+}-activated K^+ channel in MCF-7 human breast carcinoma cells: An apparent correlation of channel incidence with the rate of cell proliferation. Pflugers Arch 1991;417:562–570.
27. Nilius B, Wohlrab W: Potassium channels and regulation of proliferation of human melanoma cells. J Physiol Lond 1992;445: 537–548.
28. Huang Y, Rane S: Potassium channel induction by the Ras/Raf signal transduction cascade. J Biol Chem 1994;269:31183–31189.
29. Pepp H, Draheim H, Ruland J, Seidel G, Belse J, Presek P, Dreyer F: Profound differences in potassium current properties of normal and Rous sarcoma virus-transformed chicken embryo-fibroblasts. Proc Natl Acad Sci USA 1993;90:3403–3407.
30. Rosen LB, Ginty DD, Weber MJ, Greenberg ME: Membrane depolarization and calcium influx stimulate MEK and MAP kinase via activation of Ras. Neuron 1994;12:1207–1221.
31. Lev S, Moreno H, Martinez R, Canoll P, Peles E, Musacchio JM,

Plowman GA, Rudy B, Schlessinger J: Protein tyrosine kinase PYK 2 involved in Ca^{2+}-induced regulation of ion channel and MAP kinase functions. Nature 1995;376:737–745.
32. Prevarskaya NB, Skryma RN, Vacher P, Daniel N, Djiane, J, Dufy B: Role of tyrosine phosphorylation in potassium channel activation. Functional association with prolactin raceptor and JAK2 tyrosine kinase. J Biol Chem 1995;270:21292–21299.
33. Rui H, Lebrun JJ, Kirken RA, Kelly PA, Farrar WL: JAK 2 activation and cell proliferation induced by antibody-mediated prolactin receptor dimerization. Endocrinology 1994;135:1299–1306.
34. Abercrombie RF, Masukawa LH, Sjodin RA, Livengood D: Uptake and release of ^{45}Ca by Myxicola axoplasms. J Comp Physiol 1981;78:413–428.
35. Prevarskaya N, Skryma R, Vacher P, Daniel N, Bignon C, Djiane J, Dufy B: Early effects of PRL on ion conductances in CHO cells expressing PRL receptor. Am J Physiol 1994;267:554–562.
36. Bradford M: A rapid method for the quantitation of protein utilizing the principle of protein-dye binding. Anal Biochem 1976;72:248–254.
37. Blin N, Stafford D: A general method for isolation of high molecular weight DNA from eukaryotes. Nucleic Acids Res 1976; 3:2303.
38. Nörenberg W, Gebicke-Haerter PJ, Illes P: Voltage-dependent potassium channels in activated rat microglia. J Physiol (Lond) 1994;475:15–32.
39. Lang DG, Ritchie AL: Tetraethyl-ammonium blockade of apamin-sensitive and insensitive Ca^{2+}-activated K^+ channels in a pituitary cell line. J Physiol (Lond) 1990;450:117–132.
40. Cobbet P, Legendre P, Mason WT: Characterization of three types of potassium current in cultured neurones of rat supraoptic nucleus area. J Physiol (Lond) 1989;410:443–463.
41. Castle NA, Haylett DG, Jenkinson DH: Toxins in the characterization of potassium channels. TINS 1989;12:59–65.
42. White RE, Schonbrunn A, Armstrong DL: Somatostatin stimulates Ca^{2+}-activated K^+ channels through protein dephosphorylation. Nature 1991;351:570–573.
43. Price M, Lee SC, Deutsch C: Charybdotoxin inhibits proliferation and interleukin 2 production in human peripheral blood lymphocytes. Proc Natl Acad Sci USA 1989;86:10171–10175.
44. Harvey AL, Karlsson E: Dendrotoxin from the venom of the green mamba *Dendroaspis angusticeps*. A neurotoxin that enhances acetylcholine release of neuromuscular junctions. Naunyn Schmiedebergs Arch Pharmacol 1980;312:1–6.
45. Steinsapir J, Socci R, Reinach P: Effects of androgen on intracellular calcium of LNCaP cells. Biochem Biophys Res Commun 1991;179:90–96.
46. Sandström PE, Jonsson O, Grankvist K, Henriksson R: Identification of potassium flux pathways and their role in the cytotoxicity of estramustine in human malignant glioma, prostate carcinoma and pulmonary carcinoma cell lines. Eur J Cancer 1994; 30:1822–1826.
47. Bregestovski P, Redkozubov A, Alexeev A: Elevation of intracellular calcium reduces voltage-dependent potassium conductance in human T cells. Nature 1986;319:776–778.
48. Schlichter LC, Pahapill PA, Schumacher PA: Reciprocal regulation of K^+ channels by Ca^{2+} in intact human T lymphocytes. Receptors Channels 1993;1:201–215.
49. Skryma R, Prevarskaya N, Vacher P, Dufy B: Voltage-dependent ionic conductances in Chinese hamster ovary cells. Am J Physiol 1994;267:544–553.
50. Penner R, Petersen M, Pierau FK, Dreyer F: Dendrotoxin: A selective blocker of a non-inactivating potassium current in guinea-pig dorsal root ganglion neurones. Pflügers Arch 1986; 407:365–369.
51. Walev I, Reske K, Palmer M, Valeva A, Bhakdi S: Potassium-inhibited processing of IL-1β in human monocytes. EMBO J 1995;14:1607–1614.
52. Pappas CA, Ulrich N, Sontheimer H: Reduction of glial proliferation by K^+ channel blockers is mediated by changes in pHi. Neuroreport 1994;6:193–196.
53. Rouzaire-Dubois B, Dubois JM: A quantitative analysis of the role of K^+ channels in mitogenesis of neuroblastoma cells. Cell Signalling 1991;3:333–339.
54. Heurteaux C, Bertaina V, Widmann C, Lazdunski M: K^+ channel openers prevent global ischemia-induced expression of c-fos, c-jun, heat shock protein, and amyloid β-protein precursor genes and neuronal death in rat hippocampus. Proc Natl Acad Sci USA 1993;90:9431–9435.
55. Heurteaux C, Lazdunski M: MCD peptide and dendrotoxin I activate c-fos and c-jun expression by acting on two different types of K^+ channels. A discrimination using the K^+ channel opener lemakalim. Brain Res 1991;554:22–29.
56. Wöll E, Ritter M, Scholz W, Häussinger D, Lang F: The role of calcium in cell shrinkage and intracellular alkalinisation by bradykinin in Ha-ras oncogene expressing cells. FEBS Lett 1993; 322:261–265.

ANTICANCER RESEARCH 22: 1727-1730 (2002)

(F)

Voltage-gated Sodium Ion Channels in Prostate Cancer: Expression and Activity

MANSOOR ABDUL and NASEEMA HOOSEIN

Rumbaugh-Goodwin Institute for Cancer Research, Plantation, Florida, U.S.A.

Abstract. *Background: High levels of voltage-gated sodium channels (VGSCs) have been previously associated with the invasiveness of rat and human prostate cancer (Pca) cell lines. Materials and Methods: 4 normal prostate and 80 clinical Pca specimens on a tissue microarray slide were examined by immunohistochemistry using anti-sodium channel (III-IV linker region) antibody. The effects of a VGSC-opener and VGSC-blockers on the in vitro proliferation of 4 human Pca cell lines was examined. Results: Fifty-five% (44 out of 80) Pca specimens showed higher VGSC levels compared to normal, with 14 (of 44) showing increased focal staining. VGSC-opener veratrine (1-50 ug/mL), increased growth of PC3, DU145, LNCaP and MDA-PCA-2B Pca cells. VGSC-blockers, flunarizine (IC_{50}=2 μg/mL) and riluzole (IC_{50}=10-30 μg/mL) caused dose-dependent growth-inhibition of all four cell lines. Western analysis of cell extracts showed VGSC-immunoreactivity in the 4 Pca cell lines. Conclusion: Our results indicate increased expression of VGSCs in Pca and VGSC involvement in Pca growth.*

Electrophysiological recording (patch-clamp) studies have shown that highly metastatic rodent Mat-LyLu, Dunning prostate cancer (Pca) cells express sodium (Na+) channels, activated by membrane depolarization (1). In contrast, the weakly metastatic AT-2 Dunning Pca cells express no active Na+ channels (1). The pharmacological profile of the Mat-LyLu voltage-gated Na+ channel (VGSC) suggested that it is tetrodotoxin-sensitive (2). Study of human Pca cell lines revealed similar properties (3). A greater percentage of the aggressive, androgen-insensitive, PC3 cells express voltage-gated sodium channels (VGSCs) compared to the relatively-indolent, androgen-sensitive, LNCaP cells (3). The possible function of VGSCs expressed by strongly metastatic PC3 cells has been investigated by *in vitro* invasion assay (Boyden chamber) (3). The invasiveness of PC3 cells was reduced significantly by tetrodotoxin (2, 3). Analysis of VGSC protein levels in rat and human Pca cell lines by flow cytometry, showed a positive correlation between the proportion of channel-expressing cells and the ability of the cell line to invade reconstituted basement membrane (Matrigel) *in vitro* (4). Thus, VGSC activity appears to contribute to the invasive behavior of Pca cells. Skeletal muscle type Na+ channel mRNA has been detected in both rat and human Pca cell lines (5). We have investigated the expression of VGSCs in clinical Pca specimens for the first time and studied the effect of VGSC-channel modulators on cellular proliferation.

Correspondence to: Dr. N. Hoosein, Rumbaugh-Goodwin Institute, 1850 NW 69 Ave #5, Plantation, FL 33313, USA. e-mail:naseema@mindspring.com.

Key Words: Voltage-gated, sodium-channel, prostate cancer, veratrine, flunarizine, riluzole.

Materials and Methods

Normal and malignant prostate specimens on tissue microarray slides were obtained from the Cooperative Human Tissue Network under the Tissue Array Research Program (TARP) of the National Cancer Institute, The National Institutes of Health (Bethesda, MD, USA). Sections were deparaffinized in xylene and hydrated through graded alcohol series. After quenching endogenous peroxidase with 0.3% hydrogen peroxide in methanol, rinsing with phosphate-buffered saline (PBS) and blocking with 3% bovine serum albumin (BSA) in PBS, tissue sections were incubated in primary antibody, 3 μg in 200 μL PBS (anti-sodium channel III-IV linker region, rabbit polyclonal, Upstate Biotechnology, Lake Placid, NY, USA) for 1 hour at room temperature (RT) in a humidified chamber. Sections were then rinsed with PBS and incubated with horseradish-peroxidase (HRP)-conjugated, goat anti-rabbit antibody (BioRad, Hercules, CA, USA) at a 1:200 dilution for 1 hour at RT. Freshly prepared 3,3'-diaminobenzidine (DAB, Sigma Fast Tablets, St. Louis, MO, USA) was used as the substrate for HRP.

Effects of the VGSC-opener veratrine (Sigma, St. Loius, MO, USA) as well as VGSC-blockers, flunarizine and riluzole (Tocris, Ellisville, MO, USA), on *in vitro* cellular proliferation were determined. Four human Pca cell lines were studied: PC-3, DU145, MDA-PCA-2B and LNCaP (American Type Culture Collection). The cell lines were maintained in Leibovitz's medium (Gibco, Rockville, MD, USA) containing 100 units/mL penicillin G, 100 μg/mL streptomycin, 0.25 μg/mL amphotericin B (L-medium) and supplemented with 20% Hams F-12, 5 μg/mL insulin, 100 μg/mL transferrin, 30 nM sodium selenite and 5% fetal bovine serum. To study growth-stimulation, human Pca cell lines were plated at 7,000 cells per well in 96-well plates in supplemented L-medium. Next day the cells were changed to unsupplemented L-medium. After 48 hours the cells were treated with veratrine in unsupplemented L-medium for 72 hours and the cell numbers determined using calcein AM (Molecular Probes, Eugene, OR, USA). To study the effect of channel-blockers on growth, human Pca cells lines were plated at 15,000 cells per well in 96-well plates in serum-supplemented growth medium. Next day the cells were treated with channel-blockers in unsupplemented L-medium for 96 hours and the cell numbers determined using calcein AM.

0250-7005/2002 $2.00+.40

Cell extracts of the 4 cell lines were prepared and Western blotting done as previously described (6). Seventy-five μg of cell extracts were loaded per lane and the anti-VGSC antibody from Upstate Biotechnology was used at a 1:1000 dilution.

Results

Antibody against the VGSC III-IV intracellular loop was employed to detect VGSC expression in a human, multi-tumor tissue microarray. A moderate level of staining was observed in normal prostatic acini (Figure 1, top) with staining somewhat higher in cells lying on the basal aspect. Staining was observed both in the epithelial and stromal compartments. Fourteen (18 %) of the 80 Pca specimens examined showed similar moderate levels of staining with high levels of focal staining observed in scattered individual cells or small groups of cells (Figure 1, middle). In addition, 30 (37 %) of the 80 Pca specimens showed elevated epithelial staining (Figure 1, bottom) compared to normal (Figure 1, top).

The VGSC-opener veratrine stimulated growth of the two androgen-responsive Pca lines (LNCaP and MDA-PCA-2B) as well as the two androgen-unresponsive cell lines (PC3 and DU145). Dose-dependent growth promotion of LNCaP cells by veratrine is shown in Figure 2. A maximal 68% stimulation was observed in LNCaP cells at a concentration of 5 μg/mL veratrine. Also, maximal stimulation of 39%, 27% and 23% was observed in MDA-PCA-2B, DU145 and PC3 cell lines, respectively at concentrations between 5-50 μg/mL veratrine (Figure 2). The effect of veratrine appeared biphasic, with lower stimulation at the higher doses in three of the cell lines examined (Figure 2). Veratrine is known to support the survival of embryonal neuronal cells *in vitro*, about 20 μg/mL veratrine being as effective as a nerve growth factor (7, 8).

The VGSC-blocker flunarizine (8, 9) inhibited, in a dose-dependent manner, the growth of the androgen-insensitive PC3 and DU145 cells as well as the androgen-sensitive MDA-PCA-2B and LNCaP cell lines (Figure 3, left). Half-maximal inhibition occurred at about 2 μg/mL flunarizine (Figure 3, left). Another VGSC-blocker, riluzole (10), decreased growth of all four Pca cell lines, half-maximally at concentrations between 10-30 μg/mL (Figure 3, right). We have previously reported that other VGSC-channel blockers such as carbamazepine, phenytoin and valproate inhibit the *in vitro* proliferation of Pca cells grown in Matrigel (11). Western blot analysis of cell extracts found VGSC-immunoreactivity in all four human Pca cell lines tested (Figure 4). Any difference in the level of VGSC protein between PC3 and LNCaP cell lines was not readily detectable by Western analysis (Figure 4) as found by flow cytometry (4).

Discussion

Electrophysiological studies of weakly metastatic AT-2 and strongly metastatic MAT-LyLu rat Pca cell lines detected VGSCs only in MAT-LyLu cells (1, 12). Flow-cytometric

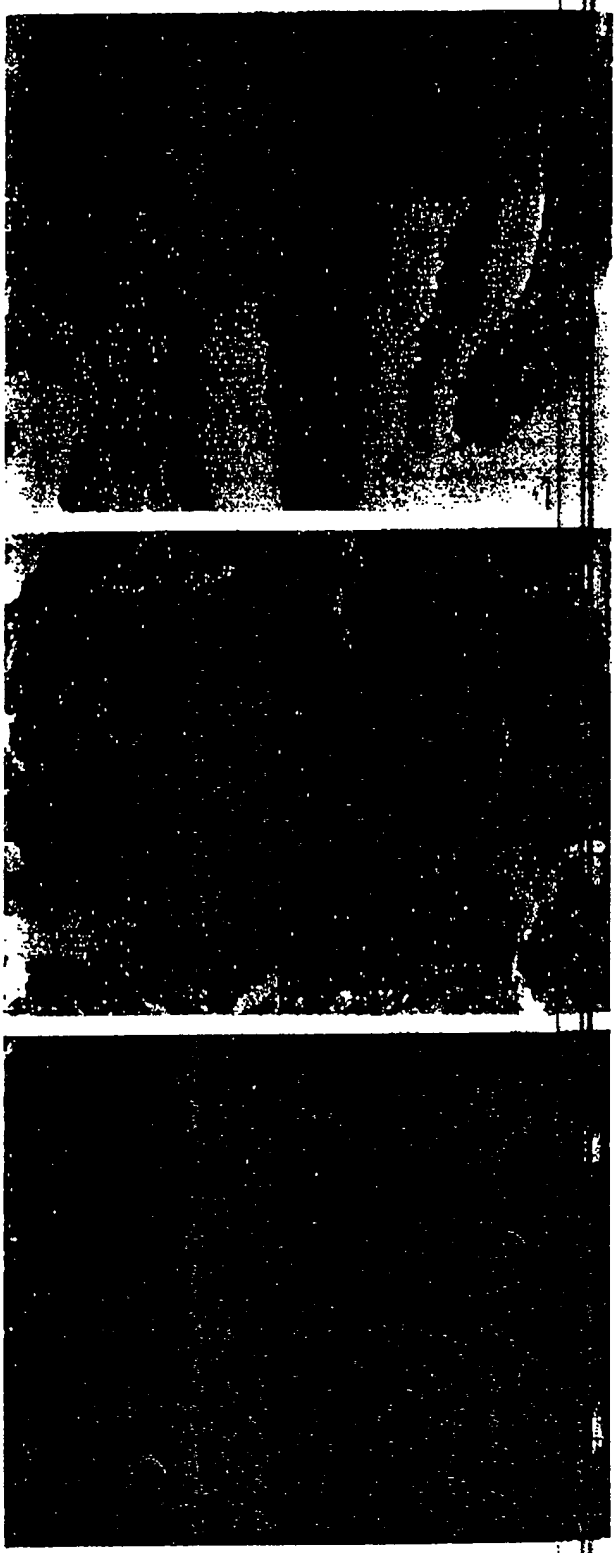

Figure 1. *Immunohistochemical staining of voltage-gated sodium ion channels in the normal human prostate (top). Representative clinical Pca specimens showing increased staining: focal (middle) and diffuse (bottom). Magnification 40X.*

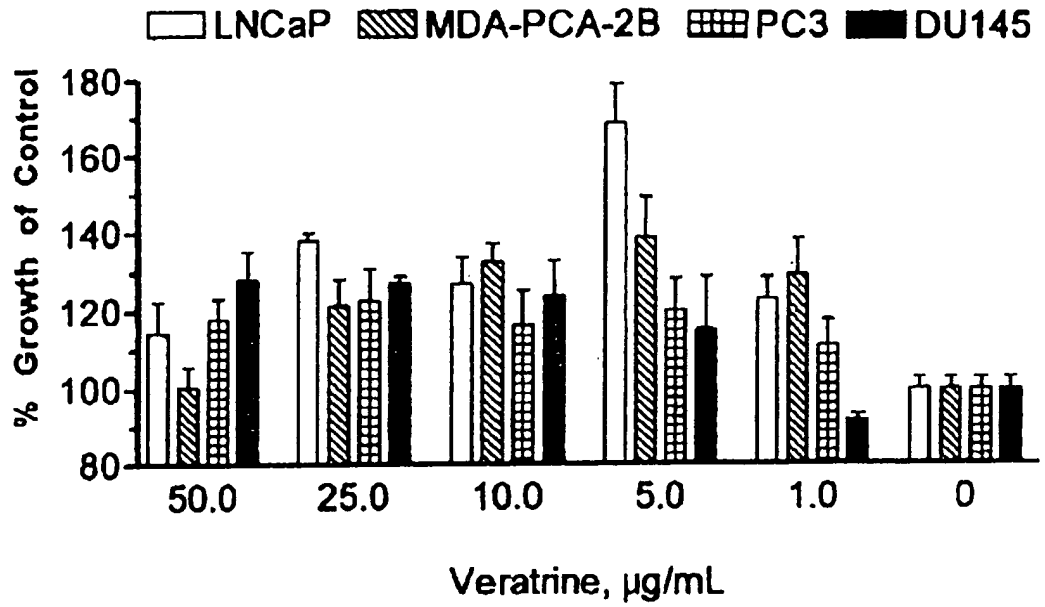

Figure 2. *Growth-stimulation of four human prostate cancer cell lines by veratrine, an activator of voltage-gated sodium ion channels. Mean and standard deviation of triplicate assay points are shown. Assays were repeated two additional times with similar results.*

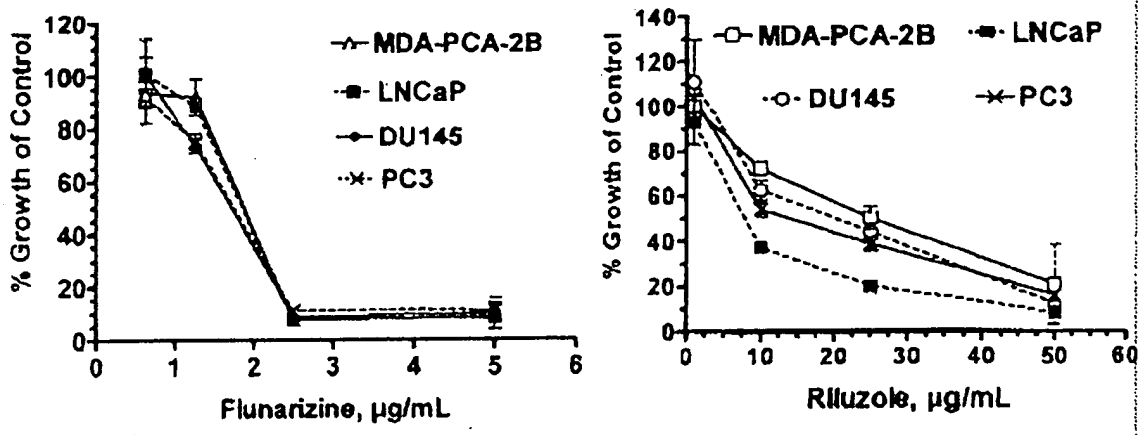

Figure 3. *Growth-inhibition of four human prostate cancer cell lines by VGSC-blockers, flunarizine (left) and riluzole (right). Mean of duplicate assay points are shown. Assays were repeated three times with similar results.*

analysis for VGSC expression in human Pca cell lines using the same commercial antibody as used in this study (Upstate Biotechnology), showed 18.8% positive cells in PC3, 13.8% positive in DU145 and only 1.6% positive in LNCaP (4). Also, transfected rat epithelial cells having high VGSC expression displayed increased *in vitro* invasiveness (4). Our finding of increased VGSC levels in a sub-set of human Pca compared to normal (Figure 1) are therefore in agreement with the previous reports of VGSCs in rat and human Pca cell lines. Differential expression of VGSCs in prostate cancer cells of varying metastatic potential, and the demonstration of their involvement in cellular behavior (such as proliferation and invasion), are consistent with VGSCs having a significant role in Pca progression (13). It is noteworthy that androgens have been shown to suppress VGSC activity in the mouse muscle C2 cell line (14). It is thus possible that increased VGSC activity is associated with progression of Pca to androgen-independence. These data support other studies showing

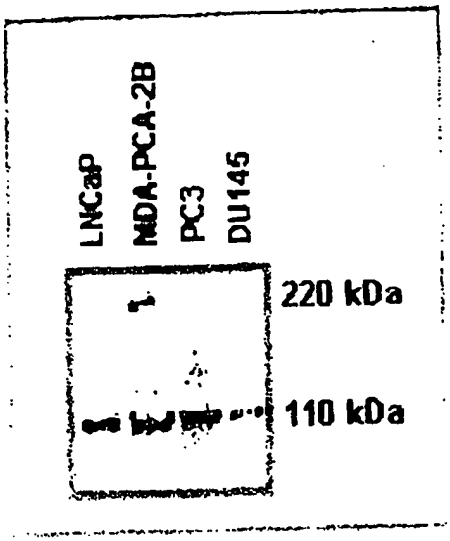

Figure 4. *Western blot of cell extracts from 4 human prostate cancer cell lines using antibody specific for the voltage-gated sodium-channel intracellular III-IV loop.*

altered voltage-gated ion-channel expression during cancer development and progression (13, 15, 16). VGSC presence in small cell lung cancer cell lines has been reported (17, 18). Our results suggest that VGSCs could serve as targets for Pca treatment. Further investigations of an association between higher VGSC expression and poor prognosis and regulation of VGSC activity in Pca are warranted.

Acknowledgements

Supported by the National Cancer Institute: Grant CA63225.

References

1 Grimes JA, Fraser SP, Stephens GJ, Downing JEG, Laniado ME, Foster CS, Abel PD and Djamgoz MBA: Differential expression of voltage-activated Na+ currents in two prostatic tumour cell lines: Contribution to invasiveness *in vitro*. FEBS Lett *369*: 290–294, 1995.

2 Grimes JA and Djamgoz MBA: Electrophysiological characterization of voltage-gated Na+ current expressed in the highly metastatic Mat-Ly-Lu cell line of rat prostate cancer. J Cell Physiol *175*: 50–58, 1998.

3 Laniado ME, Lalani EN, Fraser SP, Grimes JA, Bhangal G and Djamgoz MBA: Expression and functional analysis of voltage-activated Na+ channels in human prostate cancer cell lines and their contribution to invasion *in vitro*. Am J Pathol *150*: 1213–1221, 1997.

4 Smith P, Rhodes NP, Shortland AP, Fraser SP, Djamgoz MB: K... and Foster CS: Sodium channel protein expression enh...es ... invasiveness of rat and human prostate cancer cells. FEBS Lett ... 19–24, 1998.

5 Diss JKJ, Stewart D and Fraser SP: Expression of skeletal mu... type voltage-gated Na+ channel in rat and human prostate cancer ... lines. FEBS Lett *427*: 5–10, 1998.

6 Diaz M, Abdul M and Hoosein NM: Modulation of neuroendoc... differentiation in prostate cancer by interleukin-1 and -2. ... Prostate (Suppl) *8*: 32-36, 1998.

7 Bhave SV, Malhotra RK, Wukade TD and Wakade AR: Verat... supports the *in vitro* survival of embryonic chick sympathetic ... Neurosc Lett *109*: 201-205, 1990.

8 Tanaka S and Koike T: Veratridine delays apoptotic neuronal d... induced by NGF deprivation through a Na(+)-dependent mechan... in cultured rat sympathetic neurons. Int J Develop Neurosc *15*: 15... 1997

9 Cousin MA, Nicholls DG and Pocock JM: Flunarizine inhibits ... calcium-dependent and -independent release of glutamate ... synaptosomes and cultured neurones. Brain Res *606*: 227-36, 1993.

10 Song JH, Huang CS, Nagata K, Yeh JZ and Narahashi T: Differe... action of riluzole on tetrodotoxin-sensitive and tetrodotoxin-resi... sodium channels. J Pharmacol Experimntl Therapeutic *282*: ... 1997.

11 Abdul M and Hoosein NM: Inhibition by anticonvulsants o... prostate specific antigen and interleukin-6 secretion by human prostate ca... cells. Antican Res *21*: 2045-2048, 2001.

12 Fraser SP, Grimes JA and Djamgoz MBA: Effects of voltage-g... ion channel modulators on rat prostate cancer cell prolifera... Comparison of strongly and weakly metastatic cell lines. The Pr... *44*: 61-76, 2000.

13 Foster CS, Cumford P, Forsyth L, Djamgoz MBA and Ke Y: ... cellular and molecular basis of prostate cancer. BJU Internation... 171-194, 1999.

14 Tabb JS, Fanger GR, Wilson EM, Maue RA and Hen... Suppression of sodium channel function differentiating ... cells stably overexpressing rat androgen receptors. J Neurosc *14*: ... 773, 1994.

15 Caffrey JM, Brown AM and Hess P: Mitogens and oncogene... block the induction of specific voltage-gated ion channels. Sc... *239*: 570-573, 1987.

16 Repp H, Braheim H and Ruland J: Profound differences in pota... current properties of normal and Rous sarcoma virus-transfo... chicken embryo fibroblasts. Proc Natl Acad Sci USA *90*: 3403-... 1993.

17 Pancrazio JJ, Viglione MP, Tabbara IA and Kim YI: Vo... dependent ion channels in small-cell lung cancer cells. C... 5901-5906, 1989.

18 Blandino JK, Viglione MP, Bradley WA, Oie HK and Kim YI: ... Voltage-dependent sodium channels in human small-cell lung c... cells: role in action potentials and inhibition by Lambert-... syndrome IgG. J Membrane Biol *143*: 153-163, 1995.

Received January 14, 2002
Accepted March 12, 2002